BIO-OPTICAL PROPERTIES OF THE TURKISH SEAS

A THESIS SUBMITTED TO THE GRADUATE SCHOOL OF
MARINE SCIENCES MIDDLE EAST TECHNICAL
UNIVERSITY

BY

HASAN ÖREK

IN PARTIAL FULFILLMENT OF THE REQUIREMENTS FOR
THE DEGREE OF DOCTOR OF PHILOSOPHY IN MARINE
SCIENCES

MARCH 2007

Approval of the Graduate School of Marine Sciences

_____

Prof. Dr. Ferit Bingel Director

I certify that this thesis satisfies all the requirements as a thesis for the degree of Doctor of Philosophy.

_____
Prof. Dr. Ferit Bingel
Head of Department

This is to certify that we have read this thesis and that in our opinion it is fully adequate, in scope and quality, as a thesis for the degree of Doctor of Philosophy.

_____   _____
Assoc Prof. Dr. Dilek Ediger   Assoc. Prof Dr. Şükrü Turan Beşiktepe
        Co-Supervisor   Supervisor

Examining Committee Members

Prof. Dr. Özden Baştürk   (MersinUniversity)_____

Assoc Prof Dr. Şükrü Turan Beşiktepe   (METU-IMS)_____

Prof Dr. Ferit Bingel   (METU-IMS)_____

Assoc Prof. Dr. Dilek Ediger   (TUBITAK-MAM)_____

Assoc Prof. Dr. Zahit Uysal   (METU-IMS)._____

I hereby declare that all information in this document has been obtained and presented in accordance with academic rules and ethical conduct. I also declare that, as required by these rules and conduct, I have fully cited and referenced all material and results that are not original to this work.

Name, Last name: **Hasan Örek**

Signature   :

ABSTRACT

Bio-optical Characteristics of the Turkish Seas

Örek, Hasan

Ph.D., Graduate School of Marine Sciences

Supervisor   : Assoc. Prof. Dr. Şükrü Turan Beşiktepe

Co-Supervisor: Assoc. Prof. Dr. Dilek Ediger

March 2007, 160 pages

Optical properties of the seas surrounding Turkey (i.e. Mediterranean Sea, Black Sea and Aegean Sea) are investigated utilizing the data collected from years 2001-2005. Pigment, light (irradiance), absorption samples were collected and analyzed. SeaWiFS and MODIS satellite observations between years 1997-2006 has been collected, processed and analyzed. High temporal and spatial variability is observed in the optical properties of the three basins. The Mediterranean Sea and the Black Seas are the two typical examples of the Case I and the Case II waters, respectively. SeaWiFS and MODIS derived chlorophyll data obtained during the time period where the data were coexistent (2002-2004) gave consistent results. Thus, data from both sensors are used to establish temporal continuity. Optical classification of the water types based on the Jerlov model shows that the Mediterranean has clear (Type 1) and very clear water type characteristics and the Black Sea and the Marmara waters are turbid (Type 5). Absorption from yellow substance (or so-called CDOM) does not optically dominate the Mediterranean allowing accurate estimation of pigment concentrations by remote sensing methods. This study is further extended to analyze the main contributing phytoplankton groups to the bio-optical characteristics in the three basins. HPLC

measurements show that the diatoms are the main group in the Black Sea ecosystem. Whereas in Mediterranean *Cyanophyta* dominates. Phytoplankton group compositions in the offshore and coastal regions of the Mediterranean do not show considerable difference. The main differences are the higher *Prymnesiophyceae* (nearly two times higher then the offshore) and lower *Cyanophyta* contribution in the coastal regions compared to offshore regions.

Key Words: Mediterranean Sea, Black Sea, Optical properties, remote sensing, pigments.

ÖZ

Türkiye Denizlerinin Biyo-Optiksel Karakteristikleri

Örek, Hasan

Doktora, Deniz Bilimleri Enstitüsü

Tez Yöneticisi : Doç. Dr. Şükrü Turan Beşiktepe

Ortak Tez Yöneticisi : Doç. Dr. Dilek Ediger

Mart 2007, 160 sayfa

Türkiye denizlerinin biyo optik özellikleri, 2001-2005 yılları arasında toplanan verilerle araştırılmıştır. Işık, iz pigment ve soğurma verleri toplanarak analiz edilmiştir. Bununla birlikte, 1997-2006 tarihleri arasındaki, SeaWiFs ve MODIS uydularından toplanan verileri değerlendirilmiştir. Yapılan çalışmalar sonucunda, optik özelliklerin zamansal ve mekansal olarak büyük farklılıklar gösterdiği ortaya çıkmıştır. Akdeniz ve Karadeniz sırası ile Case I ve Case II sularına tipik örnek teşkil etmektedirler. SeaWiFS ve MODIS uydu algılayıcıları, değişik olmalarına rağmen uzun süreli ve tutarlı bir klorofil verisi üretilmiştir. Su tiplerinin Jerlov modeline göre sınıflandırılması sonucu, Akdeniz suyunun temiz ve çok temiz sınıfına giridiği ve Karadeniz ile Marmara da ise 5 dereceden bulanıklık olduğu tespit edilmiştir. Akdeniz genelinde sarı madde (CDOM) ışık soğurulmasında çok etkili olmadığından, uydularla üretilen klorofil değerleri daha doğru olmaktadır. Yüksek performanslı sıvı kromatografisi ölçüm tekniği kullanılarak iz pigmentlere bakıldığında Karadeniz'in diatomlarca zengin, Akdeniz'de ise *Cyanophyta* grubunun baskın olduğu bulunmuştur. Akdeniz kıyı ve açık suları arasında belirgin farklılıklar olmamakla birlikte, kıyı ile açık arasındaki başlıca farklılık, *Cyanophyta*'nın

kıyıda daha az olması fakat bunun yanında *Prymnesiophyceae* grubunun yaklaşık iki kat kıyıda daha yoğun olmasıdır.

Anahtar Kelimeler: Akdeniz, Karadeniz, Optik özellikler uzaktan algılama, iz-pigmentler.

TABLE OF CONTENTS

LIST OF TABLES

LIST OF FIGURES

ABBREVIATIONS

AOP: Apparent Optical Properties.

ALLO: alloxanthin

B-CAR: β-carotene

BUT: 19-butanoyloxyfucoxanthin

CDOM: Colored Dissolved Organic Matter (Gelbstoff).

CHL-a or chl a: Chlorophyll-a

CMODIS: Chinese Moderate Resolution Imaging Spectroradiometer.

CNES: Centre National d'études Spatiales (French Space Agency).

CNSA: China National Space Administration.

COCTS: Chinese Ocean Colour and Temperature Scanner.

CONAE: Comision Nacional de Actividades Espaciales (Argentine Commission on Space Activities).

CSIRO: Australian Commonwealth Scientific and Research Organization.

CZCS: Coastal Zone Colour Scanner.

CZI: Coastal Zone Imager.

DIAD: Diadinixanthin.

DLR: Deutsches Zentrum für Luft- und Raumfahrt (German Aerospace Center).

DOM: Dissolved Organic Matter.

$E_d(\lambda,z)$: Down ward Irradiance at λ (wavelength),z(depth).

EOS: Earth Observing System.

$E_u(\lambda,z)$: Upward Irradiance at λ (wavelength),z(depth).

ESA: European Space Agency.

FUX: Fucoxanthin.

GCOM: Global Change Observation Mission.

GCOM-C: Global Change Observation Mission (Climate)

Geost: Geostationary.

GES: Goddard Earth Sciences.

GLI: Global Imager.

GMES: Global Monitoring for Environment and Security.

GOCI: Geostationary Ocean Colour Imager.

HEX: 19`-Hexanoyloxyfucoxanthin.

HPLC: High Performance Liquid Chromatography.

HY-1A: HaiYang-1A.

IOP: Inherent Optical Properties.

IPO: Integrated Program Office.

IRS P3: Indian Remote Sensing.

ISRO: Indian Space Research Organization.

JAXA: (former NASDA)

KARI: Korea Aeropspace Research Institute.

K_d: Light, Vertical Attenuation Coefficient.

KOMPSAT: Korea Multi-Purpose Satellite.

KORDI: Korea Ocean Research and Development Institute.

MERIS: Medium Resolution Imaging Spectrometer.

MMRS: Mulitspectral Medium Resolution Scanner.

MODIS: Moderate Resolution Imaging Spectroradiometer

MOS: Moderate Optoelectrical Scanner.

NASA: National Aeronautics and Space Administration.

NASDA: National Space Development Agency

NPOESS: National Polar-orbiting Operational Environmental Satellite System.

NPP: The NPOESS Preparatory Project.

OCM: Ocean Colour Monitor.

OCTS: Ocean Colour and Temperature Scanner.

OCMI: Ocean Scanning Multispectral Imager.

OLCI: Ocean and Land Colour Instrument.

PA: Particle Absorption

PARASOL: Polarization & Anisotropy of Reflectances for Atmospheric Sciences coupled with Observations from a Lidar.

Phyto: Phytoplankton

POLDER: PoLarization and Directionality of the Earth's Reflectances.

PPC: Photoprotective carotenoids.

Psu: Practical Salinity Unit

RSD: Relative Standard Deviation.

R/V: Research Vessel

SAC-C: Satelite de Aplicanciones Cientificas-C.

SATELL: Satellite

SeaWiFS: Sea-viewing Wide Field-of-view Sensor.

SGLI: (SecondGeneration GLI)

SPEC-COV: Spectral Coverage.

SZ-3: Shen Zhou-3.

URL: Uniform Resource Locator.

VIIRS: Visible Infrared Imager / Radiometer Suite.

1. INTRODUCTION

Solar energy controls the dynamics and equilibriums in both terrestrial and aquatic ecosystems. Since solar radiation is transferred to the earth through the atmosphere, a major part of the solar flux is absorbed (photoionizes or dissociates) in the first layers of the atmosphere. However, the atmosphere has two highly transparent ranges, the optical window (λ=400-700 nm), and the radio window (λ=10^{-2}-10^{2} meters). Several narrow, partial infrared windows also exist. The most important part of the solar flux reaching the ecosphere is in the visible range (λ=400-700 nm, or PAR: photosynthetically active radiation) (Figure 1). The solar intensity of the visible range (λ=400-700 nm) variability is less than 1% (Thomas and Stamnes 1999).
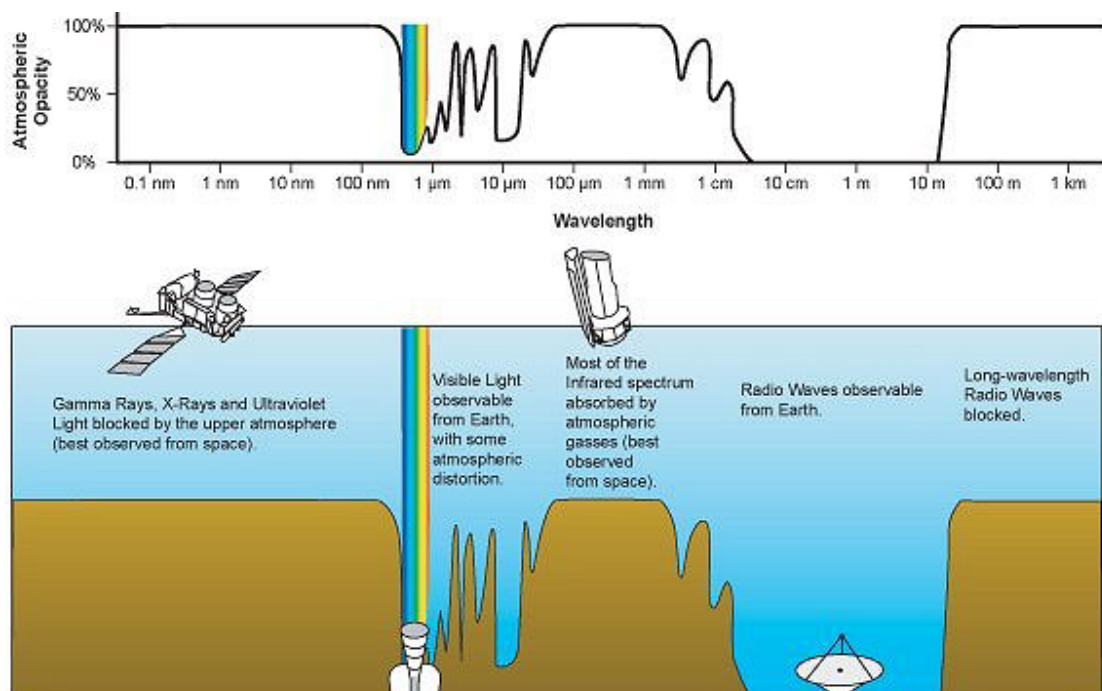
Figure 1: Electromagnetic waves and atmospheric transparency (URL1).

The visible range of the solar radiation is the most important part for ocean science, where passive remote sensing is used as a tool. Light being electromagnetic radiation behaves in two distinct ways (Gordon1994):

1. Fluctuating electric and magnetic waves: *Propagation of Energy*
2. Packets of particles called photons or quanta: *Quantify Energy.*

Properties of light such as reflection, refraction, and polarization are related to the wave like behavior. However, the intensity is related to the photon type behavior. Spectral properties of objects are utilized in various fields in earth sciences, such as in mapping forests, and urbanization through remote sensing. Recently, parallel to advances in satellite technology, optics and optical properties of the oceans have been intensively investigated.

Solar energy heats the sea and provides energy for phytoplankton, thus the energy is transferred to the other living organism. Most of the light is absorbed in the first few meters. In particular, infrared part of the spectrum is absorbed in the first few centimeters (Jerlov 1976). On the other hand, only a small amount of light is reflected. The reflected light depends upon the constituents in the water. The type and concentration of these constituents depend on both the region and/or the water body. The reflectance is used to determine various parameters, for instance, chlorophyll concentration and total suspended sediments among others. The main concept of these measurements is based on the optical properties of the particular constituent. Phytoplankton is one of the most important constituent in the sea surface, thus the color of the ocean is related to the large extent on the phytoplankton concentration and composition (Stewart 2006).

1.1. Ocean Optics and Ocean Color

1.1.1. Ocean Optics

Lights reaching the sea surface are either scattered or absorbed. Because of this processes, the seawater and constituents in it control the optical processes in the oceans. Phytoplankton groups are the most important optical constituents in the open

ocean in terms of ocean color. According to the authors (Mobley (1995), Gordon (1994), Kirk (1994), Srokosz (2000) and Morel and Maritorena (2001) optical properties of the oceans may be classified as:

    a. Inherent optical properties
    b. Apparent and/or quasi-inherent optical properties.

It is to note here that the first classification in this sense has been proposed by Preisendorfer (1961).

The Inherent Optical Properties (IOP): These are independent from the ambient light field and related with only the medium. The absorption coefficient and the volume scattering function are two fundamental IOPs. Other IOPs include the attenuation coefficients and the single scattering albedo (ratio of the scattering coefficient to the extinction coefficient, very dependent on wavelength). It is possible to derive the other IOPs from these fundamental properties (attenuation coefficients and the single scattering albedo) (Mobley 1995).

Apparent and/or quasi-inherent Optical Properties (AOP): These depend on both the medium (IOPs) and the geometric (directional) structure of the light field. Commonly used AOPs are, irradiance, average cosines (measuring the light from all directions in 180^0 surface) and various attenuation functions (K functions, like beam attenuation coefficients). Similar to the IOP fundamentals, spectral radiance is the parent of all radiometric quantities and AOPs (Mobley 1995, Kirk 1994), (Figure 2).

1.1.1.2. Case 1 and Case 2 waters

Ocean provinces are classified in two main groups, according to their spectral reflectance. In the field of remote sensing, two types of seawater have been defined: Case 1 and Case 2 waters (Morel and Prieur, 1977). This concept has been refined later (Morel and Maritorena, 2001, Mobley et al., 2004, Stramski et al., 2004). Case 1 waters are characterized by a strong correlation between scattering and absorbing

substance concentrations and the chlorophyll concentration. Thus the phytoplankton activity controls optical properties of water. Hence the characterization of Case 1 waters depends on the biological activity, mainly on the phytoplankton and its' co-variants. A strong correlation exists between the optical properties and the chlorophyll concentration (Behrenfeld and Falkowski 1997, Morel and Maritorena 2001, Mobley et al., 2004). Open ocean surface water and oligotrophic regions such as eastern Mediterranean are typical Case 1 waters. These types of water bodies cover nearly 95%-97% of the total ocean surface (Morel 1994).
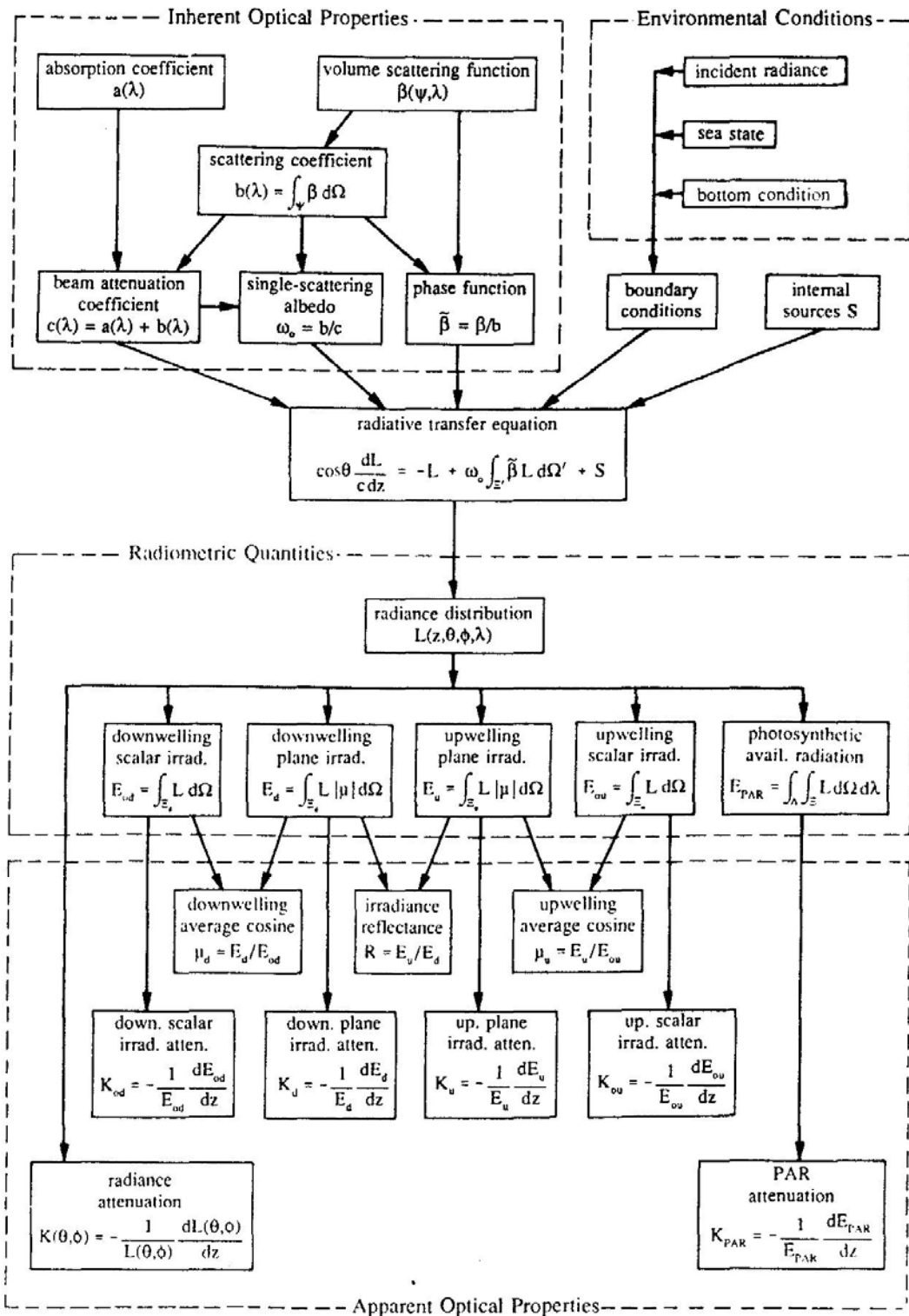
Figure 2: Schematic representation of the optical properties of the water (ocean, lake, etc...) (cf. Mobley 1995).

Case 2 waters are characterized by a lack of correlation between scattering and absorbing substance concentrations and chlorophyll concentration. Coastal waters are usually classified as Case 2 waters. The dominant optically active matter in the water is not phytoplankton only; particulate matter and colored dissolved organic matter (CDOM), which are not always related with chlorophyll, also affect the seawater optical properties. The parameterization of the Case 2 waters is more complicated than for the Case 1 waters, because the other components (particles and CDOM) are not the covariant with the phytoplanktonic or even biological activity and may have originated from anthropogenic sources. It is necessary to determine the other constituents, in order to establish a relation between chlorophyll and optical signatures (Kirk 1994, Sathyendranath 2000, Mobley et al., 2004).

1.1.2. Ocean Color

Remote sensing data from satellites has been increasingly used in physical and biological oceanography for the understanding of meso and even micro scale processes. The main goal of satellite oceanography is to acquire large amounts of data from an area (e.g., whole Back Sea) in unit time, but the resolution of the data (now, it is about 1 km) still needs to be enhanced for increasing the sensitivity. The following four basic parameters are measured (or calculated) at present.

a. Surface temperature
b. Color of near surface water
c. Surface roughness
d. Sea surface height

For measurement of these parameters either active or passive sensors are used. The active sensors generate their own signals while the passive ones detect the radiation that reflects (remote sensing reflectance) from ocean. Most important active sensors are the radars and altimeters. These systems work by sending a beam (either radar wave or micro wave) and then receiving the reflected beam from the sea

surface. The conditions of the surface altimetry and roughness are calculated according to the Doppler shift principles (for detailed information see: URL2).

Ocean color and ocean optic studies began in 1960. Water optic studies extend to much earlier dates, however intensive studies were carried out around early 1960 (Jerlov and Nielsen 1974). Ocean color studies are somewhat more complicated and problematic than the other parameters that are measured by remote sensing. Calibration of the ocean color instruments and verification of the ocean color data requires comparison with in-situ bio-optical measurements. Except for the surface temperature, all other parameters are measured using active sensors. The constituents, which give the color of the ocean are many and varying depending on time or/and region. Most of these constituents may behave as co-variants or even mask each other. The other parameters measured by satellites are physical characteristics of the water, however ocean color is the derivation from the reflectance to parameters such as chlorophyll, DOM (Dissolved organic matter) or particulate matter (Sathyendranath 2000, Hansell and Carlson 2001). The principle of the derivation is to compare the reflectance of different wave bands for the desired parameter.

The color of the sea varies with place and time. This variability is used to determine various parameters in the sea, such as chlorophyll a concentration. The ocean color concept became an important tool after the ocean color satellites. The possibility and, now the reality of the determination of the chlorophyll a from the space is the driving force of the ocean color studies. These studies are parallel to the bio-optical studies and atmospheric studies.

1.1.2.1. Ocean Color Sensors

The Costal Zone Color Scanner (CZCS) revolutionized ocean color studies. It was launched on the Nimbus-7 satellite, from the Vandenburg Air Force Base, California, and October 24, 1978. The CZCS mission ended in 1986. Unfortunately, the ocean color community, had to wait another ten years to for ocean color data from a satellite. After the CZCS, a number of sensors were launched; some of them

are still in operation. (Table1, Table 2). Beside current active ocean color sensors, some other sensors are also scheduled to be deployed (Table 3).

Table 1: Historical Ocean-Color Sensors (from: URL 3, updated 01-10-2007).

SENSOR	AGENCY	SATELL	OPERATION PERIOD	SWATH (km)	RES (m)	# OF BANDS	SPEC COV. (nm)	ORBIT
CZCS	NASA (USA)	Nimbus7 (USA)	24/10/78 - 22/6/86	1556	825	6	433-12500	Polar
CMODIS	CNSA (China)	SZ-3 (China)	25/3/02 – 15/9/02	-	400	34	403-12500	Polar
COCTS	CNSA (China)	HY-1A (China)	15/5/02 – 1/4/04	1400	1100	10	402-12500	Polar
CZI	CNSA (China)	HY-1A (China)	15/5/02 – 1/4/04	500	250	4	420-890	Polar
GLI	NASDA (Japan)	ADEOSII (Japan)	25/1/03 - 24/10/03	1600	250/1000	36	375-12500	Polar
MOS	DLR (Germany)	IRS P3 (India)	21/3/96 - 31/5/04	200	500	18	408-1600	Polar
OCTS	NASDA (Japan)	ADEOS (Japan)	03/9/96 - 29/6/97	1400	700	12	402-12500	Polar
POLDER	CNES (France)	ADEOS (Japan)	16/9/96 - 29/6/97	2400	6 km	9	443-910	Polar
POLDER-2	CNES (France)	ADEOSII (Japan)	01/2/03 - 24/10/03	2400	6000	9	443-910	Polar

Table 2: Current Ocean-Color Sensors (from: URL 3, updated 01-10-2007).

SENSORS	AGENCY	SATELL	LAUNCH DATE	SWATH (km)	RES (m)	# OF BANDS	SPEC. COV (nm)	ORBIT
MERIS	ESA (Europe)	ENVISAT (Europe)	01/03/02	1150	300/1200	15	412-1050	Polar
MMRS	CONAE (Argentina)	SAC-C (Argentina)	21/11/00	360	175	5	480-1700	Polar
MODIS-Aqua	NASA (USA)	Aqua EOS-PM1	04/05/02	2330	1000	36	405-14385	Polar
MODIS-Terra	NASA (USA)	Terra (USA)	18/12/99	2330	1000	36	405-14385	Polar
OCM	ISRO (India)	IRS-P4 (India)	26/05/99	1420	350	8	402-885	Polar
OSMI	KARI (Korea)	KOMPSAT (Korea)	20/12/99	800	850	6	400-900	Polar
PARASOL	CNES (France)	Myriade Series	18/12/04	2100	6000	9	443-1020	Polar
SeaWiFS	NASA (USA)	Seastar (USA)	01/08/97	2806	1100	8	402-885	Polar

Table 3: Scheduled Ocean-Color Sensors (from: URL 3, updated 01-10-2007).

SENSORS	AGENCY	SATELL	SCHED. LAUNCH	SWATH (km)	RES (m)	# OF BANDS	SPEC. COV (nm)	ORBIT
COCTS	CNSA (China)	HY-1B (Korea)	2007 (April)	1400	1100	10	402 - 12,500	Polar
CZI	CNSA (China)	HY-1B (Korea)	2007 (April)	500	250	4	420 - 890	Polar
GOCI	KARI/ KORDI	COMS-1 (Korea)	2009	2500	500	8	400 - 865	Geost
OCM-II	ISRO (India)	IRS-P7 (India)	2008	1400	1 - 4 km	8	400 - 900	Polar
OLCI	ESA (Europe)	GMES-Sentinel 3 (ESA)	2012	1120	< 300	15	400 - 900	Polar
S-GLI	JAXA (Japan)	GCOM-C (Japan)	2012	1150	250/1000	19	375 - 12,500	Polar
VIIRS	NASA / IPO	NPP	2009	3000	370 / 740	22	402 - 11,800	Polar
VIIRS	NASA / IPO	NPOESS	2012	3000	370 / 740	22	402 - 11,800	Polar

Different than the previous polar orbiting satellites, geostationary satellites are being planned for observing a fixed geographic region. This will allow the observations on daily chlorophyll fluctuations. The first geostationary ocean color satellite is scheduled to be launched in 2009 (Table 3).

Determination of ocean is based on the blue and green light ratio. It is well known that chlorophyll selectively absorbs the blue light and reflects the green. Hence the ratio between the blue and green light is directly related with the chlorophyll concentration in the water. Without exception all ocean color sensors have bands at the blue and green region of the spectrum (O'Reilly et al., 2000). However, this information is not sufficient to determine species diversity, because chlorophyll is the common pigment for all the phytoplankton groups. The detection of a single species by remote sensing is only possible during harmful algal blooms or for unique species such as *Trichodesmium* sp. and *Emilliana sp*. These species have unique properties making it possible to distinguish them by satellite (Brown and Podesda 1997, Lamperta et al., 2002, Subramaniama et al., 2002).

1.2. Connections of Phytoplankton and Optical Properties of Seawater

The most evident bio-optical characteristics of phytoplankton groups is that hey absorb blue light and reflect green light. However every group, even every single species has its own peculiarity, and influences different parts of the light spectrum (Hoepffner and Sathyendranath 1993). It is very important to understand the bio-optical characteristics of the general phytoplankton groups such as dinoflagellate, cyanobacteria or diatoms present in the region and at the time of the investigation.

Estimation of the phytoplankton biomass is the main objective of remote sensing. All ocean color algorithms are based on *chl a*; the phytoplankton biomass is calculated from the *chl a* measurements, or more truly derived from reflectance (O'Reilly et al., 2000). *Chl a* cannot be measured separately by optical measurements (either remote sensing or in-situ), because of the other constituents present in the water column.

Optical studies including remote sensing utilize light from an active source or sunlight. The light reaching an object is either reflected, or absorbed, or both. For chlorophyll measurements, two bands are sufficient. However, it is impossible to analyze any other pigments except chlorophyll with the two bands. Concentration of the Chlorophyll is the ratio between green to blue light in the remote sensing reflectance (O'Reilly et al., 2000).

Investigations on the bio-optics of the phytoplankton groups are very limited. Most of the studies have concentrated on the amount of production by primary producers, or the concentration of the *chl a* (Morel and Maritorena 2001). The present study is a new contribution in the bio-optical context, and the only one carried out in the Turkish seas in this aspect of bio-optic.

The bio-optical studies are not limited with the chlorophyll concentration or primary production measurements. Several of the different studies investigated the relations between phytoplankton and the light, nutrient, other abiotic factors and also the inter-cellular activities/or composition, such as pigment concentration and the behaviors of the pigments under various conditions mentioned above.

Mitchell and Kiefer (1988) measured the *chl a* specific absorption and fluorescence excitation spectra of the pigmented particles retained on filters, under variable light conditions. This study was done on algae cultures of three different species. The absorption, fluorescence efficiency spectra showed spectral shifts associated with increases in the reactive contribution in the accessory pigment bands compared to *Chl a* peak at 435 nm. They conclude that the ratio of the fluorescence signal in the accessory pigments band to the signal at 435 nm may be used as an indicator of photo adaptation for field populations.

Platt and Sathyendranath (1988) established conversion methods including light data and regional chlorophyll distributions, for calculating the production in water column. This method was applied on both regional and global scales. The model is based on the irradiance and the biomass profiles. The study was applied on the three depth zones (shelf, slope and oceanic), where the light and biomass profiles are different from each other.

The main problem with remote sensing data is the effect of atmospheric perturbations. Either models or data (atmospheric optical thickness) are used to eliminate the disturbance. However, for the model development it is essential to know how much radiance is reflected from atmosphere and how much from the ocean surface. Zibordi et al., (1990) using airborne sensors over the Northern Adriatic, on channels as the CZCS, evaluated the chlorophyll and sediment concentration. The objective was to evaluate the fluorescence index, which could be helpful in separating chlorophyll from other materials suspended or dissolved in turbid coastal waters, where the blue/green algorithms fails. Parallel with this procedure in situ measurements at the same time were carried out (atmospheric transmittance, meteorological data, and concentration of suspended and dissolved materials). The measurements were done in different regions, and in different seasons. The measurements taken from the field and over-flight data generally showed good accuracy, even though the relationships applied in computing concentrations are not related to specific seasonal water type, and relationships computing the water-leaving radiance in the reference channel used for atmospheric correction have not been proposed specifically for the Northern Adriatic.

Direct measurement of in vivo phytoplankton are difficult, considering the low concentration of algal cells in nature as compared to cultures and the distribution of photons between phytoplankton and other particulate material such as detritus and

sediments (Hoepffner and Sathyendranah 1992). Hoepffner and Sathyendranah (1992) studied the effect of pigment distribution on absorption spectra. They addressed the question: how important is the intracellular pigment composition in explaining variability in the *Chl a* specific absorption spectra of phytoplankton (at 440 nm). The results show that strong variability in the specific absorption coefficient of phytoplankton is indeed closely related to changes in pigment composition, which in turn is directly associated with the structure of the phytoplankton community.

The number of bands is the limitation for resolving pigment types and concentrations. However, increasing the bands on the sensors puts an extra load and increases the cost. Curve analyses are used to resolve this problem. The analysis resolves the problem by plotting the results from radiometers into a smaller number of peaks which correspond to the components of that curve. The absorption spectrum of the phytoplankton is complex due to the mixtures of the pigments and associated proteins. Identification of these pigments by optical analyses is very difficult. Most of the peaks overlap each other. For resolving these peaks derivative spectral analyses was applied. Gomez et al., (2001) used Gaussian curve fitting or Lorenzian curve fitting according to the shape of the curve. Usually the second derivative of the Lorenzian curves was sufficient for resolving the peaks. However, to resolve all the Gaussian peaks it was necessary to continue up to the fourth derivative.

Nezlin (2000) analyzed several years of CZCS at surface pigment's concentrations in the Black Sea to appraise the seasonal and inter-annual fluctuations of phytoplankton biomass, and to understand the causes of these fluctuations in terms of the Black Sea's general dynamics. The pattern of year-to-year variations seems to correlate with cyclic oscillations of winter air temperature.

Ocean color studies are progressing gradually to the phytoplankton differentiation. The approach for the determination of *Chl a* is nearly solved; however the accuracy is not sufficient for every region. The problem now is to differentiate the species and even predict the blooms. The optical approach to understand the pigment types is to either increase of the number of bands, or curve analyses to eliminate the overlapping effect.

A multi-spectral classification scheme was developed to detect the cyanobacteria *Trichodesmium* spp. by Subramaniama et al., (2002). The criteria for this scheme were established from spectral characteristics derived from (1) SeaWiFS

imagery of a *Trichodesmium* bloom located in the South Atlantic Bight and (2) modeled remote sensing reflectance of *Trichodesmium* and other phytoplankton.

Trichodesmium is well suited for identification from space because its population maximum is usually at 15–30m and it has a combination of specific ultra-structure and biochemical features that result in a relatively unique spectral signature that should be detectable by ocean color sensors (Subramaniama et al., 1999). These features include high backscatter due to the presence of gas vesicles and the absorption and fluorescence of its accessory pigment phycoerythrin.

An optical model developed by Subramaniama et al., (1999) predicted that the magnitude of water-leaving radiances at 412nm for *Trichodesmium* always should be lower than that of other phytoplankton due its higher chlorophyll-specific absorption, while the water-leaving radiance at 555nm always should be higher for *Trichodesmium* than other phytoplankton due to the influence of phycoerythrin fluorescence.

Trichodesmium is an organism with a unique combination of absorption, scattering and fluorescence properties that permit it to be spectrally identified in satellite ocean color imagery. They have demonstrated that it is possible to identify *Trichodesmium* when it is present in sufficient quantities, even in optically complex coastal waters rich in CDOM and sediments. The classification scheme presented here detects only moderate concentrations of *Trichodesmium*.

Bowers et al., (2001) reported that there is a robust relation between the color of the sea, as measured by the 490-nm/570 nm irradiance reflection ratio, and the chlorophyll concentration, valid for algal blooms detection, monitoring and prediction in 367 nm wide ranges of chlorophyll concentrations. Their result confirms the effectiveness of a color ratio as an indicator of chlorophyll concentration in Case 1 waters and implies that ocean color sensors can be used to measure chlorophyll concentrations in these waters with a minimum of calibration information.

Gomez et al., (2001) reported that pigment ratios and differences have traditionally been used in ocean color studies, but they are restricted to a small number of spectral bands. The advent of high-spectral-resolution sensors requires the use of improved methods of study such as the derivative analysis. The derivative method tackles many of the problems of quantitative analysis in a more effective way than ratios and differences by taking into account a larger amount of data, which

stands for more information potentially available. Derivative analysis can be applied to spectra obtained by high spectral-resolution sensors. These sensors can be defined as those having a bandwidth less than 5nm and/or more than 100 spectral bands. Thus, high-spectral-resolution sensors can provide information about smaller spectral variations than can coarse bands. The derivative method is used for minimizing low-frequency background noise and for resolving overlapping spectra (Butler and Hopkins 1970). This method has successfully been applied in remote sensing studies of vegetation (Demetriades- Shah et al., 1990) and suspended solids in water (Chen et al., 1992, Goodin et al., 1993) and can also be applied to marine remote sensing studies. As contemporary optical sensors develop higher spectral resolution, there is potential for a greater wealth of information relating to the absorption capabilities of phytoplankton that could help in identifying the major differences in taxonomic groups.

The results obtained show that derivative of the reflectance spectra of marine waters can be used to identify absorption bands of different pigments present in natural populations of algae. Even though it could be easier to detect pigment signatures from dense algal communities, the results shown here are promising and can be applied to natural seawaters. Therefore, remote sensing of accessory pigments may be successfully applied in other environments (e.g. relatively colored coastal areas and eutrophic lakes or in oceanic waters).

Chlorophyll concentration was estimated using a bio-optical model from natural fluorescence flux over the emission of chlorophyll a, incident irradiance, chlorophyll specific absorption coefficient, and quantum yield of fluorescence in Gerlache and Bransfield Strait waters (Figueroa 2002). Beam attenuation coefficient at 660 nm, which is a good estimator of the particulate material concentration, ranged from 0.85–2.5 m^{-1} in the upper mixed layer. He reported that the highest correlations between chlorophyll and K_d were found in the blue wavelengths, agreeing with previous measurements in Antarctic waters (Mitchell and Holm-Hansen 1991, Stambler et al., 1997); but in contrast to the above mentioned papers, there was also a good correlation in red and green wavelengths. The high correlation between chlorophyll and K_d in green wavelengths in Gerlache is explained by the relatively high proportion of cryptomonads, which absorb in the green region due to the presence of phycoerythrin.

Bricaud et al., (2002), showed that OCTS (Ocean Color and Temperature Scanner) POLDER (Polarization and Directionality of the Earth's Reflectance) SeaWiFS (Sea-viewing Wide Field-of-view Sensor) sensors tend to overestimate chlorophyll concentrations in oligotrophic waters. A ''regional algorithm'' is proposed to reduce this bias.

The bio-optical studies in the Turkish waters are very limited. The light penetration and PAR measurements were first studied by Verdaguer (1995) in the Turkish waters. According to Verdaguer (1995), K_d values found for the Mediterranean changed between 0.015-0.07 m^{-1} and for the Black Sea K_d values changed between 0.06-0.13 m^{-1}. Other studies carried out in the Turkish waters were mostly concentrated on the chlorophyll-a distribution and deep chlorophyll maxima (Yılmaz et al., 1994, Ediger and Yılmaz 1996). Within the bio-optical context, the most recent work was done by Sancak et al., (2005) and they proposed a new regional SeaWifs chlorophyll algorithm, instead of the global algorithm for the Mediterranean waters (Case 1). The algorithm used 412 nm instead of 451 nm, because the reflectance peak shifts from 440-450 to 410-420 nm in the Mediterranean.

The pigment composition of the various communities strongly influences the pattern of absorption in phytoplankton cells, and these properties have been examined for the various regions (Barlow et al., 2002, Mitchell et al., 2002).

Barlow et al., (2002), estimated absorption coefficients from reconstructed spectra utilizing the pigment data. The major role of chlorophyll *a* is to absorb light for photosynthesis, but there is also a range of pigments, such as, chlorophylls *b* and *c* plus a variety of carotenoids, that have a significant function in extending the light-harvesting spectrum in the phytoplankton, thus ensuring optimal absorption efficiencies (Kirk, 1994). Other carotenoids, however, serve to protect microalgal cells against the effects of high irradiances, which may damage the photosynthetic apparatus, and these pigments may be termed photoprotective carotenoids (PPC) (Kirk, 1994).

The distribution of accessory pigments provided information concerning the components of the phytoplankton community. Fucoxanthin concentrations (diatoms) were most prominent on the European shelf, the NW African upwelling zone and in the Falklands region, while peridinin (dinoflagellates) was only significant at 45–

50N. A summation of 19-hexanoyloxyfucoxanthin, 19- butanoyloxyfucoxanthin, alloxanthin and chlorophyll b was a useful combined signature for nanoflagellates.

Chlorophyll only accounts for about 50% of the total pigment in most marine ecosystems and absorb light in the blue part of the spectrum between 400 and 470 nm with the secondary absorption being around 670 nm. Chlorophylls b and c plus the carotenoids all absorb light across the blue–green region of the spectrum (400–550 nm), which overlaps the chlorophyll a absorption. Interpretation of ocean color data is, therefore, quite complex, because all pigments need to be considered instead of chlorophyll a alone.

1.3. Aim of the study

The bio-optical characteristics of the oceans and the regional seas are very important. Phytoplankton groups are the main bio-optical constituents in the seawater. Every group, even every single species have their own peculiarity, thus influencing different parts of the spectrum. Therefore, it is very important to understand the bio-optical characteristics of the general groups in time and space.

The aim of the thesis is to determine the contribution of the different parameters on the bio-optical characteristics of the Turkish seas. Overall goal of the research was to understand the bio-optical properties of Turkish seas and classification of the sub-regions within Turkish seas. Linking the phytoplanktonic activities, including particle absorption, CDOM absorption and in-situ irradiance are the objectives of this study. A realization of these objectives requires multidisciplinary data. Diversity of the phytoplankton species adds complexity to the data. For an understanding of field conditions general group dependent characteristics of phytoplankton species, bio-optical properties of the water have to be known. In this connection, a large number of parameters have been measured to find out the phytoplankton contribution to the bio-optics. For this purpose, reflectance particular to the phytoplankton groups is determined. However the process is not simple because of other constituents in the water, which perturb the reflectance. Therefore, these parameters need to be measured parallel to the phytoplankton measurements (HPLC measurements and satellite data).

The further step in the bio-optics applied here is to understand the optical properties of the phytoplankton groups and their variability between the regions. Certain groups, such as *Trichodesmium* can be easily detected by their unique properties, however not all species have clear identifying properties. Phytoplankton groups have different pigment compositions. These biomarkers can be extracted from absorption spectra (Devred et al., 2006). Understanding and detecting the groups at workable precision level will allow building more reliable ecosystem and primary production models, since every species have their own rates for biological activities.

2. MATERIAL AND METHODS

2.1 Study Area.

The study area covers nearly all the Turkish seas but is concentrated on the North Eastern Mediterranean (Figure 3, 4). Sampling stations were chosen from optically different regions. However, the majority of the stations were located in the North Eastern Mediterranean (including the İskenderun Bay, Figure 4). This region is not well understood in terms of bio-optics. Almost no bio-optical studies have been done in this region except that by Sancak et al., (2005). The basin includes relatively high and low chlorophyll regions and also shelf and offshore regions. The North Eastern Mediterranean is the largest basin in eastern Mediterranean, and receives a relatively high amount of fresh water. Especially the İskenderun Bay and the Mersin Bay are two productive regions (Figure 5). The shelf width in this region is relatively larger than other parts of the Basin (Figure 6).
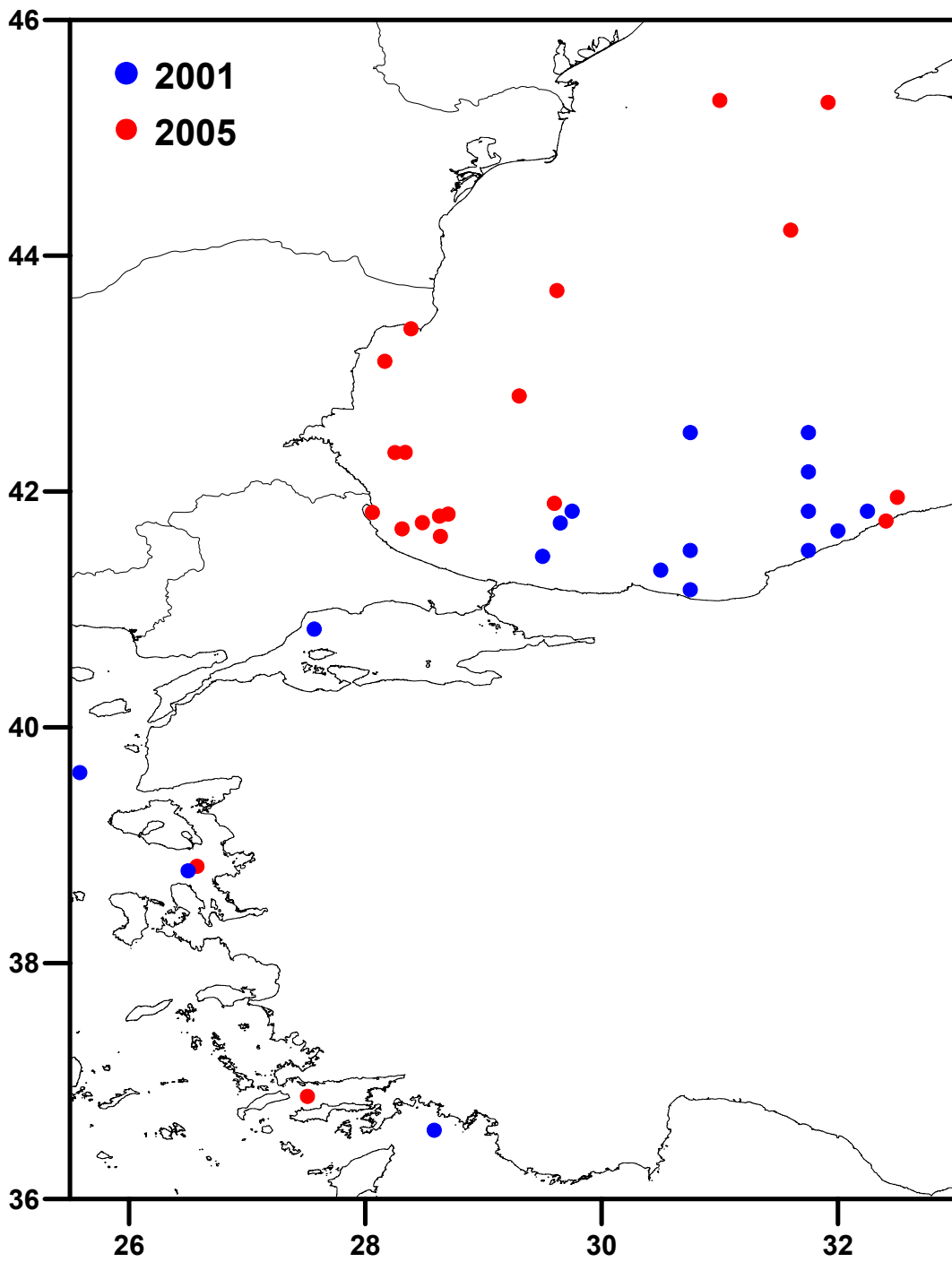
Figure 3: Locations of sampling stations in May and June 2001, March 2005 and September-October 2005.
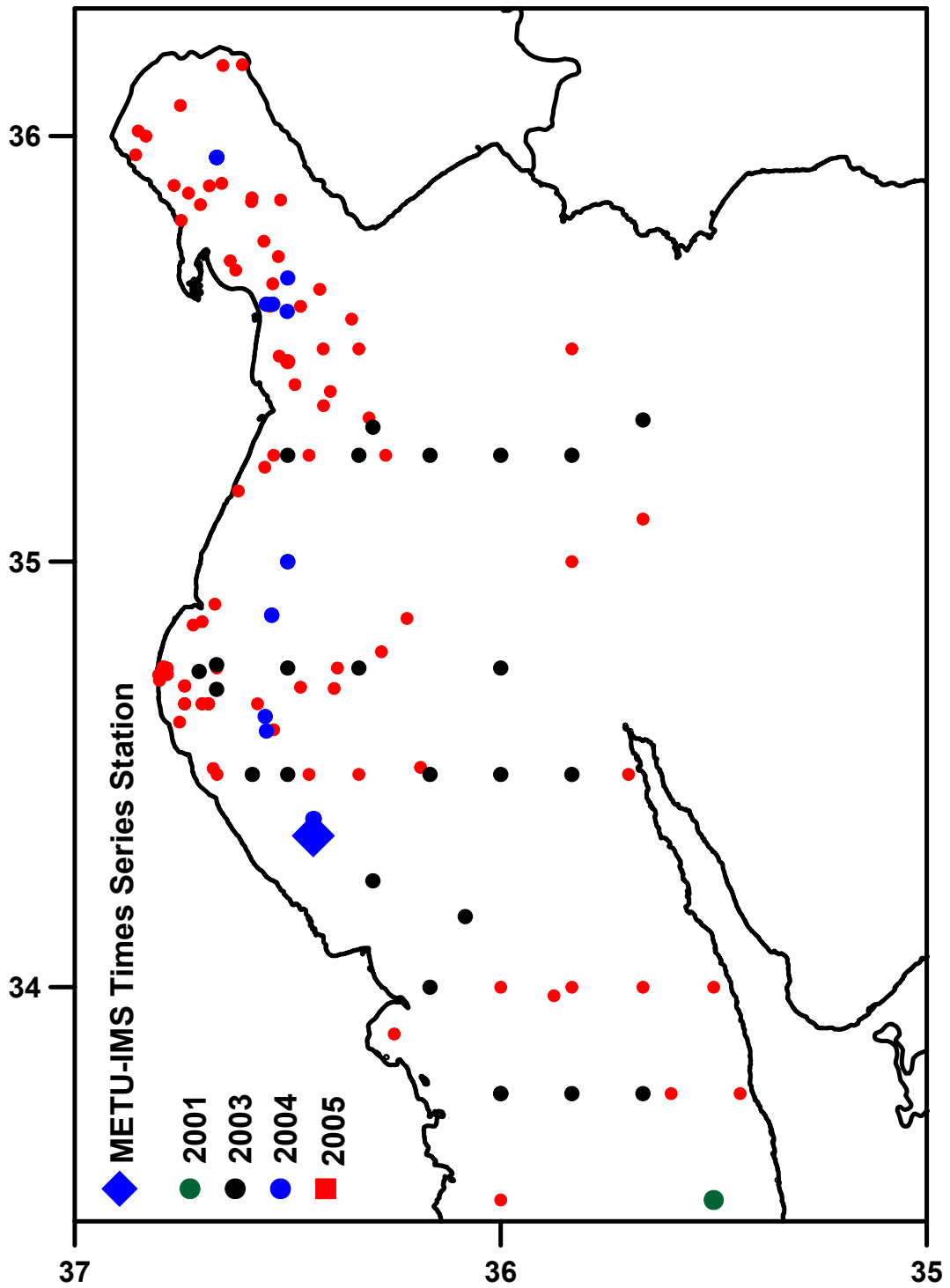
Figure 4: Locations of sampling stations in July 2001, December 2003, May-December 2004 and February-December 2005.
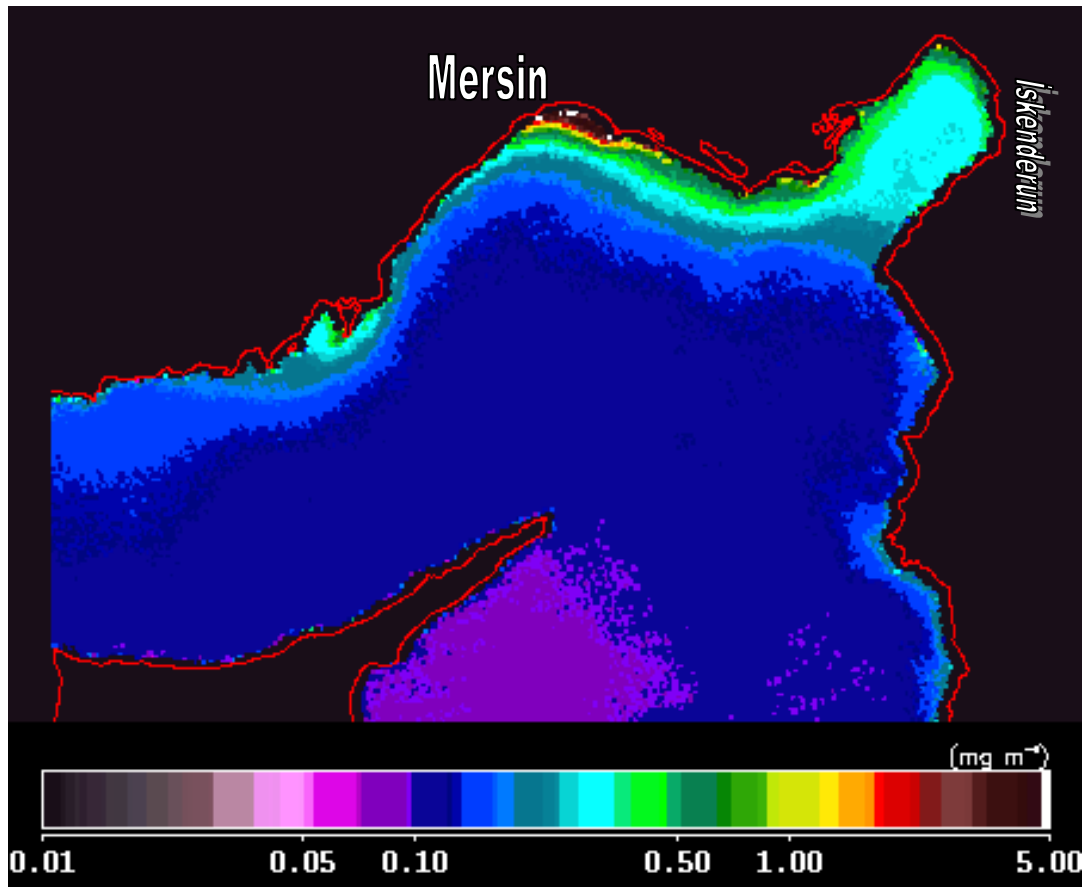
Figure 5: Mean surface chlorophyll-a concentration (mg m^{-3}) in North Eastern Mediterranean in year 2005, derived from MODIS Aqua data.
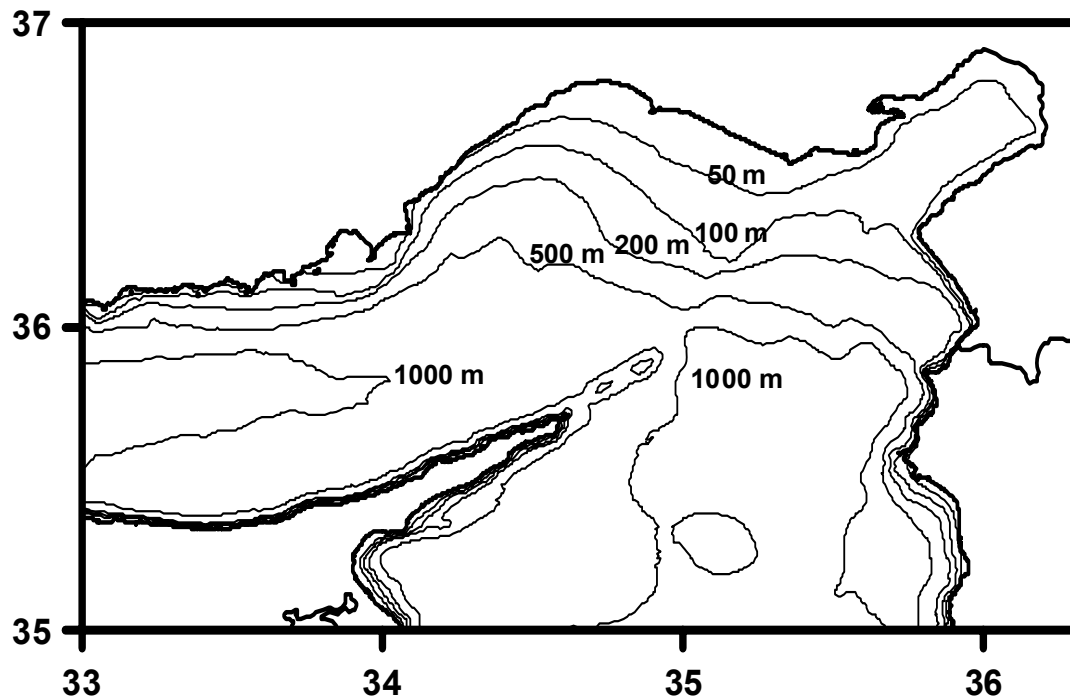
Figure 6: North Eastern Mediterranean bathymetry map (Ediger et al., 2005).

2.2 Field Sampling and Measurements

The study consists of four parts:

1. Field sampling and measurements
2. Laboratory work
3. Analysis
4. Satellite data correlation.

Samples were collected from various cruises between 2001 and 2005. However, most of the data were collected during year 2005 (Table 4. See also % distribution on the following pi chart further below).

Table 4: Dates names and locations of the stations during the study period. MED=METU-IMS time series Station, ISK=İskenderun.

Date	Station	Lat	Lon	Date	Station	Lat	Lon
24.05.2001	M30M45	42.500	30.750	26.09.2004	G40S57	36.666	35.950
25.05.2001	M10N45	42.100	31.750	27.09.2004	METU-IMS	36.441	34.396
25.05.2001	M30N45	42.500	31.750	02.10.2004	MERSIN	36.550	34.602
26.05.2001	L50N45	41.833	31.750	03.10.2004	G40S57	36.666	35.950
27.05.2001	L10M45	41.167	30.750	04.11.2004	METU-IMS	36.438	34.396
27.05.2001	L30M45	41.500	30.750	28.12.2004	METU-IMS	36.438	34.356
17.06.2001	L27L30	41.500	31.750	10.02.2005	MED02	36.440	34.356
17.06.2001	L30N45	41.450	29.500	11.02.2005	Karataş	36.500	35.470
18.06.2001	L44L39	41.733	29.650	18.02.2005	Karaduvar	36.791	34.750
24.06.2001	K50J34	40.833	27.567	07.03.2005	K2	41.900	29.600
25.06.2001	J37H35	39.616	25.583	09.03.2005	Çandarlı	38.821	26.575
26.06.2001	I47I30	38.783	26.500	10.03.2005	Gökova	36.870	27.510
28.06.2001	G35K35	36.583	28.583	25.03.2005	MED03	36.440	34.356
03.07.2001	F30Q30	35.500	33.500	21.04.2005	MED04	36.440	34.356
20.12.2003	F40Q45	35.666	33.750	03.05.2005	MED05	36.440	34.356
20.12.2003	F50Q45	35.833	33.750	10.05.2005	MEDPOL18	36.783	34.735
20.12.2003	G00Q45	36.000	33.750	10.05.2005	MEDPOL15	36.701	34.666
20.12.2003	G00R30	36.000	34.500	13.05.2005	MED05	36.440	34.356
21.12.2003	F50R30	35.833	33.750	20.05.2005	F30R00	35.500	34.000
21.12.2003	G00R45	36.000	33.750	20.05.2005	F35Q45	35.600	33.750
22.12.2003	G18S19	36.300	35.316	20.05.2005	F40R00	35.666	34.000
22.12.2003	G20S15	36.333	35.250	20.05.2005	F26.50Q45	35.438	33.750
22.12.2003	G30R45	36.500	34.750	20.05.2005	F50R00	35.833	34.000
22.12.2003	G30S00	36.500	35.000	20.05.2005	G00Q45	36.000	33.750
22.12.2003	G30S15	36.500	35.250	20.05.2005	G00R00	36.000	34.000
27.12.2003	G30R30	36.500	34.500	20.05.2005	G00R45	36.000	34.750
27.12.2003	G35R30	36.583	34.500	21.05.2005	G00Q30	36.000	33.500
28.12.2003	F40S20	35.666	35.333	21.05.2005	G00R30	36.000	34.500
28.12.2003	F50S15	35.833	35.250	21.05.2005	G10R30	36.166	34.500
28.12.2003	G00Q45	36.000	33.750	21.05.2005	G20R30	36.333	34.500
28.12.2003	G00S15	36.000	35.250	21.05.2005	G27R30	36.450	34.500
28.12.2003	G10S15	36.166	35.250	21.05.2005	G30R30	36.500	34.500
28.12.2003	G20R45	36.333	34.750	22.05.2005	F50S30	35.833	35.500
29.12.2003	G05R10	36.083	34.166	22.05.2005	F50S00	35.833	35.000
29.12.2003	G10R00	36.166	34.000	22.05.2005	F50S15	35.833	35.250
29.12.2003	G10R30	36.166	34.500	23.05.2005	G20S30	36.333	35.500
29.12.2003	G18R15	36.300	34.250	23.05.2005	G25.8S38.7	36.425	35.640
16.03.2004	METU-IMS	36.438	34.396	23.05.2005	G28.3S36	36.470	35.600
08.07.2004	ISK.BAY	35.535	35.605	23.05.2005	G31S33.30	36.517	35.850
10.07.2004	FRONT	36.501	35.588	23.05.2005	G32.30S39.30	36.535	35.653
19.07.2004	METU-IMS	36.438	34.396	23.05.2005	G33.6S45.3	36.556	35.753
22.07.2004	ISK.BAY	36.550	35.605	23.05.2005	G35.10S51.50	36.584	35.855
24.07.2004	MERSIN	36.537	34.874	23.05.2005	ISK.BAY	36.606	36.167
12.08.2004	ISK.BAY	36.500	35.666	24.05.2005	G18.9S20.45	36.309	35.337
14.08.2004	G40S57	36.666	35.950	24.05.2005	G24S24	36.400	35.400
15.08.2004	MERSIN	36.553	34.636	24.05.2005	G25S30	36.417	35.500
26.08.2004	G40S57	36.666	35.950	24.05.2005	G27S15	36.450	35.250
27.08.2004	G30S00	36.500	35.000	24.05.2005	G30S00	36.500	35.000
14.09.2004	G40S57	36.666	35.950	24.05.2005	G40R45	36.667	34.750
16.09.2004	MERSIN	36.537	34.874	26.05.2005	MP15A	36.686	34.666
18.09.2004	G40S57	36.666	35.950	08.06.2005	G17R47.5	36.280	34.788

Table 4 Continued.

Date	Station	Lat	Lon	Date	Station	Lat	Lon
08.06.2005	G23R45	36.383	34.750	06.08.2005	G42.12R51.93	36.701	34.859
08.06.2005	G28.5R42.5	36.470	34.705	06.08.2005	G31.66S46.07	36.522	35.717
08.06.2005	G34.5R40	36.571	34.666	06.08.2005	G38.40S53.60	36.655	35.889
08.06.2005	G40R30	36.666	34.500	06.08.2005	G45.16T04.91	36.752	36.072
09.06.2005	F40S06	35.666	35.100	06.09.2005	MP13	36.742	34.708
09.06.2005	G16.5S15	36.270	35.250	06.09.2005	MP14	36.742	34.666
09.06.2005	G32S15	36.533	35.250	07.09.2005	MED09	36.440	34.356
09.06.2005	G40.5R54	36.671	34.900	07.09.2005	MP3	36.754	34.623
10.06.2005	G29S25	36.483	35.416	29.09.2005	P1	43.380	28.386
10.06.2005	G32.8S35.95	36.542	35.600	29.09.2005	ST4	43.105	28.165
10.06.2005	G38.2S42.7	36.635	35.707	30.09.2005	P4	42.331	28.251
10.06.2005	G39.2T10	36.652	36.166	30.09.2005	P5	42.332	28.337
10.06.2005	G44S52	36.733	35.866	30.09.2005	P7	41.822	28.059
10.06.2005	G50T00	36.833	36.000	01.10.2005	P2	41.683	28.311
11.06.2005	F42R30	35.700	34.500	01.10.2005	P3	41.736	28.483
12.06.2005	MED06	36.440	34.356	01.10.2005	P4	41.791	28.628
01.07.2005	MP13	36.742	34.708	07.10.2005	1	41.750	32.407
01.07.2005	MP14	36.742	34.666	08.10.2005	3	41.951	32.503
01.07.2005	MP15	36.701	34.666	10.10.2005	18	45.300	31.917
01.07.2005	MP15A	36.686	34.666	11.10.2005	27	45.317	31.000
01.07.2005	MP16	36.801	34.721	12.10.2005	30	44.217	31.600
01.07.2005	MP17	36.803	34.734	13.10.2005	39	43.704	29.621
01.07.2005	MP18	36.783	34.735	14.10.2005	52	42.810	29.302
02.07.2005	MED07	36.440	34.356	14.10.2005	56X	41.808	28.700
02.08.2005	MED08	36.440	34.356	14.10.2005	57X	41.620	28.635
02.08.2005	G11.50R31	36.188	34.517	26.10.2005	MP13	36.742	34.708
03.08.2005	G32R36.50	36.533	34.605	26.10.2005	MP14	36.742	34.666
03.08.2005	G13.50R52	36.220	34.867	26.10.2005	MP15	36.701	34.666
04.08.2005	G37S01	36.616	35.166	26.10.2005	MP15A	36.686	34.666
04.08.2005	G33.41S13.61	36.554	35.222	27.10.2005	MED10	36.440	34.356
04.0820.05	G25S22	36.416	35.367	16.11.2005	MP13	36.742	34.708
04.08.2005	G31.50S29	36.520	35.483	16.11.2005	MP14	36.742	34.666
04.08.2005	G21S34.50	36.350	35.570	16.11.2005	MP15	36.701	34.666
04.08.2005	G42.05S50.6	36.705	35.839	16.11.2005	MP15A	36.686	34.666
05.08.2005	G37.66S41.26	36.622	35.685	18.11.2005	IST11	36.675	34.514
05.08.2005	G45S48.20	36.750	35.802	22.11.2005	IST24	36.585	35.846
05.0820.05	G41.38S53.08	36.684	35.883	23.11.2005	IST9	36.391	34.702
05.08.2005	g46.07s53.04	36.767	35.884	24.11.2005	IST28	36.250	33.890
05.08.2005	G51.70S57.60	36.857	35.956	24.11.2005	IST33	35.875	33.980
05.08.2005	G51.16T0012	36.851	36.012	27.11.2005	MED11	36.440	34.356
06.08.2005	G47R45	36.783	34.750	29.12.2005	MED12	36.440	34.356
06.08.2005	G43.97R51.07	36.722	34.851				
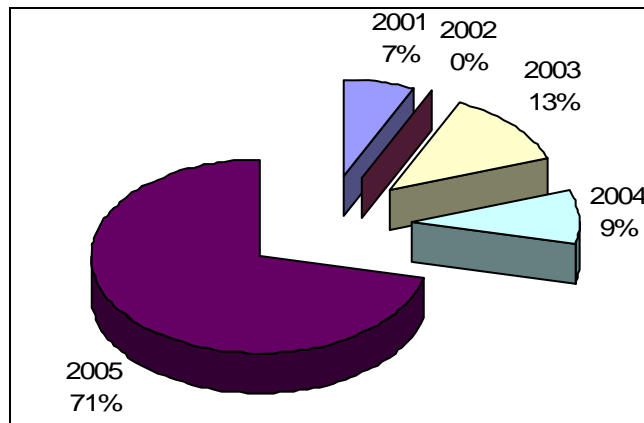
Samples were collected from the Black Sea, the Sea of Marmara, the Aegean Sea, and the Mediterranean Sea. Seawater samples were taken for particle absorption, Chlorophyll-*a,* and HPLC-derived pigment, colored dissolved organic matter (CDOM). During the cruise, samples were either kept in refrigerator or in liquid nitrogen. All the samples were transferred to the liquid nitrogen at the end of the cruise for further storage. Samples were not kept in refrigerator more than one month. Usually, storage period did not exceed a week.

2.2.1 Field Sampling

Field samples were taken on board R/V Bilim, R/V Lamas, R/V Erdemli and a few samples were taken by artisanal fishermen boats. Samples were collected (usually) between 10:00 and 15:00 o'clock, when the sun position is relatively perpendicular, ensuring the sampling area received sunlight with minimum solar zenith angle. Water samples were taken by either 5 lt or 30 lt Niskin bottles. During the warm seasons, water samples were immediately filtered or stored in dark bottles in refrigerator, until filtration. In winter or in cooler periods the samples were kept in shadow in dark bottles, until filtration. Field measurements were conducted according to the ocean color protocols and key manuals on pigment measurement (Jeffrey et al., 1997, Mueller and Forgain 2002, Mueller et al., 2003, Mueller,

Fargion and McClain. 2004) (Table 5). Sampling and measuring were arranged according to the time arrived at the station. The sequence of the sampling and measurements were arranged to light conditions. Usually the time of the minimum solar zenith angle period was utilized for light measurements, thus eliminating both shadows and decreasing scattering.

Table 5: In-situ measurements needed for calibration/validation of satellite ocean color. Table derived from; Mueller and Forgain (2002), Mueller et al., (2003), Mueller, Fargion and McClain (2004).

Required Measurements	
Cruise Data Acquisition	**Instrumentation System**
Downwelled Irradiance	Licor UW 1800
Upwelled Radiance	
Upwelled Irradiance	Licor UW 1800
Incident Irradiance	
Aerosol Optical Depth	Data taken from NOAA
Phytoplankton Pigment Concentration	HPLC
Chlorophyll-a and Phaeopigment Conc	Fluorometer
Latitude and Longitude	GPS
Wind Speed and Direction	From log book of the ship
Surface Barometric Pressure	From log book of the ship
Air Temp/Relative Humidity	From log book of the ship
Cloud Cover	From log book of the ship
Secchi Depth	Secchi disk
Highly Desired Measurements	
Cruise Data Acquisition	**Instrumentation System**
Beam Attenuation	Calculated from E_d
Beam Attenuation profiles	Wetlabs C-Star
Particle Absorption	Diode Array Spectrophotometer
Dissolved Material Absorption (CDOM)	Diode Array Spectrophotometer
Non-Pigment Particle Absorption	Diode Array Spectrophotometer
Phytoplankton Absorption	Diode Array Spectrophotometer
Fluorometric Profiles	Chelsea
Whitecap Condition	Eye Check
Conductivity and Temperature Profiles	SeaBird (CTD)
Conductivity Temperature Along track	Falmouth TSG

2.2.2. In-situ Measurements

In-situ measurements were carried out in two ways. One is related with the CTD casting and the second is related with light measurements, in other words with the upward and downward irradiance measurements detailed below. In these sense the bio-optical measurements were carried out in the Black Sea, Sea of Marmara, Aegean Sea and the Mediterranean Sea. However, most of the data have been collected from the North Eastern Mediterranean. Satellite data obtained additionally corresponds to the sampling dates. Those are transferred to monthly-binned images for all sampling period, in which more than 100 stations have been visited between 2001 and 2005, but most of the data have been collected in year 2005 (Figure 3, 4).

2.2.2.1. CTD measurements

At each station, temperature and salinity profiles were recorded using a Seabird (Model SBE 19 plus) sensor mounted on the frame of sampling pump. A software program calculated the water density (sigma-theta σ_t) using temperature and salinity measured. The CTD probe was lowered at a rate of 0.3-0.8 m/sec and it records at a rate of 24 Hz. The signals were formatted and transferred to a PC.

CTD casts were taken at all stations for the determination of the general hydrographic conditions. Usually, temperature, salinity, density, relative fluorescence, PAR (photosynthetically active radiation), and oxygen concentration were measured.

2.2.2.2. Light Measurements (Upward and Downward Irradiance Measurements)

An underwater spectroradiometer, Li-Cor Model LI-1800 was used to measure the light intensity with a 180° viewing cosine receptor in the 350-850 nm wavelength range, at 1 nm resolution. Both upward and downward light intensities were measured. As mentioned before, light measurements were done around 11:00-15:00 (local time). It was aimed to carry out the light measurements, under calm sea and clear sky conditions; however it was not always possible to catch such ideal conditions during the cruises. Instead of waiting for the ideal conditions, light measurements were carried out even at the limited conditions. Light measurements, were done from the surface (means 0-1 m depth) to 50-70 mt depths, at discrete depths.

Downward and upward spectral irradiances, $E_d(\lambda,z)$ and $E_u(\lambda,z)$ respectively, expressed as W m^{-2} nm^{-1}, were measured at discrete depths. Downward spectral irradiances were measured with the collector facing upward and receiving the downward flux, the and upward spectral irradiances after having turned the instrument upside down in such a way that it receives the upward flux. The data were recorded every 2 nm, in favorable sea and sky conditions at around noontime.

Spectral distribution of the downward and upward irradiances in the water column was carried out in 2001, 2003, 2004 and 2005, in the Black Sea, the Aegean Sea and the Mediterranean Sea. Majority of the measurements carried out in the North Eastern Mediterranean. The up-welled and down-welled irradiances were measured between the 300 nm (or 350 nm)-850 nm in all stations, with 1 or 2 nm resolution. Irradiance reflectance spectra were calculated as a ratio of up-welled to down-welled irradiances measured at each depth. Spectral distribution of the downward diffuse attenuation coefficient, was calculated through water column between the depths of downward irradiance measurements by

$$K(\lambda)=(-1/(z_2-z_1))\ln(E(z_2,\lambda)/E(z_1,\lambda),$$

Where λ is the wavelength, z_1 and z_2 depths, E is the downward irradiance.

The downward diffusivity (vertical attenuation coefficient or absorption coefficient) is the apparent property of seawater. It depends on the concentration and composition of the matter in the seawater (Kirk 1994, Mobley 1994).

Light measurements carried out between May and June 2001 covered the area from the Black Sea to the Mediterranean (Figure 3). Comparisons of the spectral irradiance profiles from the different basins were done using data collected in relatively short time. In December 2003, irradiance measurements were carried out at 5 stations in the North Eastern Mediterranean (Figure 4). Majority of the irradiance measurements were done in 2005. However, these stations were concentrated in North Eastern Mediterranean and only one station from Back Sea and two from Aegean Sea (Figure 3, 4).

2.3. Laboratory Work

2.3.1. Spectrofluorometric Method of Chlorophyll-a

Seawater samples (0.5 to 3 liters) were collected from each depth for chlorophyll-a analysis. Seawater was filtered through Whatman GF/F filters (0.7μm pore size and 47 mm diameter) at a vacuum of less than 0.5 atm. Samples were stored in liquid nitrogen until analyzed. The filters were extracted with 5 ml 90% acetone solution by using ultrasonicator (60 Hz for 1 min). Following the extraction, the volume of the extract was made up to exactly 10 ml. The samples were allowed to extract overnight (about 12 hours) in the dark at 4 °C (in the refrigerator). Samples were centrifuged at 3500 rpm for 10 min to remove cellular debris.

Fluorometric analysis was performed using a Hitachi F-3000 type fluorescence spectrophotometer. Prior to measurement the fluorometer was set to zero with 90% acetone, then fluorescence intensity of 2 ml extract was measured before and after acidification at 420 nm excitation and 669 nm emission wavelength (Strickland and Parsons, 1972). Chlorophyll-a and phaeopigment concentration was calculated by following formula;

$$\text{Chl-a } (\mu g L^{-1}) = F_m \times (F_o - F_a) \times V_{ext} \times K_s / (F_m - 1) \times V_{flt}$$

$$\text{Phaeo } (\mu g L^{-1}) = F_m \times [(F_m \times F_a) - F_o] \times V_{ext} \times K_s / (F_m - 1) \times V_{flt}$$

Where;

Fm, acidification coefficient (F_o/F_a) for pure chl-a (usually 2.2)

F_o, reading before acidification

F_a, reading after acidification

K_s, door factor from calibration calculations (1/slope)

V^{ext}, extraction volume (ml)

V_{flt}, filtration volume (ml)

Chlorophyll-a standard obtained from Sigma was used to quantify the sample fluorescence intensities and the concentration of the standard stock solution was determined spectrophotometrically. A minimum of five dilutions was prepared from this standard and emission and excitation wavelengths were adjusted using the same standard. Fluorometer readings were recorded before and after acidification with 2 drops of 1N HCl. The detection limit was about 0.01 µg/l. The precision was better than 7% (Relative Standard Deviation, RSD).

2.3.2. Pigment Measurements

The HPLC method was applied to the determination of the pigment composition of the samples. Samples were collected mostly from the surface, but there were some profile stations also. Including the previous studies nearly 200 samples were utilized. Depending on the suspended material concentration in the

sample, 1 to 6 liters of water was filtered over 25 Ø mm GF/F filter. Filtration procedure was stopped after visual check of filters or if a decrease in filtration rate was observed. Filters were kept according to the procedure mentioned below.

Extraction was carried out with 90% HPLC grade acetone by using sonication (60Hz for 1min) and centrifugation (3500 rpm for 10 min). Extracted samples were stored overnight at 4^oC. 500 µl of the extract was filtered through 0.2 µm pore size Millipore filters and mixed with 500 µl 1M ammonium acetate ion pairing solution. The buffered extracts were injected (100µl) to the Thermo Hypersil MOS-2 C8 column (150 x 4.6 mm, 3µm particle size, 120Å pore size and 6.5% carbon loading) using a Agilent HPLC system (Quaterner pump, manual injector) having 100µl loop.

Pigments were separated using a binary mobile phase system with linear gradient. Mobile phases used in the gradient elution consisted of primary eluant (A) consisting of methanol and 1M ammonium acetate (80:20 v/v), and a secondary eluant (B) consisting of 100 % methanol. Pigment were separated at a flow rate of 1 ml min^{-1} by a linear gradient programmed as follows (minutes; % solvent A; % solvent B): (0;75;25), (1;50;50), (20;30;70), (25;0;100), (32;0;100). The column was then reconditioned to original conditions over a further 7 min (Barlow et al., 1997). Ammonium acetate was used as an ion pairing reagent, and it is recommended that it should be present in both the sample and mobile phase to improve pigment separation and suppressed dissociation of isolated compounds (Mantoura and Llewellyn 1983). Pigments were detected by absorbance at 440 nm using an Agilent variable wavelength detector. Data collection and integration were performed using a PC-based Chemstation chromatography package. Pigment identity was determined by comprising with authentic pigments: chlorophyll *a* was obtained from Sigma Chemical Co., chlorophyll *c*2, chlorophyll *c*3, peridinin, 19-butanoyloxyfucoxanthin, fucoxanthin, 19-hexanoyloxyfucoxanthin, diadinoxanthin, alloxanthin, lutein, zeaxanthin, divinyl chlorophyll-a and β-carotene from VKI, Denmark. Concentrations of pigments were calculated according the 'external standard' equation (Jeffrey et al., 1997).

$$C_p = A_p \text{ x } V_{ext} \text{ x } 10 \text{ / B x } V_{flt} \text{ x } V_{inj} \text{ x } 1000 \text{ x } Rf$$

Where;

C_p (μg L^{-1}); concentration of a particular pigment

A_p (mAU*s); peak area of the eluting pigment

Rf (ng mAU^{-1}); the slope of the calibration curve (ng column^{-1})

V_{filt} (l); the volume of filtered seawater

V_{ext} (ml); the solvent used for the extraction;

V_{inj} (μl); the solvent injected to the chromatographic system and

B; the buffer dilution factor

2.3.3. Particle Absorption

Particle absorption samples were collected from the surface part of the water column and filtered for approximately the same amount as HPLC samples through 25 Ø mm GF/F filter, and were kept in liquid nitrogen or freezer. Blanks were taken beside the samples. Blanks were kept under the same conditions as the samples. Preparation of the blanks was carried out by filtering the pre-filtered seawater through 0.2μ pore size nucleopore filters, over the 25 Ø mm GF/F filter. Filtered seawater (from 0.2μ pore size nucleopore filter) was kept for nearly the same time as the samples filtration period on the blank filter.

Particle absorption measurements were performed by using the single beam Helios spectrophotometer. After defrosting, the samples (usually defrosting 3 samples in each set) were put on the quartz window, which is placed on a special holder perpendicular to the light beam. After placing the sample, scanning procedure was applied from 320 to 850 nm at 1 nm interval and the data is kept in the text file on a PC. The blank is subtracted manually after the end of the measurements.

The particle absorption measurements give 3 parameters:

1. Total absorption
2. Detritus absorption
3. Phytoplankton absorption

After getting the total absorption, the filters were put on the filtration towers again and treated by 3 series of 15-30 ml 100% methanol for 10-15 minutes each. The extracted samples were measured again to obtain the detritus absorption or de-pigmented fraction of the total particles. Phytoplankton absorption was obtained by subtracting detritus absorption from total absorption (Kishino et al., 1985, and Kishino 1995).

The absorption coefficients of the particles are not the same in the liquid and on the filter. The particles are concentrated on the filter, which artificially amplifies the optical density (OD = Absorption value reading by spectrophotometer) measured by spectrophotometer. This amplification is called path length amplification (β) and should be corrected. The samples were corrected according to their pigment compositions. The absorption by different phytoplankton species and different sizes has different amplification factors (More et al., 1995, Mitchell et al., 2000, 2002). However, most of the experiments were carried out on various mix species. Field samples showed more or less the same results. The difference between the results is not greater then 20% (Mitchell et al., 2000). However, samples from oligotrophic waters, such as the Saragossa Sea, where the phytoplankton is dominated by small sized groups (like Prochloroccocus), the amplification factor differs by nearly 50% (Moore et al 1995, Allali et al., 1997). Therefore, different correction factors should be applied. Ancillary data such as size fraction, HPLC or flow-cytometry and HPLC pigments would be useful to evaluate the ideal correction factors (Mitchell et al., 2000). In this study, HPLC measurements are utilized for choosing the amplification factor.

Pathlength amplification corrections were made according to laboratory investigations, in which the suspended and filtered samples were compared. The relation between the filtered and suspension samples can be expressed by quadratic or power function (Hoepffner and Sathyendranath 1993, Suzuki et al., 1998, Mitchell et al., 2000, 2003).

According to the Mitchell et al., (2000) the path length amplification (β) equations are:

$$\beta = [C_1 + C_2[OD_f(\lambda) - OD_{null}(\lambda)]]^{-1} \dots\dots\dots\dots\dots\dots\dots\dots\dots\dots\dots\dots\dots\dots 1$$
or
$$\beta = [C_0 + C_1[OD_f(\lambda) - OD_{null}(\lambda)]^{C_2} \dots\dots\dots\dots\dots\dots\dots\dots\dots\dots\dots\dots\dots\dots 2$$

Where C_0, C_1, C_2 are the constants, $OD_f(\lambda)$ is optical density of the filtered sample, $OD_{null}(\lambda)$ is the null absorption value which is the OD at 750nm for this study.

The equations (1 or 2) can be expressed simply as:
$$OD_s = C_1 \, OD_f(\lambda) + C_2 \, OD_f(\lambda)^2 \dots\dots\dots\dots\dots\dots\dots\dots\dots\dots\dots\dots\dots\dots\dots 3$$

According to the equation 3, the absorption coefficients in m^{-1} calculated as:
$$a_p = [2.303 \times [C_1 \, OD_f(\lambda) + C_2 \, OD_f(\lambda)^2] \times A] / V \dots\dots\dots\dots\dots\dots\dots\dots\dots\dots\dots 4$$

* $OD_f(\lambda)$ is getting after subtracting the null and blank values.

Where 2.303 is a constant used in the ocean optics protocols to covert the dimensionless OD to base-e representation of absorbance. A is the clearance area of the filter in m^2 and V is the volume of the water filtered in m^3.

The constants (C_1, and C_2) used in this study are taken from Cleveland and Weidemann (1993) for mix compositions and the constants from Moore et al., (1995) used for the *Prochlorococcus and Synechococcus* dominated waters. HPLC measurements have been used to determine the phytoplankton composition of the sample. The equations with these constants for the mix composition and *Prochlorococcus and Synechococcus* dominated waters are:

Mix composition:
$$a_p = [2.303 \times [0.378 \, OD_f(\lambda) + 0.523 \, OD_f(\lambda)^2] \times 0.00038] / V$$

Prochlorococcus and Synechococcus dominated

$$a_p = [2.303 \times [0.291 \, OD_f(\lambda) + 0.051 \, OD_f(\lambda)^2] \times 0.00038] / V$$

2.3.4. Colored Dissolved Organic Matter (CDOM)

CDOM measurements were usually carried out on board R/V Bilim. However in some cases, especially during the daily cruises the samples were kept in the refrigerator until analyzed. According to the accepted concept dissolved matter is the fraction of the matter that can pass through the 0.45-1μm-pore size filter, where the particulate matter cannot pass (Hedges 2002). However, more accurate measurements can be achieved by using the 0.2μm pore size filters (Mitchell et al., 2002).

The Helios spectrophotometer was used to measure the spectral absorption by CDOM. For this purpose, 10 cm path length quartz windowed cell is used. Water samples taken from the surface were immediately transferred to the refrigerator in a dark bottle. At the end of the day all collected samples were filtered through the 0.2 μm pore size filters and the filtered water was poured to the cell for measurement of the absorption spectra. Setting of the spectrophotometer was the same as the particle absorption settings. Reagent blank was measured by high quality Milli-Q (Ultra pure Water Purification Systems) water. The blanks were subtracted from the samples afterwards.

All the instruments used in this experiment, were cleaned with acid and organic solvent methanol or acetone, and then rinsed with the Milli-Q water. The filtration flask rinsed with the first filtered seawater, and then the second was transferred to the cell. The cell was rinsed a few times with sample and then measured by the spectrophotometer. This procedure minimizes the contamination of the samples from each other.

For converting the CDOM OD (Optical Density) to m^{-1} unit, the following equation of Mitchell et al., (2002) is used.

$$a_g(\lambda) = 2.303/l \times [OD_s(\lambda) - OD_{bs}(\lambda)] - [OD_{null}]]$$

Where; l is the cuvette path length in meters (here l is 0.1 mt), $OD_s(\lambda)$ is optical density of the sample, $OD_{bs}(\lambda)$ optical density of the pure water (Milli-Q water), OD_{null} is the null absorption value which is the mean OD at after 600 nm-650 nm for this study.

2.4. Chemtax

Total phytoplankton standing stock is estimated as chlorophyll-a concentration and algal classes are identified from the presence of marker pigments (Figure 7). Furthermore, the biomass of each taxa is calculated as a proportion of total chl-a using marker pigment/chl-a ratios. For this purpose, CHEMTAX-Program is used in the present study.

CHEMical TAXonomy (CHEMTAX) is a matrix-factorization program for calculating algal class abundances from concentrations of algal marker pigments (chlorophylls and carotenoid) (Mackey et al. 1996, 1997, Wright et al. 1996). CHEMTAX Software (a product of CSIRO Division of Oceanography-Hobart, Australia) is used to calculate contribution of different phytoplankton group to total chl-a.

The program uses a steepest-descent algorithm to determine the best fit based on an initial estimate of pigment ratios for algal classes. Input for the program consists of a raw-data matrix of pigment concentrations obtained by HPLC analyses and an initial pigment-ratio file. Relatively large errors in the initial estimates of pigment ratios have little influence on the final determination of algal class abundances (Mackey et al., 1996). The data matrix is subjected to a factor-minimization algorithm that calculates a best-fit pigment ratio matrix and a final phytoplankton class-composition matrix. The class composition matrix can be expressed as relative or absolute values for specified photo-pigments. The absolute chlorophyll-a contribution of each class is particularly useful because it partitions the total chlorophyll-a into major phytoplankton groups.

Figure 7 — Marker pigments and the major phytoplankton groups. ● = present (major), · = present (minor).

Pigment	Raphidophyceae	Chrysophyceae	Prymnesiophyceae	Dinophyta	Bacillariophyta	Eustigmatophyta	Euglenophyta	Prasinophyceae	Chlorophyceae	Cryptophyta	Rhodophyta	Prochlorophyta	Cyanophyta	Group
chl a	●	●	●	●	●	●	●	●	●	●	●		●	Chlorophylls
chl b							●	●	●					Chlorophylls
chl c1	●		●		●									Chlorophylls
chl c2	●	●	●	●	●					●				Chlorophylls
chl c3		●	●											Chlorophylls
MgDVP								●						Chlorophylls
DV a												●		Chlorophylls
DV b												●		Chlorophylls
β,ε – car			·					·	●	●	●	●		
β,β – car	●	·	·	·	·	●	●	●	●			●	●	
Allo										●				Xanthophylls
19 BF		●	●											Xanthophylls
Diadino	●	●	●	●	●		●							Xanthophylls
Dino				●										Xanthophylls
Fuco	●	●	●		●									Xanthophylls
19HF			●											Xanthophylls
Lut								●	●					Xanthophylls
Neo							·	●	●					Xanthophylls
Per				●										Xanthophylls
Pras								●						Xanthophylls
Viola						●		●	●					Xanthophylls
Zea						·			●		●	●	●	Xanthophylls
P/cyanin										●	·		●	
P/erythrin										●	●		●	

Figure 7: Marker pigments and the major phytoplankton groups. (Summarized from, Jeffery et al., 1997).

2.5. Satellite Data and Evaluation

Both SeaWiFS (Sea-viewing Wide Field-of-view Sensor) and MODIS (Moderate Resolution Imaging Spectroradiometer) data were utilized in the study. Satellite data were obtained from the NASA Goddard Earth Sciences (GES) Data and Information Services Center (DISC) (URL: 4), and Ocean color Web; (URL: 5). Satellite data, was processed by SeaDAS (SeaWiFS Data Analysis System) version 4.9.4. This software is capable to process both SeaWiFS and MODIS data from level 0 (raw instrument data at original resolution, time ordered, with duplicate packets removed) to level 3 (variables mapped on uniform space-time grid scales, usually with some completeness and consistency) data formats.

Chlorophyll-a, sea surface temperature and water leaving radiances are processed from the satellite data. These parameters were compared with the in-situ data and analyzed as temporally and spatially. Whole level 2 (derived geophysical variables at the same resolution and location as the level 1 source data) data were downloaded for the North Eastern Mediterranean.

Chlorophyll-a is the key pigment of the marine and terrestrial ecosystems, harvesting the light for photosynthesis. Hence, to know the chlorophyll concentration or the variability is crucial for the ecosystem based research activities. The variability of the phytoplanktonic biomass can directly be linked with the chlorophyll-a concentration.

SeaWiFS and MODIS are the two major sensors through which chlorophyll data can be derived daily. The data sets of SeaWifs were available from September 1997 to present. However, SeaWifs is a joint project with NASA and Orbimage Inc. and the high-resolution data transfer for scientific usage after 2004 is limited. Thus, the swaths coinciding with the North Eastern Mediterranean are effectively available until October 2004. MODIS data is available since end of the June 2002 to present and there is no any limitation on the ocean color data, it is freely downloadable from internet. The consistency of these two sensors is critically important to create long-term time series of chlorophyll.

Evaluation of the data sets obtained from SeaWiFS and MODIS are compared with the time series data collected from the METU-IMS time series station, between December 2001-2005 (HPLC data from 2001 and 2002 was kindly provided by Dr. Doruk Yılmaz). Daily, 1 km resolution data were downloaded from the ocean color data browser (URL 5). Data were extracted from the images for the determination of a 10x10 km square centered at the IMS station. The data points within this square were averaged to obtain a single value, which was assumed to represent the area concerned. The in situ data were obtained from HPLC measurements for the period of 2002-2005. Chlorophyll-*a*, and Divinyl chlorophyll-*a* values are utilized for the comparison of the satellite data.

Chlorophyll-*a* variability in the basin was analyzed by selecting six typical locations representing different characteristics within the Cilician Basin. Two stations were chosen in the (productive) coastal waters in Mersin area (# 3 in Fig. 8). Another coastal station was located near the İskenderun city (# 6 in Fig. 8). Stations in the offshore waters were #1 and # 4 in Fig. 8. One of the other two stations is located at the Middle of the İskenderun bay (# 5 in Fig 8) and the second one was the time series station area of IMS (# 2 in Fig 8). At the time series stations bi-weakly chlorophyll-*a* sampling was carried out between, January 2003 and December 2005.
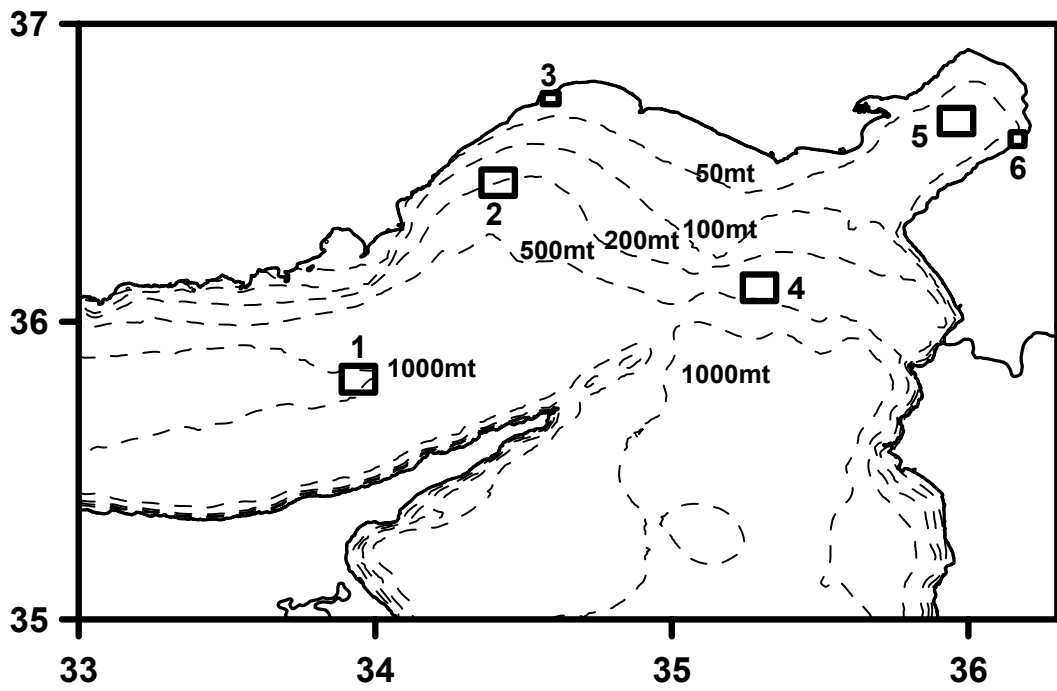
Figure 8: Areas selected for the analysis of chl-a. Numbers 1, 2, 4 and 5 are squares of 10x10 km and numbers 3, 6 are squares of 5x5km.

3. RESULTS

3.1. Hydrography

Temperature of the North Eastern Mediterranean water undergoes considerable variations throughout the year. The sea surface temperature of the whole water starts to decrease in autumn and minimum sea surface temperature occurs in February-March and extends to the bottom layers (Figure 9).
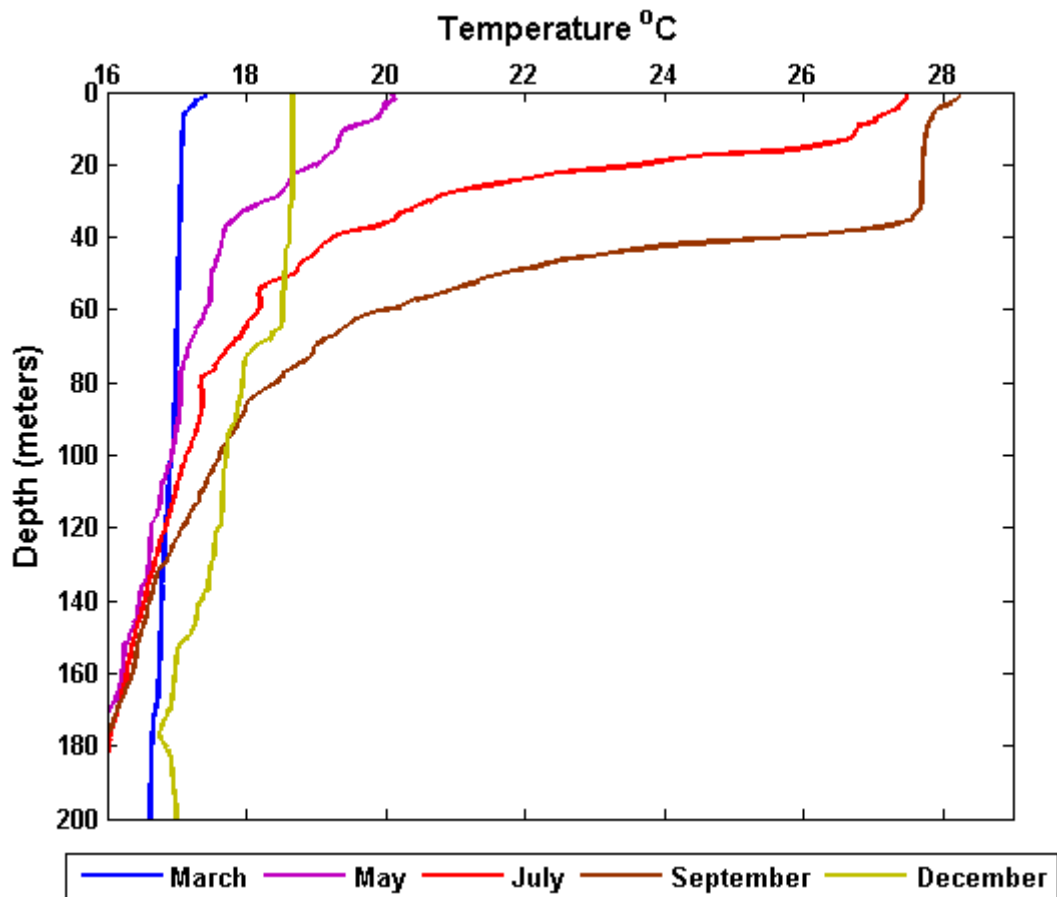
Figure 9: Temperature profiles of the METU-IMS time series station (see figure 4 for station location and latitude and longitude values are given in table 4), from different months of 2005.

Salinity increases during the summer periods due to evaporation. The whole water column was well mixed in winter around 17 ^{o}C temperature and around 39 psu salinity. The surface salinity increases from 39.05 to about 39.6 psu through the end of the year (Figure 10).
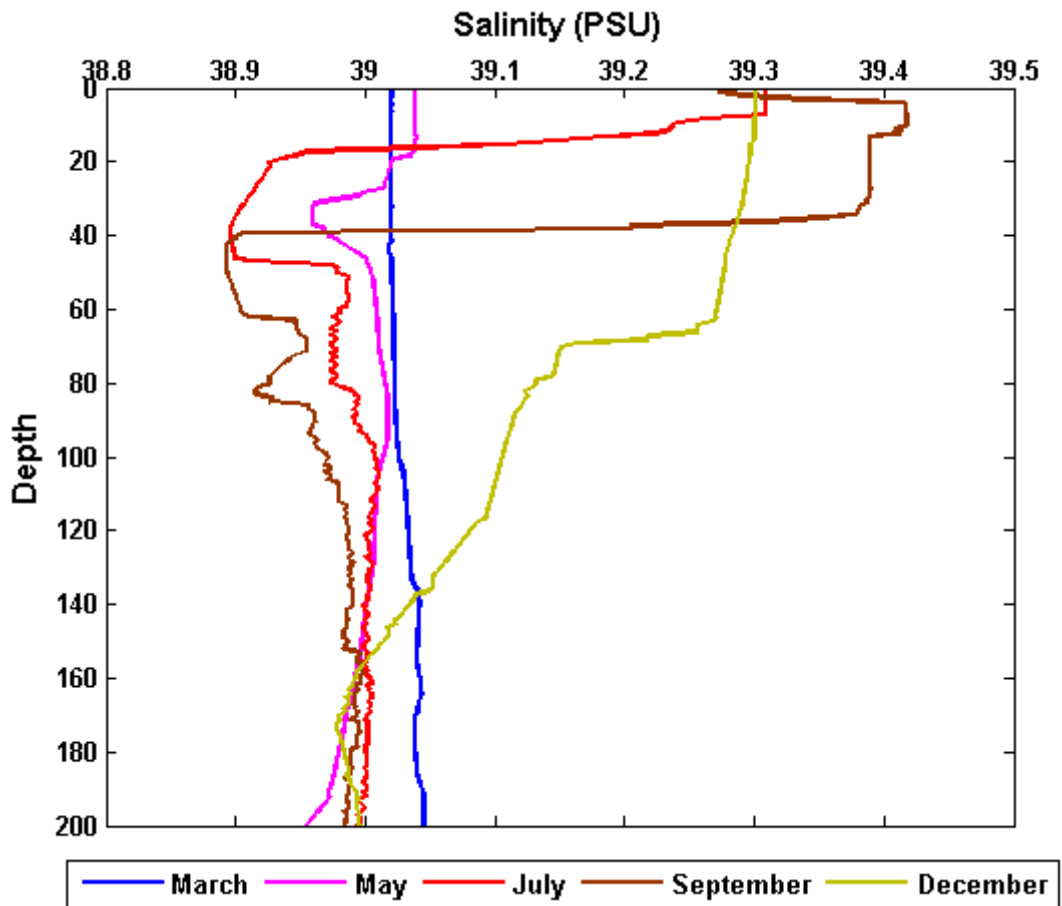
Figure 10: Salinity profiles of the METU-IMS time series (see figure 4 for station location and latitude and longitude values are given in table 4) station, from different months of 2005.

The mixing and stratification period was clearly observed, in 2005. The mixing started during November-December and extended until April. Stratification started during May and extended until October (Figure 11). Surface mixed layer was between 20-50m with a relatively high salinity (39.3–39.6 psu). The surface temperatures vary between 17–30°C. During the winter period, whole water column is mixed, even in the deeper parts of the basin (Figure 12).
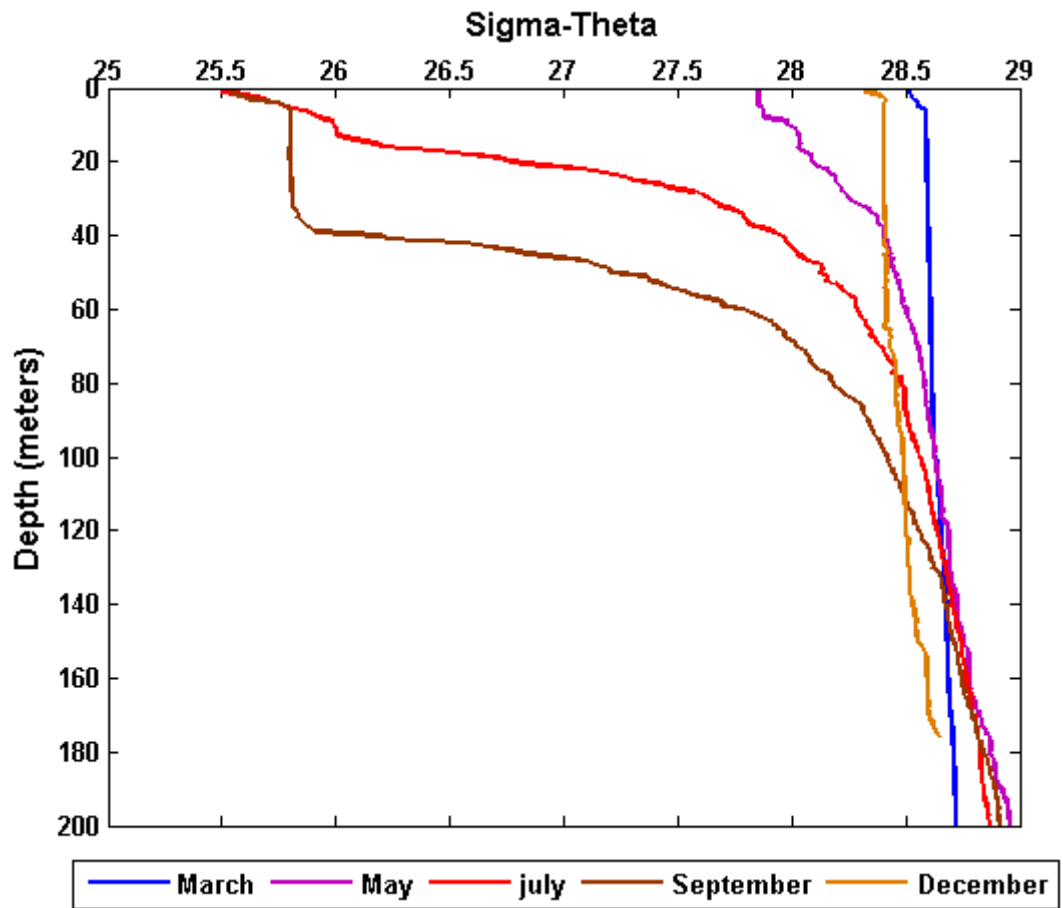
Figure 11: Density profiles of the METU-IMS time series station (see figure 4 for station location and latitude and longitude values are given in table 4), from different months of 2005.
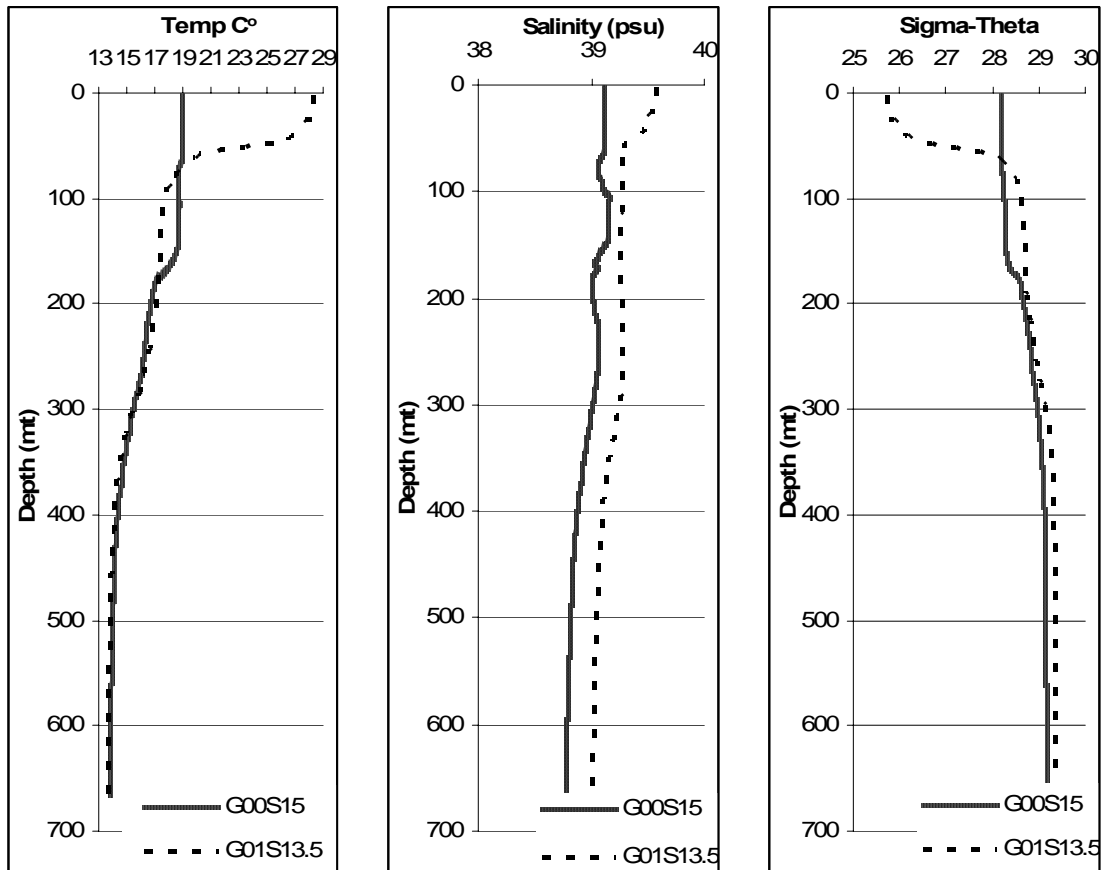
Figure 12: Temperature, Salinity and Density Profiles, at station G00S15 (28-12-2003) and station G01S13.5 (03-08-2005) see figure 4 for station locations and latitude and longitude values are given in table 4.

The stations (G00S15 and G01S13.5, see figure 4 for station locations and latitude and longitude values are given in table 4) presented here represent offshore waters of the North Eastern Mediterranean. However, low salinity and turbid inshore waters along the coast, with a well-marked outer boundary is persistent feature to the west of Seyhan River. This river water is transported to the west by mean westerly coastal flow. The effects of this coastal water on the optical properties of the North Eastern Mediterranean and how open and coastal waters optically different will be investigated in detail within the context of this study.

3.2. Evaluation of the SeaWifs and MODIS Sensors in North Eastern Mediterranean.

METU-IMS time series data collected between 2001 to 2005 December were used to evaluate the SeaWifs and the MODIS sensors. In-situ chlorophyll-a values changed between 0.01 to 0.59 mg/m³. However, satellite values varied between 0.046 to 0.59 for SeaWifs and 0.046 to 0.255 mg/m³ for MODIS (Table 6).

Table 6: In-situ and satellite data sets.

Date	MODIS Chl-a mg/m³	In-Situ Date	In-Situ Chl-a mg/m³	SeaWifs Date	SeaWifs Chl-a mg/m³	In-Situ Date	In-Situ Chl-a mg/m³
10.07.2002	0.079	10.07.2002	0.040	10.12.2001	0.225	11.12.2001	0.210
18.09.2002	0.146	18.09.2002	0.030	23.01.2002	0.430	23.01.2002	0.590
24.10.2002	0.046	24.10.2002	0.050	19.02.2002	0.166	19.02.2002	0.120
20.11.2002	0.165	21.11.2002	0.260	13.05.2002	0.152	13.05.2002	0.100
25.12.2002	0.193	24.12.2002	0.220	18.06.2002	0.100	18.06.2002	0.050
29.01.2003	0.162	29.01.2003	0.280	10.07.2002	0.097	10.07.2002	0.040
28.02.2003	0.197	27.02.2003	0.170	10.07.2002	0.050	10.07.2002	0.040
28.03.2003	0.171	28.03.2003	0.220	02.08.2002	0.110	01.08.2002	0.120
05.06.2003	0.156	05.06.2003	0.010	18.09.2002	0.161	18.09.2002	0.030
16.07.2003	0.082	15.07.2003	0.070	24.10.2002	0.142	24.10.2002	0.050
31.07.2003	0.076	31.07.2003	0.020	21.11.2002	0.085	21.11.2002	0.260
22.09.2003	0.147	22.09.2003	0.130	25.12.2002	0.225	24.12.2002	0.220
23.12.2003	0.179	24.12.2003	0.240	29.01.2003	0.105	29.01.2003	0.280
19.07.2004	0.067	19.07.2004	0.080	26.02.2003	0.174	27.02.2003	0.170
27.09.2004	0.146	27.09.2004	0.170	28.03.2003	0.267	28.03.2003	0.220
05.11.2004	0.255	04.11.2004	0.290	05.06.2003	0.063	05.06.2003	0.010
27.12.2004	0.182	28.12.2004	0.270	15.07.2003	0.114	15.07.2003	0.070
10.02.2005	0.223	10.02.2005	0.470	31.07.2003	0.059	31.07.2003	0.020
25.03.2005	0.185	25.03.2005	0.390	22.09.2003	0.119	22.09.2003	0.130
12.06.2005	0.091	12.06.2005	0.020	23.12.2003	0.249	24.12.2003	0.240
02.07.2005	0.086	02.07.2005	0.040	19.07.2004	0.046	19.07.2004	0.080
03.08.2005	0.067	02.08.2005	0.030	27.09.2004	0.184	27.09.2004	0.170
07.09.2005	0.100	07.09.2005	0.010				
27.10.2005	0.136	27.10.2005	0.120				
28.11.2005	0.147	27.11.2005	0.190				
28.12.2005	0.218	29.12.2005	0.240				

Seasonal and inter-annual variability of SeaWiF and MODIS derived and in-situ chlorophyll-a concentrations in METU-IMS time series followed similar trends from November 2001 to January 2006 (Figure 13).
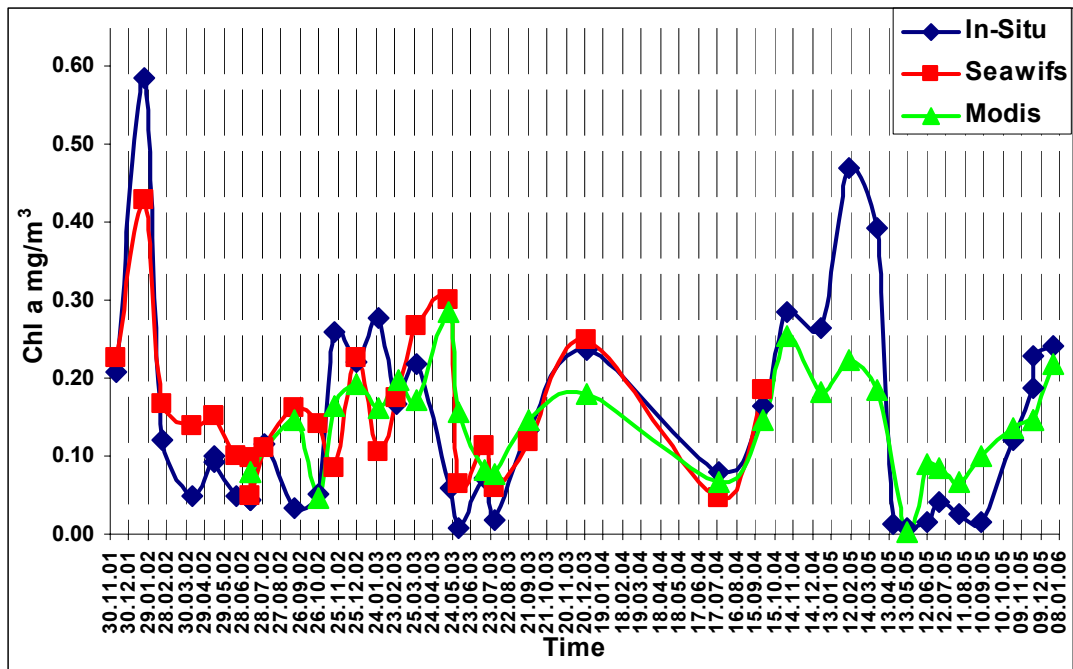
Figure 13: Variability of the Chlorophyll-*a;* In situ (METU-IMS Time series station, see figure 4 for station locations and latitude and longitude values are given in table 4), SeaWifs and MODIS.

The satellite and the in-situ chlorophyll-a measurements agreed well qualitatively. Maximum concentrations both in-situ and satellite data appeared every winter and minimum concentrations in every summer. In some points, in-situ and satellite data are not really following each other, however at these points, unavailability of the satellite data were recovered from previous days (one day before) or after (one day later) (Table 6). This method is mostly satisfactory in many occasions but may vary a lot at some points.

MODIS and SeaWiFS derived chlorophyll-a values are consistent with each other. However, both satellites underestimate the chlorophyll-a during winter and overestimate during summer periods.

3.2.1. Inter Annual Chlorophyll-*a* Variability in the North Eastern Mediterranean

Five regions have been chosen (Figure 8) to analyze inter annual chlorophyll variability in the North Eastern Mediterranean, utilizing the SeaWiFS and MODIS data. As it was shown in previous section, these two sensors data are consistent, and hence provides temporal continuity, across changes in sensors.

Chlorophyll-a fluctuations in the coastal regions are much more irregular, relative to the offshore waters. Dynamic structure of the coastal systems and anthropogenic influences are the possible reasons of these irregularities. In coastal areas, in-situ measurements and satellite chlorophyll-a measurements are not really fitting each other; usually chlorophyll algorithms over estimate in-situ values, because of the optical complexity of the coastal waters, which is very well known for the Case II waters (Sathyendranath 2000).

The general trend of the in-situ and satellite derived chlorophyll values at the coastal areas (area #3 and #6 in Fig. 8) were not parallel to each other. Chlorophyll concentrations in the Mersin station (area #3 in Fig. 8) are much higher than the İskenderun station (Figures 14 and 15). This is a clear impact of the Mersin city discharge system, which is not much away from the sampling area. Chlorophyll-a values fluctuated between 0.1 to 5 mg/m^3 according to the in-situ measurements. However, satellite derived chlorophyll-a values fluctuated between 0.7 to 10.5 mg/m^3 (Figure 14).
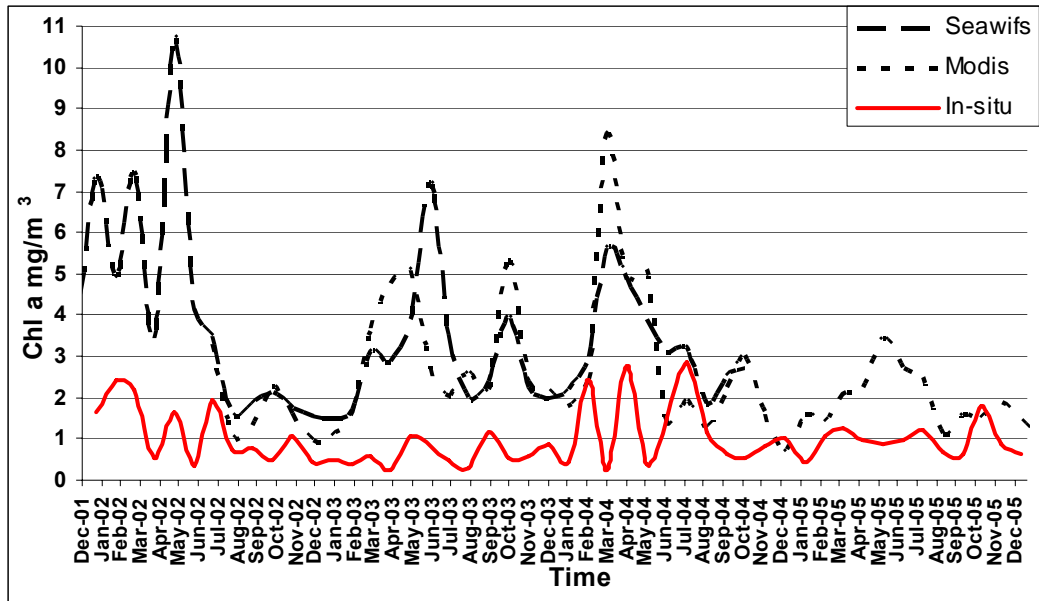
Figure 14: Comparison of the in-situ chlorophyll a and satellite derived, monthly averaged chlorophyll a values in Mersin area (area #3 in Figure. 8).

Neither SeaWifs nor MODIS derived chlorophyll-a values fluctuated parallel to the in-situ data. According to satellite derived chlorophyll-a values, main peaks occurred in January, March, April, May, June and October, although, peaks occurred in February, March, April, May, July, and October, according to the in situ data.

The fluctuation of the chlorophyll-*a* in the İskenderun Bay station was more irregular than the Mersin station (Figure 14). The concentration of the chlorophyll-*a* in the station changes between 0.1 to 2.03 mg/m^3 (Figure 15). However, satellite derived chlorophyll concentration changed between 0.3 to 1.45 mg/m^3. Contrary to the Mersin area, satellite chlorophyll-*a* values did not always overestimate the in-situ values (Figure 15).
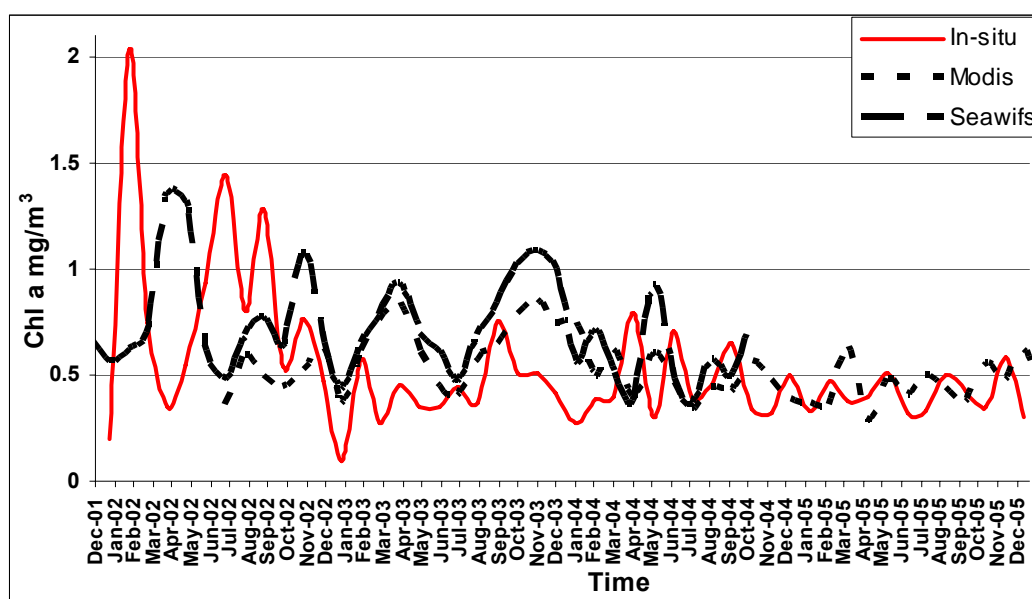
Figure 15: Comparison of the in-situ chlorophyll-a and satellite derived, monthly averaged chlorophyll-a values in İskenderun area (area #6 in Figure 8).

The major chlorophyll-*a* peaks of the satellite derived and in situ values were highly variable. The highest peaks of the satellite derived data observed in May, April and November, December. On the other hand, highest peaks observed in February, April, June and September according to in situ values.

Offshore areas (#1 and #4 in Fig. 8) and also METU-IMS time series station (area #2 in Fig. 8) showed clear inter annual variability. Clear chlorophyll *a* peaks, were observed in winter periods (Figure 16).
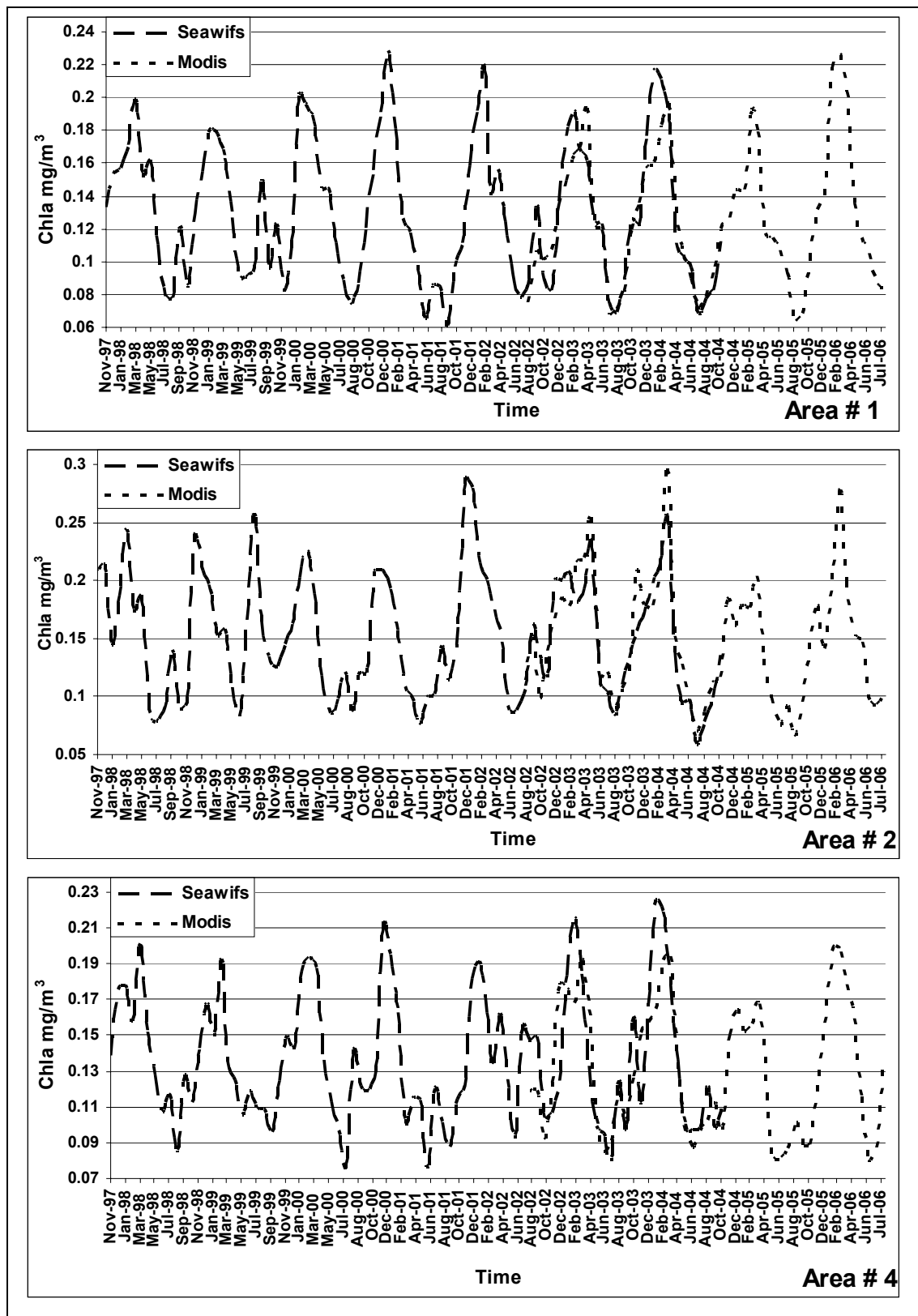
Figure 16: Monthly averaged annual chlorophyll *a* variability in the offshore areas (#1, #2, #4 in Figure 8).

As mentioned above, chlorophyll-*a* peaks occurred in winter period. However a peak was also observed in August 1999 and May 2003 in METU-IMS time series station (area # 2 in Fig. 8). The winter peaks usually appeared between January and March. In very few occasions, winter peak may extend until April or May (area # 2 in Fig. 8, between: December 2002-May 2003). In these periods, peaks were more broad, but were not high as the sharp peaks (e.g., in area 4 in Fig. 8; February 2004 peak maxima around 0.23 mg/m^3 (sharp) and December 2004-April 2005 peak maxima around 0.16 mg/m^3 (broad) (Figure 16). If the broader peak did not occur, winter peaks occurred between December and March. Most frequent winter peaks occurred in January and February for the #1 and #4 areas 4 in Fig. 8; March was the most frequent month for METU-IMS time series station (area #2 in Fig. 8). Besides the main peaks, shoulders or relatively shorter peaks occurred. These shoulders and secondary peaks appeared in nearly all months except winter, but in area # 4 in Fig. 8, four peaks occurred in August. Secondary peaks and shoulders in area 1 and 2 (in Fig. 8) have similar periodicity. In these stations peaks and shoulders appeared in April and May or August and September. Seasonal winds or post bloom periods are considered as the possible reasons of the secondary peaks and shoulders. For all that the general trend in the basin was not really changed, except the peak observed in August 1999 (Figure 17). The major feature of the offshore waters is the winter peaks.
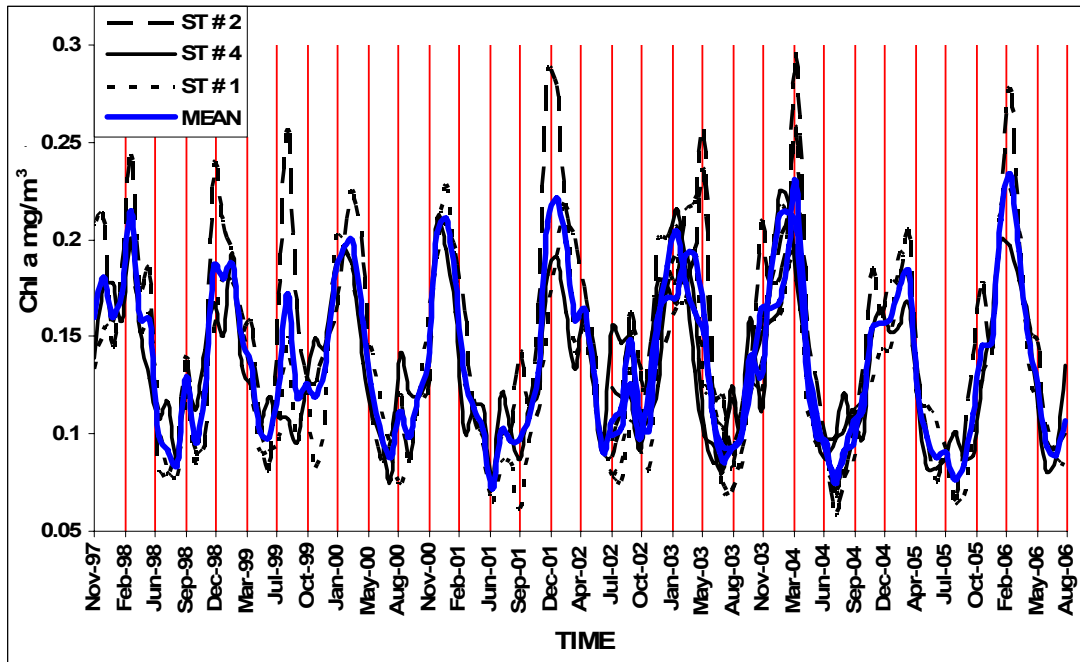
Figure 17: Average monthly chlorophyll-a fluctuation in areas #1, #2 and #4 in Figure 8 and the mean chlorophyll-*a* fluctuation.

İskenderun Bay is the shallowest part of the North Eastern Mediterranean (Figure 8). River and industrial sewage inputs are the important nutrient pollution sources in the İskenderun Bay. Thus, higher chlorophyll concentrations occurred in the Bay (Figure 5). Location of area # 5 in Fig. 8 has nearly the same distance from land from three sides of the Bay. Inter annual fluctuation of the chlorophyll-a concentration at this station was rather different than the others. Fluctuation within this area is showing (mostly) two peaks in the year, from which only one is identical in the areas #1, #2, and #4 in Fig. 8. The winter peak was observed in the Iskenderun Bay also (December – January). In addition to the winter peak, another peak occurred at spring time in April and May (Figure 18).
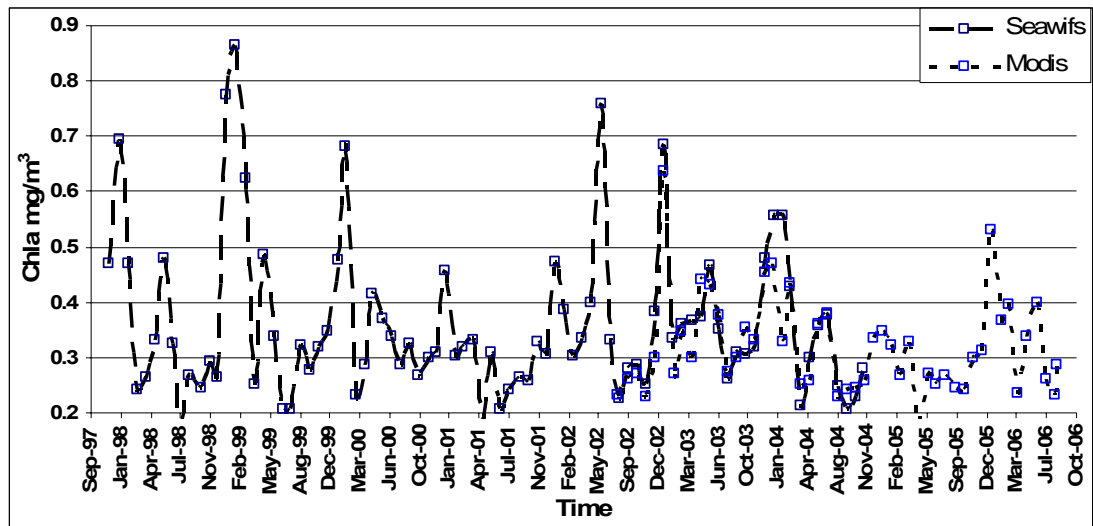
Figure 18: Monthly average chlorophyll-a variability at the area # 5 (in Figure 8).

Chlorophyll-a concentration at the area #5 (in Fig 8) has changed periodically. After the winter peak, spring peak follows accordingly and no peaks occurred in summer and autumn. Spring peak is smaller than the winter peak, but May 2002 peak was higher than December 2001 and December 2002 peaks. Besides inter annual fluctuations, stationary stages were observed. These periods were between January 2000 to May 2002 and December 2003 to December 2005. At these periods May peak is replaced with April peak and the values were relatively lower than in the May, practically lower than 0.5 mg/m^3.

3.3. Bio-Optical Measurements

Bio-optical data set collected within this study includes coincident observations of inherent optical properties (spectral absorption) and apparent optical properties (spectral irradiance). Following is the results of the measurements carried out in the seas surrounding Turkey.

3.3.1. Particle Absorption

Particle absorption measurements carried out at the Western Black Sea, the Aegean Sea and the Mediterranean Sea, revealed five regions as follows:

a. Western Black Sea Offshore (Figure 19)
b. Western Black Sea Costal (Figure 20)
c. North Eastern Mediterranean Offshore (Figure 21)
d. North Eastern Mediterranean Coastal (Figure 22)
e. North Eastern Mediterranean Iskenderun Bay (Figure 23)
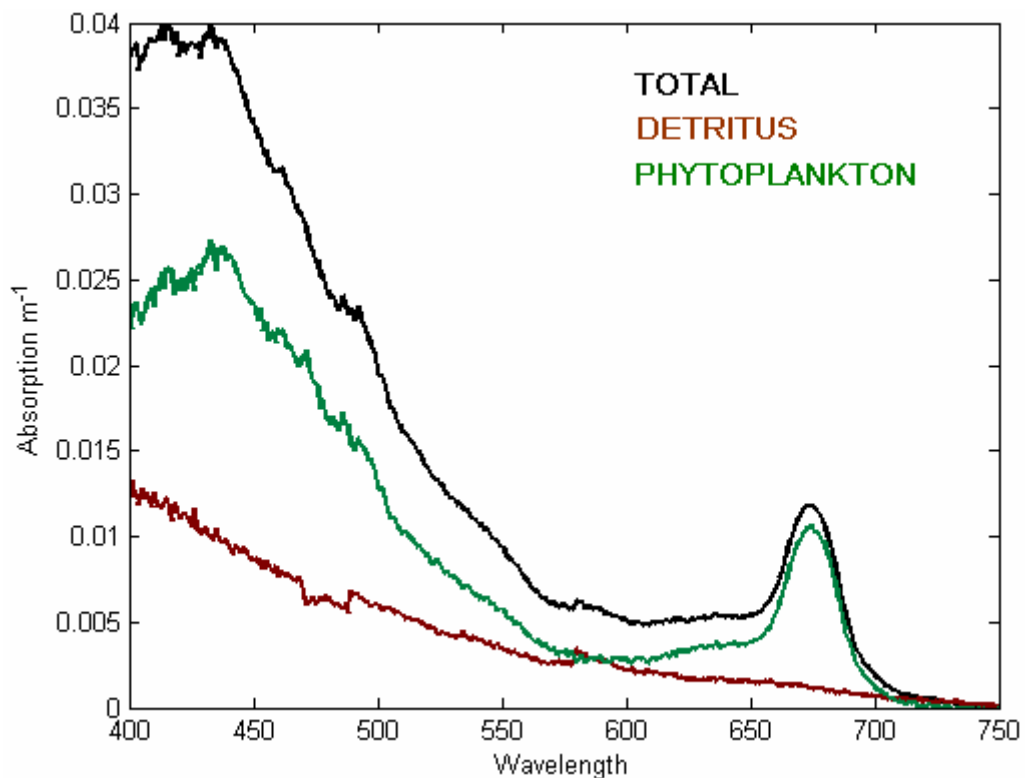
Figure 19: Western Black Sea offshore particle absorption values.
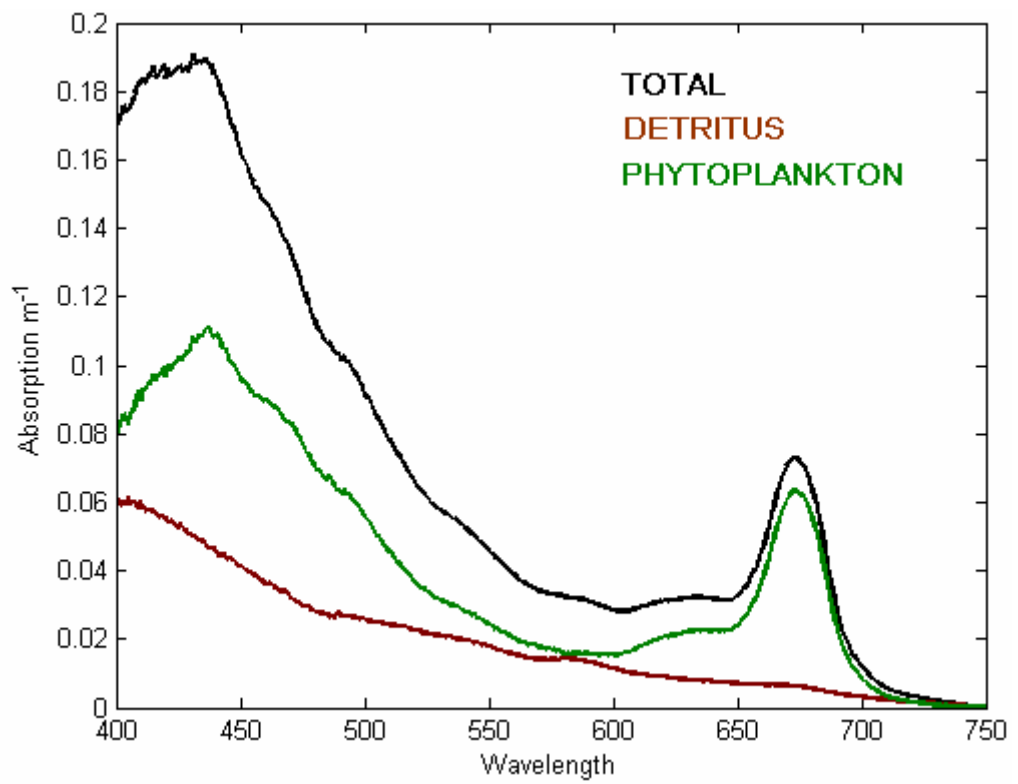
Figure 20: Western Black Sea coastal particle absorption values.
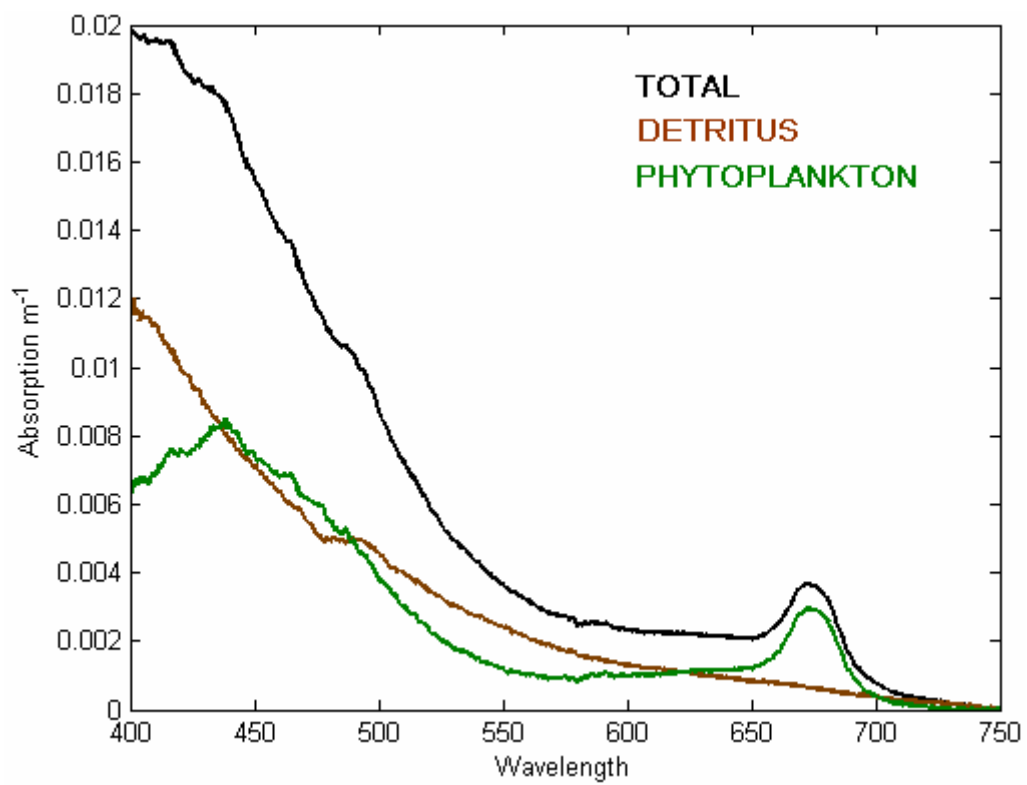
Figure 21: Offshore North Eastern Mediterranean particle absorption values.
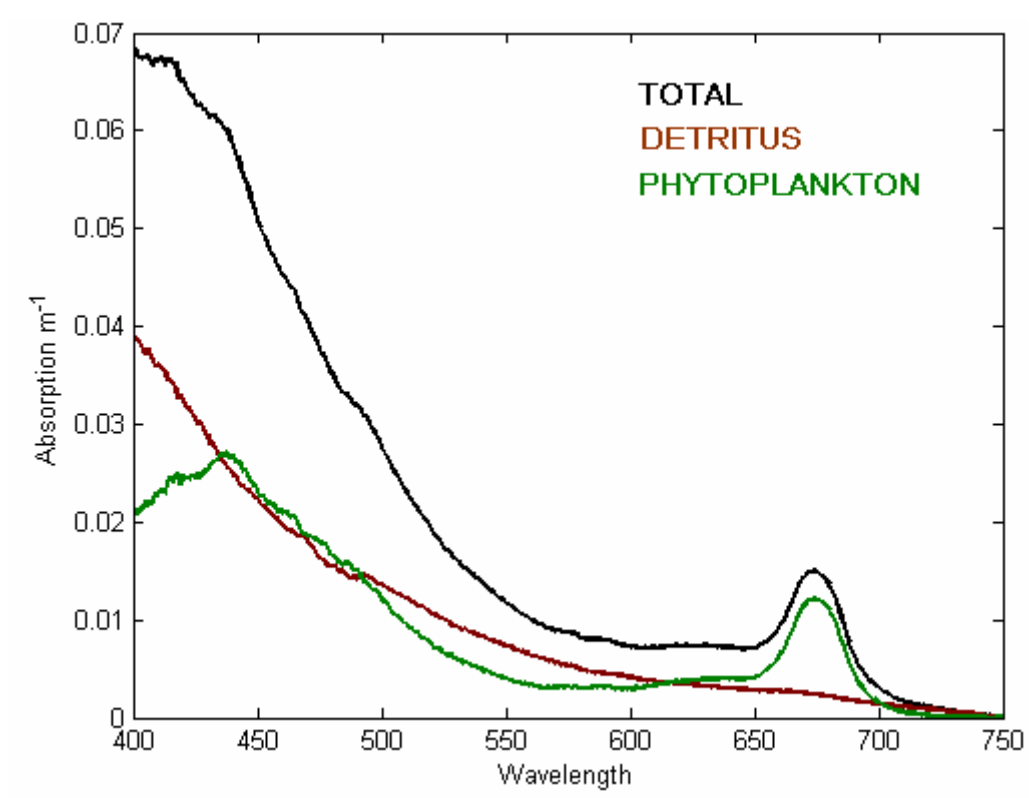
Figure 22: Coastal North Eastern Mediterranean particle absorption values.
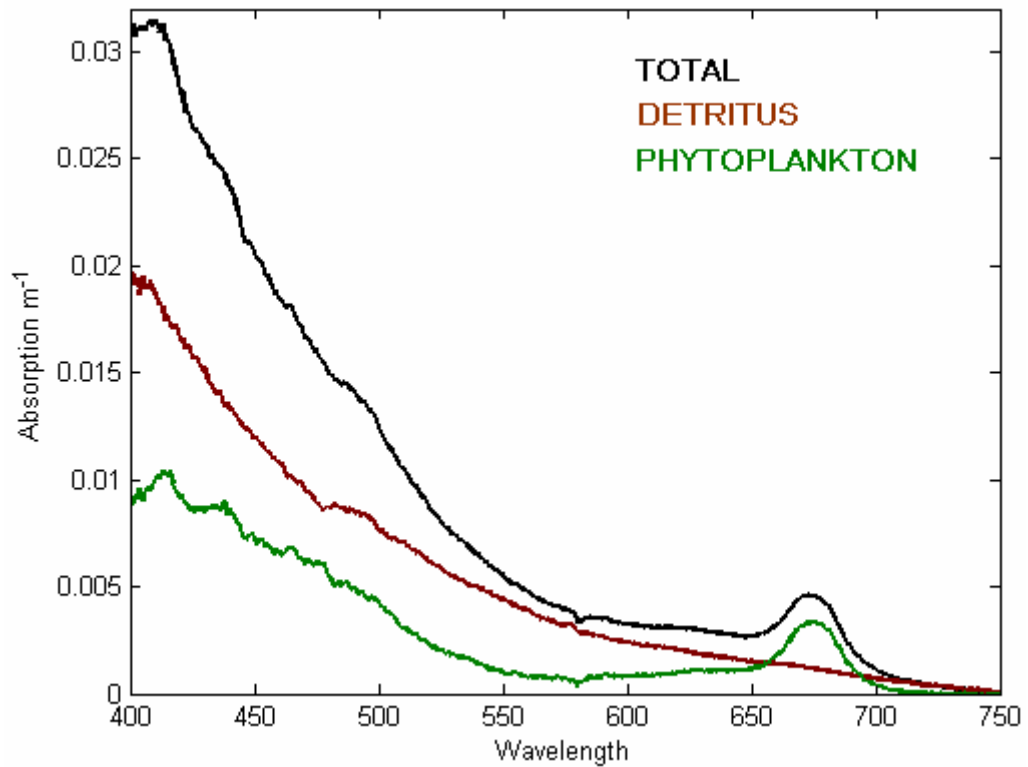
Figure 23: İskenderun Bay particle absorption values.

Particle absorption values for samples collected between 2001 and 2005 decreased starting from Western Black Sea towards the North Eastern Mediterranean Sea. However, coastal (usually estuarine) part of the North Eastern Mediterranean Sea shows higher absorption values as compared to the offshore of the North Eastern Mediterranean waters and even as compared to Western Black Sea offshore waters (Figure 24, 25, 26). Spatial and temporal variability are observed in the sampling areas. The spatial variability has been observed between the Western Black Sea coastal and offshore areas. Similar variability is also valid for the North Eastern Mediterranean Sea and İskenderun Bay's coastal and offshore areas. However the İskenderun Bay has its individual characteristic and differs from others (Figure 5, 15, 18, 23).
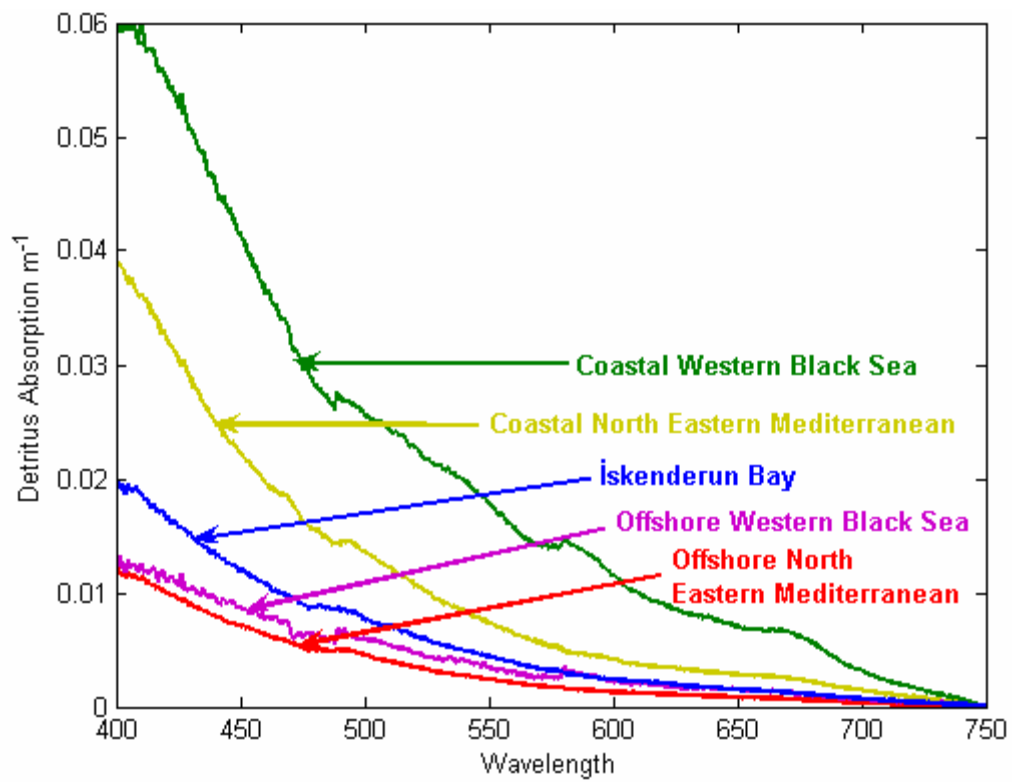
Figure 24: Spatial comparison of the mean detritus absorption coefficients.
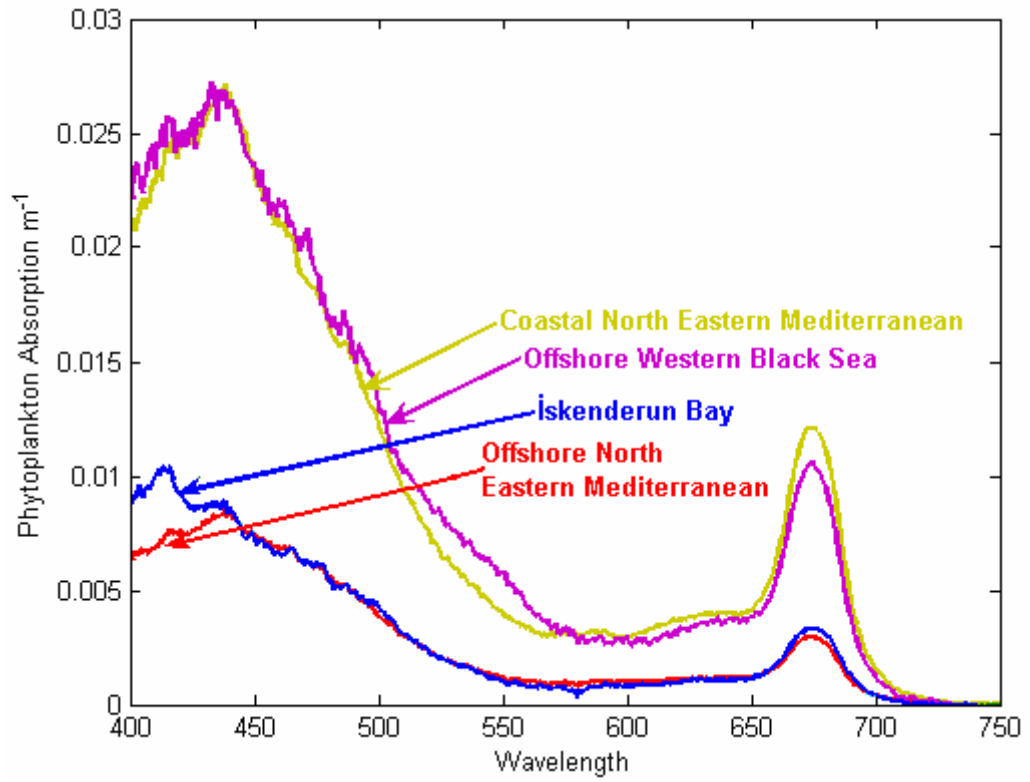
Figure 25: Spatial comparison of the mean phytoplankton absorption coefficients.
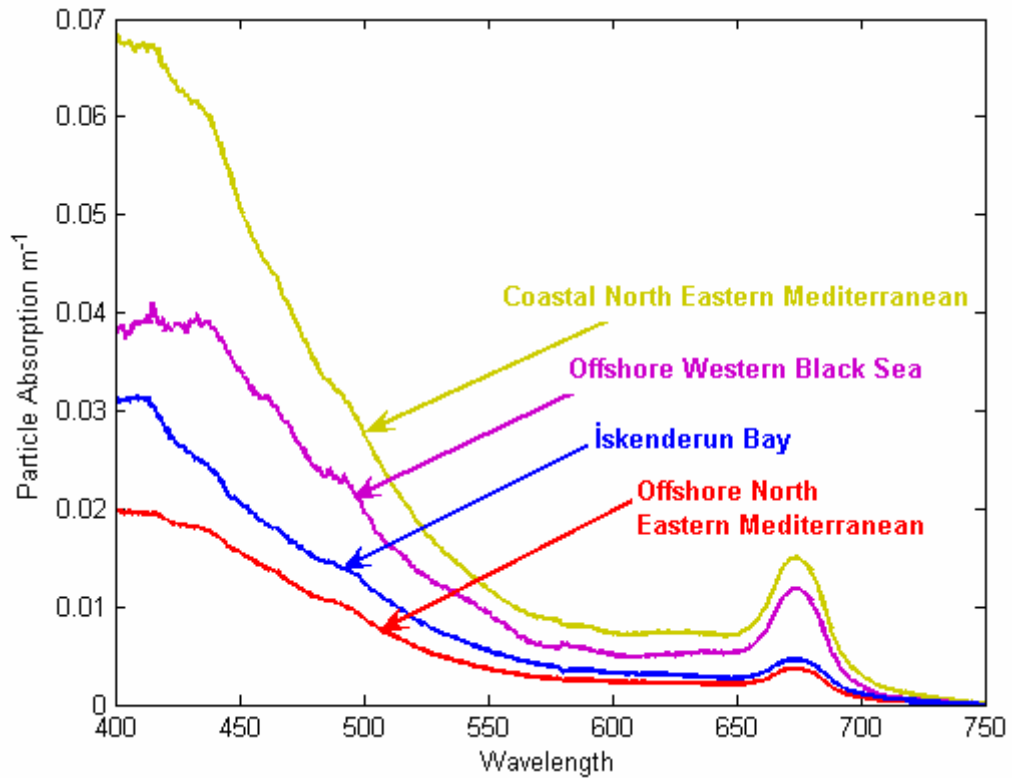
Figure 26: Spatial comparison of the mean total particle absorption coefficients.

The components of the total particle absorption coefficients differed within the regions. These differences in the components are observed either in the shape or the ratios or both. In the Western Black Sea, phytoplankton absorption coefficients are always higher within the measured range of the wavelengths. The only exception is around 580-590 nm, where the phytoplankton and detritus absorption curves cut each other (Figure 19, 20). The shape of the detritus spectra is like an exponential curve and typical for all the regions. The only difference is a decreasing range occurring between 470-490 nm apart from the gradual trend. The phytoplankton absorption spectra gave two typical peaks at 440 nm and 675 nm, showing a smaller peak around 420 nm. Beside these main features, there is a hump appearing between 600-650 nm and smaller peaks around 460, 470 and 485 nm. The total absorption spectra look like phytoplankton absorption spectra, but at the shorter wavelengths, possibly because of the high absorption by detritus. Shape of the total absorption spectra is flattened between 400-450 nm (Figure 19, 20, 21, 22, and 23).

The highest absorption coefficients were observed in the coastal Western Black Sea region (Figure 20). Especially phytoplankton and also total absorption coefficients were nearly ten times higher than the other regions. Apart from the total and phytoplankton absorption coefficients, the detritus absorption coefficients are comparable with the other regions (Figure 24). The detritus absorption coefficients are lower than the phytoplankton absorption coefficients over all spectrums between 400-750 nm. Detritus and phytoplankton absorption spectra are only touching each other at 583 nm. Detritus absorption spectrum is like exponential curve. Detritus absorption curve gradients changed, to more gradual trend from 490 to 750 nm. There are very small up and rise features. This can be observed between, 550 and 600 nm and there is a small hump remaining around 670-680 nm, from the de-pigmentation, procedure. The phytoplankton absorption peak has two main peaks at 440 nm and 675 nm. The shape of the spectra has a wave like fluctuation between 450 and 500 nm and a clear hump is appearing between 600-650 nm. The shape of total absorption spectra is reflecting the features observed in phytoplankton absorption curve. The main difference has occurred at the shorter wavelengths beyond 440 nm, where the detritus absorption coefficients are highest at that area (Figure 20).

According to the spectral characteristics of the absorption coefficients, the North Eastern Mediterranean may be divided into three sub-regions. Different than the Western Black Sea, in the North Eastern Mediterranean, detritus absorption coefficients are either equal to the phytoplankton absorption coefficients or even higher (Figure 21, 22, 23).

Offshore North Eastern Mediterranean waters are known for their oligotrophic characteristics. The absorption coefficients of the detritus and phytoplankton are usually equal to each other or follow the same trend, except the wavelengths beyond 440 nm. The detritus absorption spectra are exponential shaped curve. The only exception on this curve is a straight part between 475-500 nm, and then the curve extends exponentially. The phytoplankton absorption spectra have two main typical peaks at 440 and 675 nm. The other features of the spectra are the smaller peak at 420 nm and a hump between 460-490 nm. The absorption coefficients are almost flat between 550 and 650 nm. The total absorption coefficients are linearly decreasing from 435 to 545 nm. The other features are the small hump, between the 430-440 nm and a flat line from 400 to 420 nm (Figure 21).

Coastal waters of the North Eastern Mediterranean Sea are much more productive then the offshore waters. Thus the absorption coefficients observed in the coastal parts are much higher than the offshore waters. However, the shapes of the absorption spectra are very similar. The value of the detritus and the phytoplankton absorption coefficients are very close to each other, except beyond 440 nm where the detritus absorption coefficients are higher. Phytoplankton absorption coefficients are higher between 660 to 690 nm. The detritus absorption spectrum is like an exponential curve. The only exception on this curve is a linear part between 488-498 nm. The phytoplankton absorption spectrum has two main peaks at 440 and 675 nm respectively, and a smaller peak at 420 nm. In addition, there are several smaller peaks located between 450-490 nm. Starting from 550 nm shape of the absorption spectrum is flatten and making a little hump between 600-650 nm. The total absorption spectrum is linearly decreasing from 450 to 550 nm. The spectrum has rather straight part between 400-420 nm and very small variation observed at around 435 nm. Small hump, which is observed in the phytoplankton absorption, is not observed here (Figure 22).

The particle absorption characteristics of the İskenderun Bay differed from both offshore and coastal North Eastern Mediterranean regions. The detritus absorption coefficients are higher than the phytoplankton absorption coefficients except between 660-695 nm. The shape of the detritus absorption spectra is like an exponential curve, except a small peak around 480 nm. The phytoplankton absorption spectra are identical, with the peak at the 416 nm. Phytoplankton absorption coefficients were parallel to detritus coefficients, between 420 to 550 nm. The main peaks are located at the 416, 440, 675 nm. Some smaller peaks are located between 485 and 500 nm. The total absorption spectrum has nearly linear decreasing shape between 413 to 580 nm. The flat part of the spectrum is located between 400 to 413 nm and small variations occurred on the linear part at 425 to 450 and 485 to 510 nm. Only clear peak on the total absorption spectra is observed at 675 nm (Figure 23).

The absorption coefficients of the regions are different from each other, with their shapes and magnitudes. Highest absorption values are observed in the Western Black Sea coastal region. The detritus absorption is the parameter where the shape is very close within all regions. Although small differences may (and should) be observed between the regions, the general exponential shape is preserved. The

highest absorption coefficients were observed at coastal Western Black Sea, coastal North Eastern Mediterranean Sea, İskenderun Bay, offshore Western Black Sea and offshore of North Eastern Mediterranean Sea respectively (Figure 24).

The phytoplankton absorption coefficients show noticeable difference in patterns as compared to the detritus absorption coefficients. The highest coefficients were observed in the coastal Western Back Sea. Values are 5-10 times higher then the other regions. The shape of the phytoplankton absorption coefficients of the regions is different from each other. The general shape and the magnitude of the offshore Western Black Sea and coastal North Eastern Mediterranean Sea are similar. The main differences between the shapes are the little peaks on the Western Black Sea spectra around 420, 460, 470 and 485 nm and a relatively large hump on the coastal North Eastern Mediterranean spectra between 600-650 nm (Figure 25). The magnitude of the offshore North Eastern Mediterranean and the İskenderun Bay are nearly half of the magnitudes of the offshore Western Black Sea and the coastal North Eastern Mediterranean Sea. The general shape of these two spectrums is similar to each other. The main exception between these two spectrums is the peak at 416 nm and the smaller peak between 450 to 500 nm on the İskenderun Bay spectra (Figure 25).

Magnitude of the total absorption coefficients is differentiated. Unlike the phytoplankton or detritus absorption spectrums; all the regions are separated from each other. The coastal Western Black Sea absorption spectrum is 5 to 10 times higher than the other regions. The shapes of the spectrums are also differing, but the flat part from 550 nm to 650 nm and peak arise from chlorophyll a at 675 nm are common for all (Figure 25). The main differences occur between 400-450 nm. The coastal North Eastern Mediterranean spectrum is starting with a flat part until 420 nm then two raises are observed around 440 and 490 nm. Two small peaks appear at 416 and 430 on the flat part, which is extending until 440 nm, on the Western Black Sea offshore spectrum. In addition, two smaller peaks are appearing at 462 and 490 nm. The İskenderun Bay total particle absorption spectrum is looking like coastal North Eastern Mediterranean. After a short flat part (from 400 to 413 nm), there are two raises around 440 and 490 nm. The lowest total absorption coefficients are observed at the offshore North Eastern Mediterranean region. The shape of the spectrum is similar to Iskenderun and coastal North Eastern Mediterranean. After the flat part,

which is extending until 417 nm, there are two raises appearing around 435 and 490 nm (Figure 25).

Variability of the absorption coefficients within the study region is high. Absorption coefficients changed 20 fold at the shorter wavelengths. The temporal changes of the particle absorption coefficients were observed at the METU-IMS time series station (see figure 4 for station location and latitude and longitude value is given in table 4). The data that were collected from December 2004 to December 2005 (January data is absent) showed inter annual variability. The total absorption coefficients are higher during winter-autumn and lower during spring-summer months. Increasing of the absorption coefficients is parallel to the increasing the 675 nm peak. A peak or a relatively flat region appears between 400-440 nm on the winter-autumn spectrums. On the other hand, relatively linear decrease from 400 to 550 nm occurred on the spring-summer spectrums. Beside these general features, a raise appears on the spectrums between April and August. Within these periods the peak at the 675 nm is nearly ten times smaller than the other months (Figure 27).

Shape of the detritus absorption curves was very similar, except April, May and June, in METU-IMS time series station (see figure 4 for station location and latitude and longitude values are given in table 4. All of the detritus absorption spectrums are typically exponential shaped. However, a raise around 500 nm appeared on the spectrums, which may arise from measurement noise or a residue of a pigment. This raise is smaller on the December and August spectrums (Figure 28).
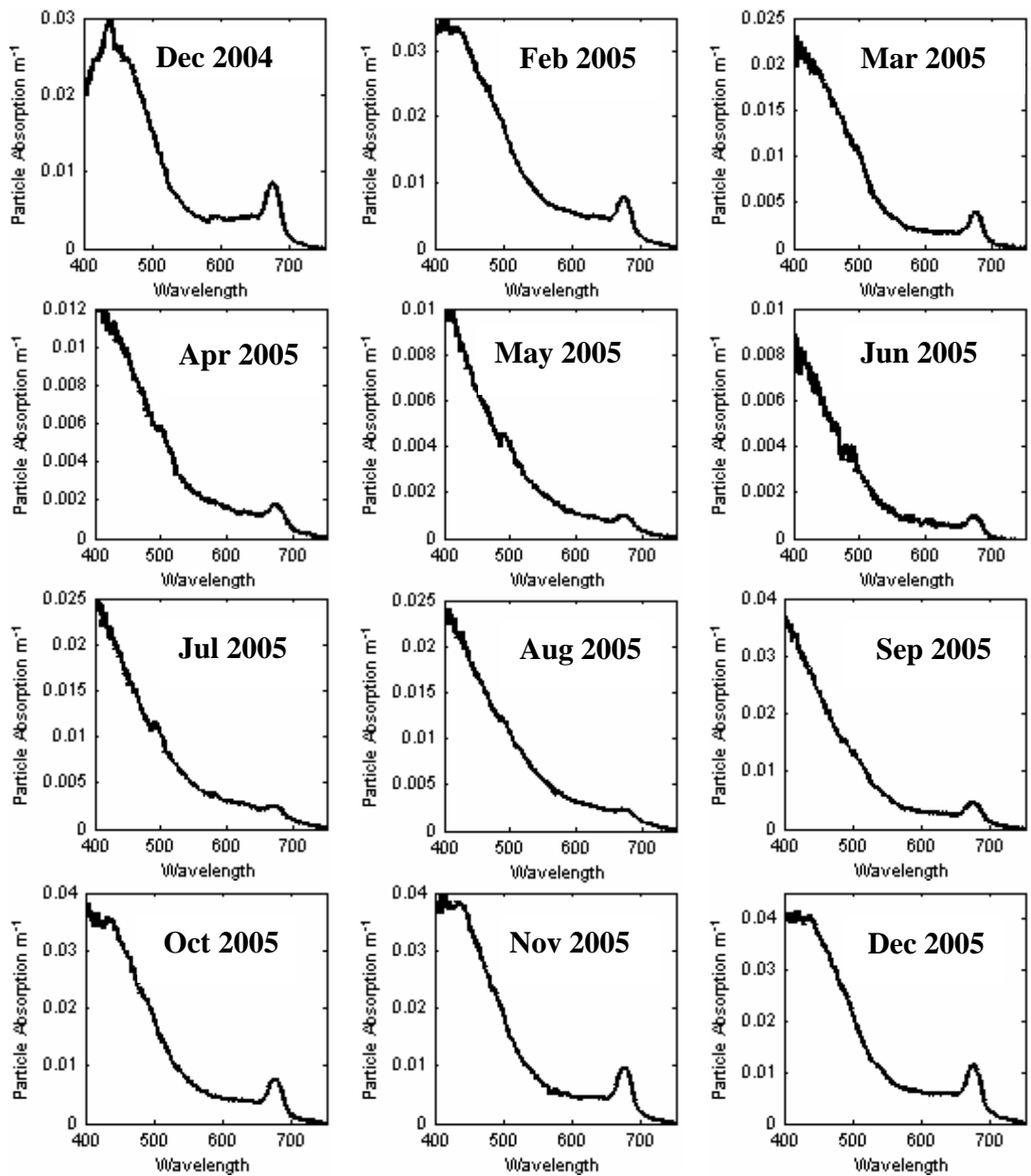
Figure 27: Monthly total particle absorption coefficients at METU-IMS time series station (see figure 4 for station location and latitude and longitude values are given in table 4).
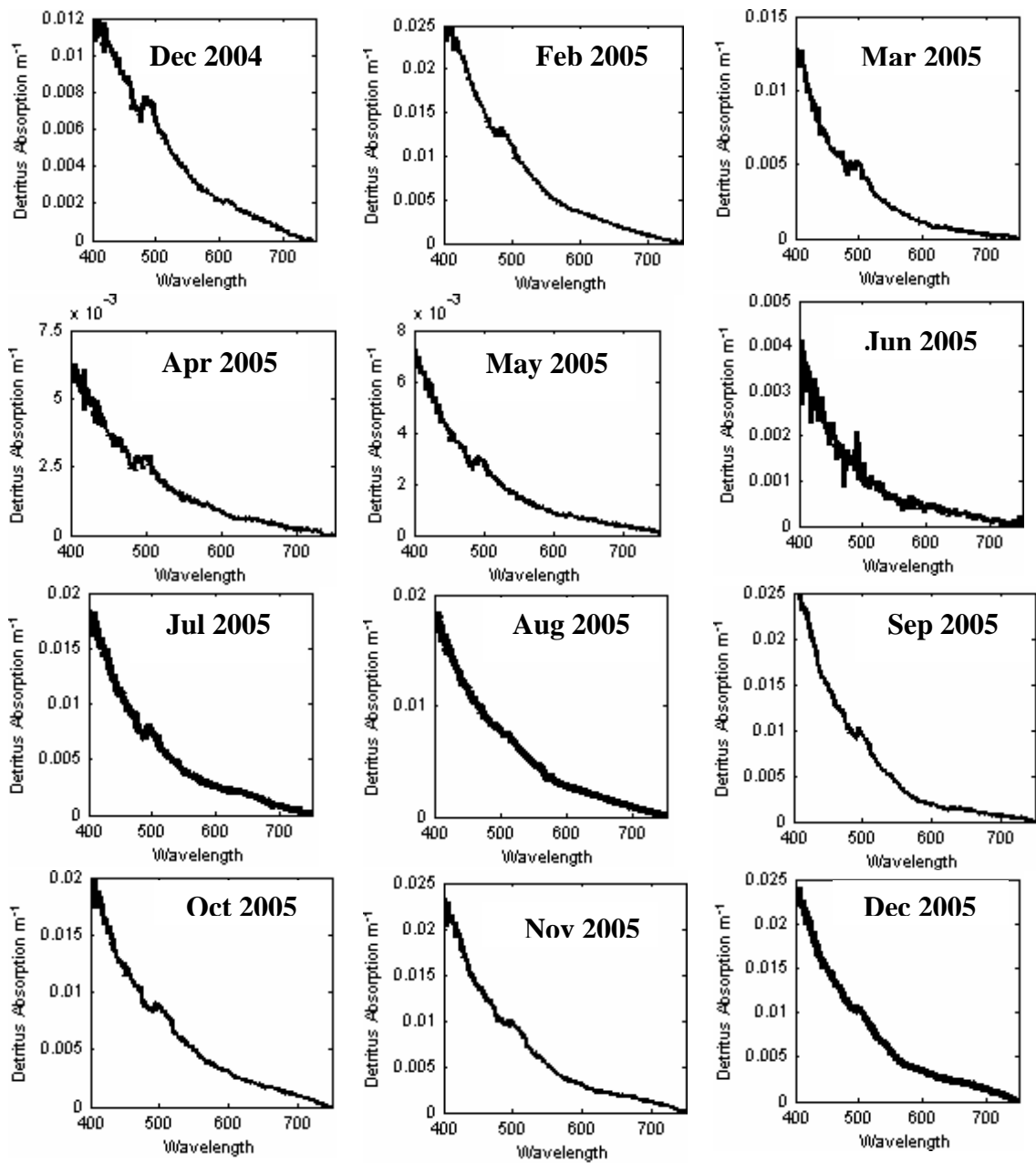
Figure 28: Monthly detritus absorption coefficients at METU-IMS time series station (see figure 4 for station location and latitude and longitude values are given in table 4).

The phytoplankton absorption coefficients have similar fluctuating pattern as total absorption coefficients. However, spectra shapes are differentiated. December 2004 and February 2005 spectrums are similar. Main peaks in December occurred at 440, 460 and 675 nm. However, in February, second peak moved to 470 nm. After the second peak, steep decrease occurred until 550 nm, and then a hump appeared between 550-600 nm in these months. The gradual increase is followed by hump until the starting of the peak at 675 nm (Figure 29). Peaks at the rest of the winter-autumn months (March, October, November, and December 2005) occurred at 440 and 675 nm. Other noticeable features were a hump or gradual increase occurred between 550 and 650 nm. During the spring summer, noisy shaped spectrums have occurred, because of the low absorption coefficients. Between April and June, the spectrums are characterized by nearly linear decrease from 420 nm to 550 nm, and then a flat plateau following until 650 nm. In addition, July and August spectrums have a shoulder around 500 nm. Autumn-winter period has from September, but the absorption coefficients are not high enough to account as in the autumn-winter period. September appears as a transition period between summer and autumn (Figure 29).
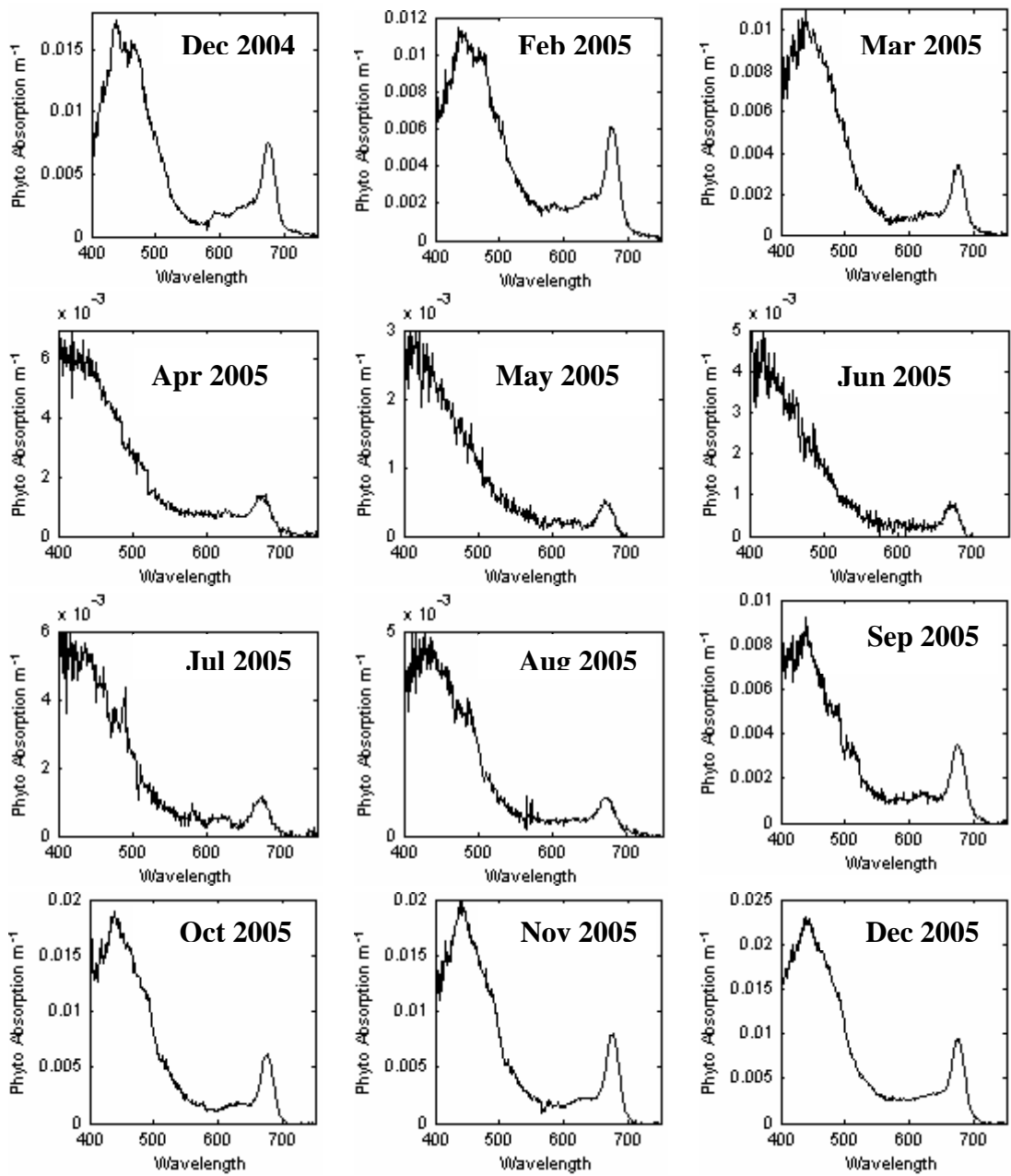
Figure 29: Monthly phytoplankton absorption coefficients at METU-IMS time series station (see figure 4 for station location and latitude and longitude values are given in table 4).

3.3.2. CDOM (Colored Dissolve Organic Matter).

First CDOM measurements were done in Western Black Sea during the 2001 May-June cruise. This cruise ended at July 2001 in the Mediterranean (Figure 3). Highest CDOM absorption values were measured at the Western Black Sea (including Marmara), then Aegean Sea, Western and Eastern Mediterranean Sea, respectively (Figure 30). Shapes and magnitudes of the CDOM curves obtained for all stations in the Western Black Sea were similar. The CDOM absorption coefficients at the shorter wavelengths were very variable between the regions. The Western Black Sea CDOM absorption coefficients between 400 to 500 nm are ten to fifty times higher than the other regions within the same wavelength range. As clearly seen from Figure 30, CDOM absorption coefficient values are decreasing from the Western Black Sea to the Mediterranean Sea.

Figure 30: Comparison of the CDOM absorption coefficients collected from different regions during May-July 2001 (see figure 3, 4 for station locations and latitude and longitude values are given in table 4).

In 2005, most of the samples were collected from the North Eastern Mediterranean. According to the CDOM absorption coefficients, two sub regions were separated (Figure 31).

    a. Offshore
    b. Coastal
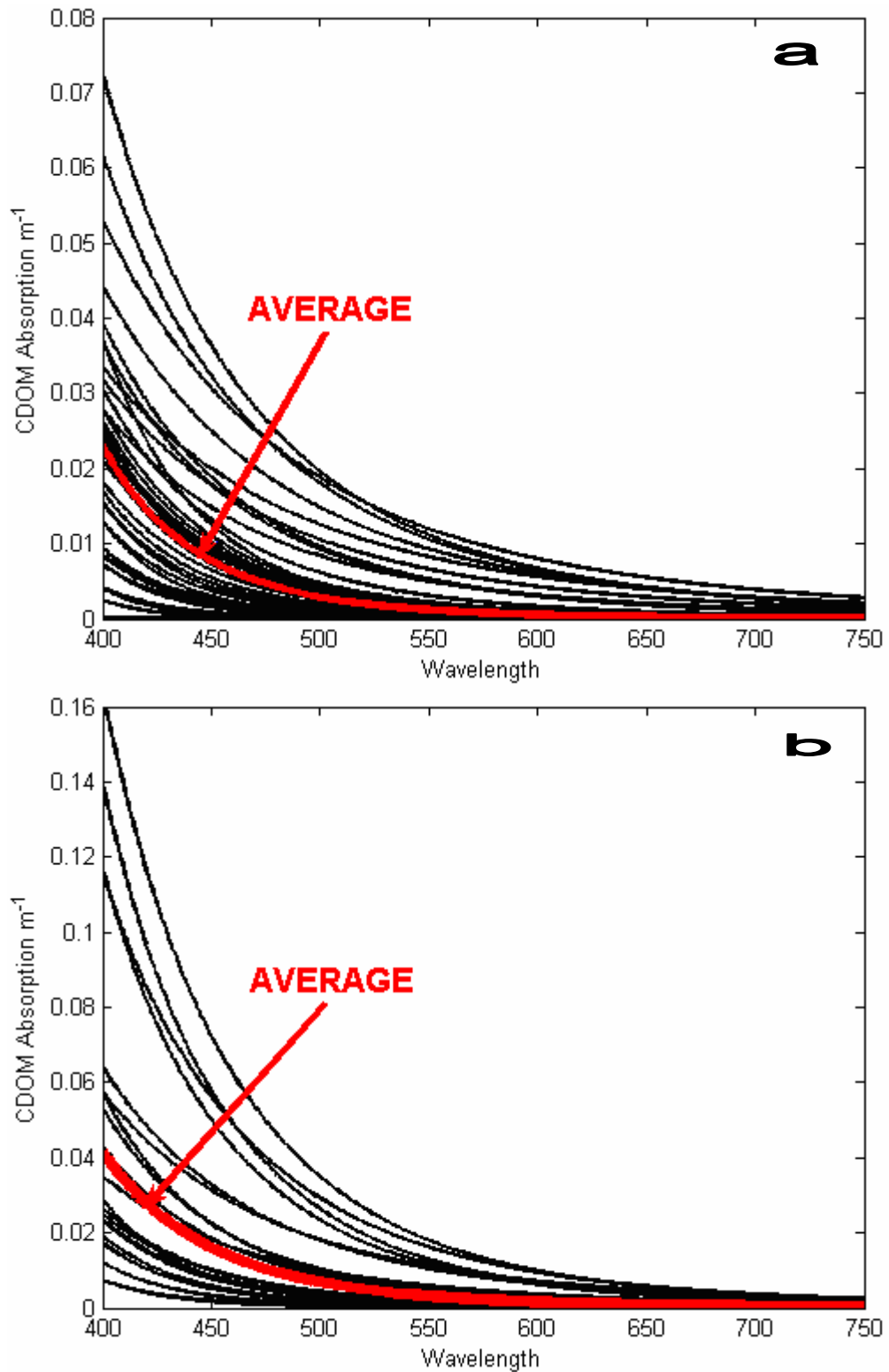
Figure 31: Average North Eastern Mediterranean CDOM coefficients, a: Offshore, b: Coastal (see figure 3, 4 for station locations and latitude and longitude values are given in table 4).

Although, the particle absorption pattern of the Iskenderun Bay is special, the average CDOM absorption coefficients were not different than the average coastal North Eastern Mediterranean CDOM absorption coefficients (Figure 32).
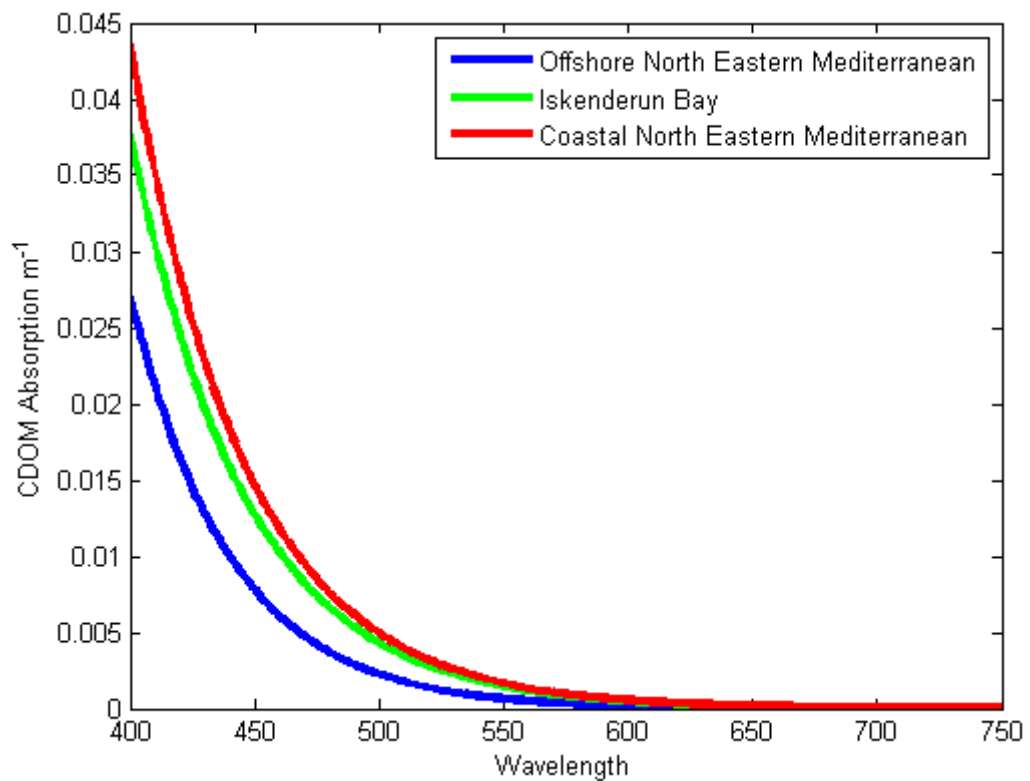
Figure 32: Comparison of the CDOM absorption coefficients within the North Eastern Mediterranean and Iskenderun Bay.

The data collected from the North Eastern Mediterranean was distributed during the whole year. Coastal and offshore waters of the North Eastern Mediterranean were covered. Besides the spatial coverage, monthly measurements have been taken from METU-IMS time series station (see figure 4 for station location and latitude and longitude values are given in table 4). The CDOM

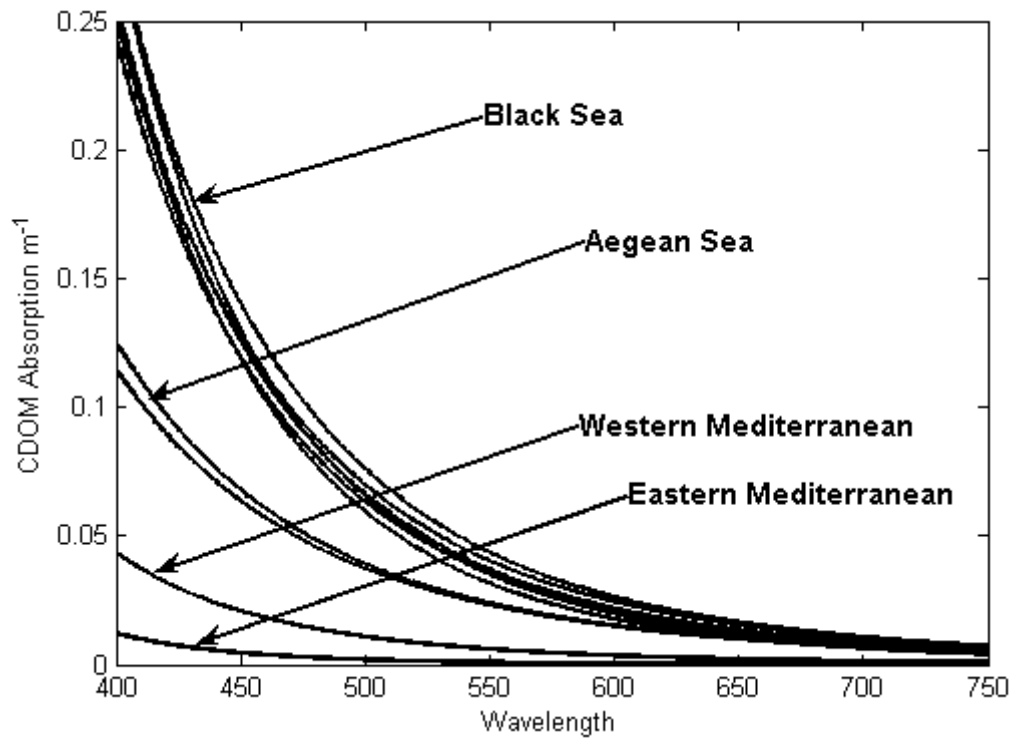absorption coefficients during the sampling period fluctuated seasonally, which is not observed in any other bio-optical measurements (e.g. particle absorption). CDOM absorption coefficients were relatively higher during February, April, July, and October. In February, extreme CDOM absorption values were recorded (Figure 33). In contrast to February very low CDOM absorption values were recorded in June (Figure 33).
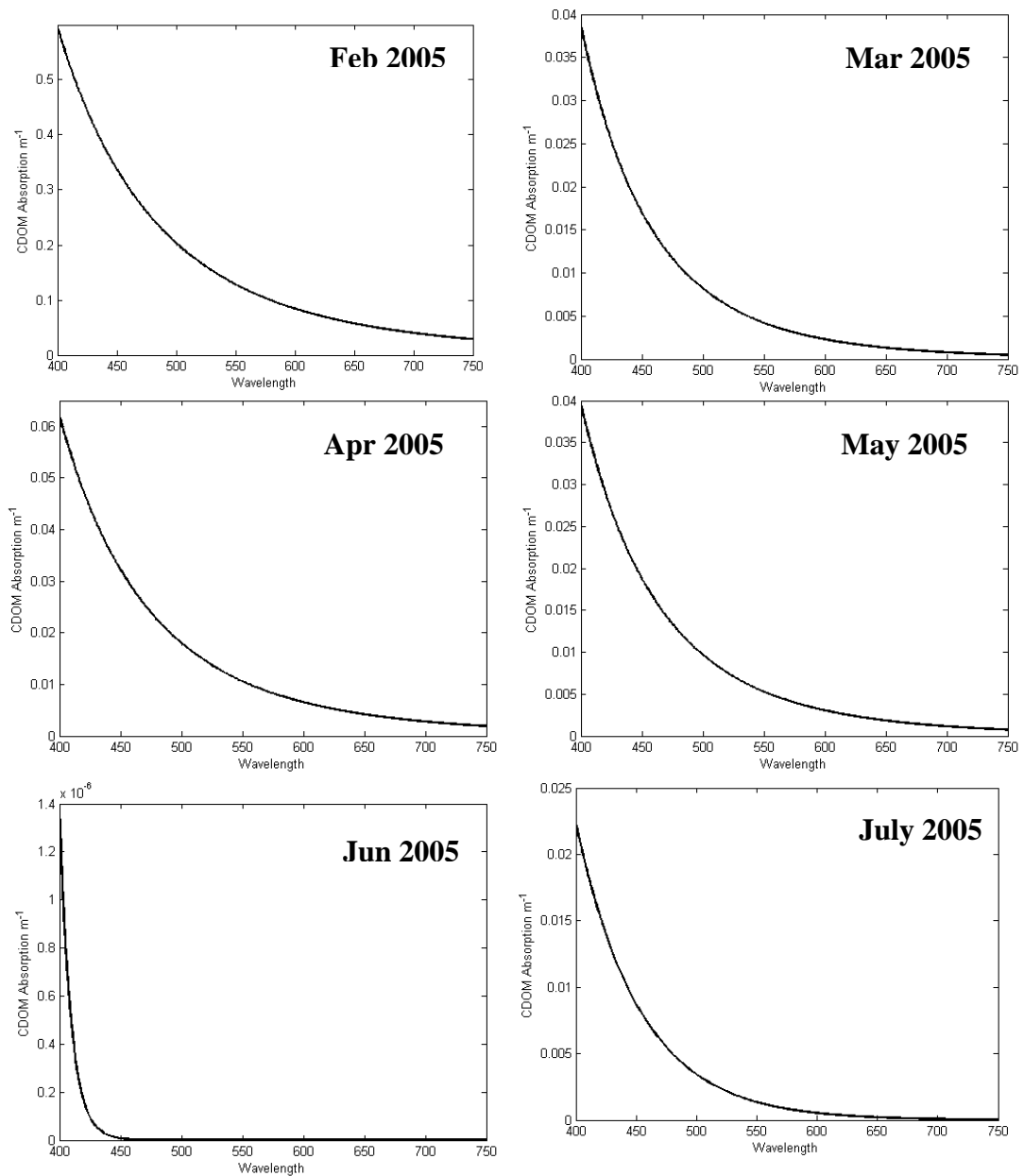
Figure 33: CDOM measurements from METU-IMS Time Series Station (see figure 4 for station location and latitude and longitude values are given in table 4).

Figure: 33 Continued
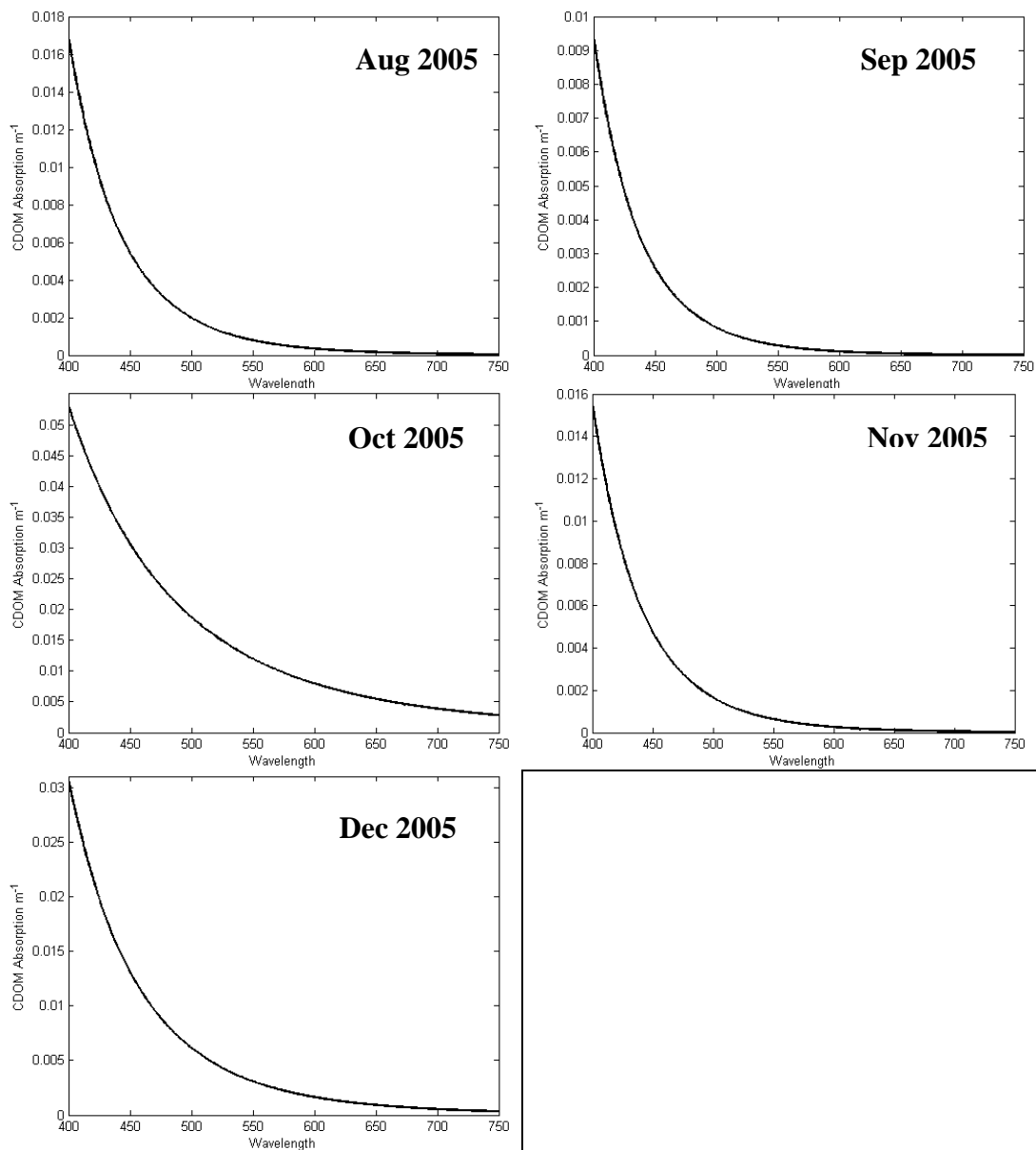
The CDOM absorption coefficients in the North Eastern Mediterranean increased in the coastal waters and decreased in the offshore waters. Although the mean coastal North Eastern Mediterranean CDOM absorption is higher than the offshore, sometimes the coastal CDOM absorption coefficients may decrease. Actually, the mean values of the North Eastern Mediterranean region are very close to each other, because higher and lower absorption values are distributed in the whole region (Figure 34, 35). The stations G50T00 and G44S52 (see figure 4 for station locations and latitude and longitude values are given in table 4) are about 10

knots away from each other and located nearly at the same distance from the shoreline. However, the CDOM absorption coefficients are differentiated (Figure 34). Determination of the regional properties is very difficult, because of the availability of the wide range of CDOM absorption coefficients in the regions (Figure 34, 35).
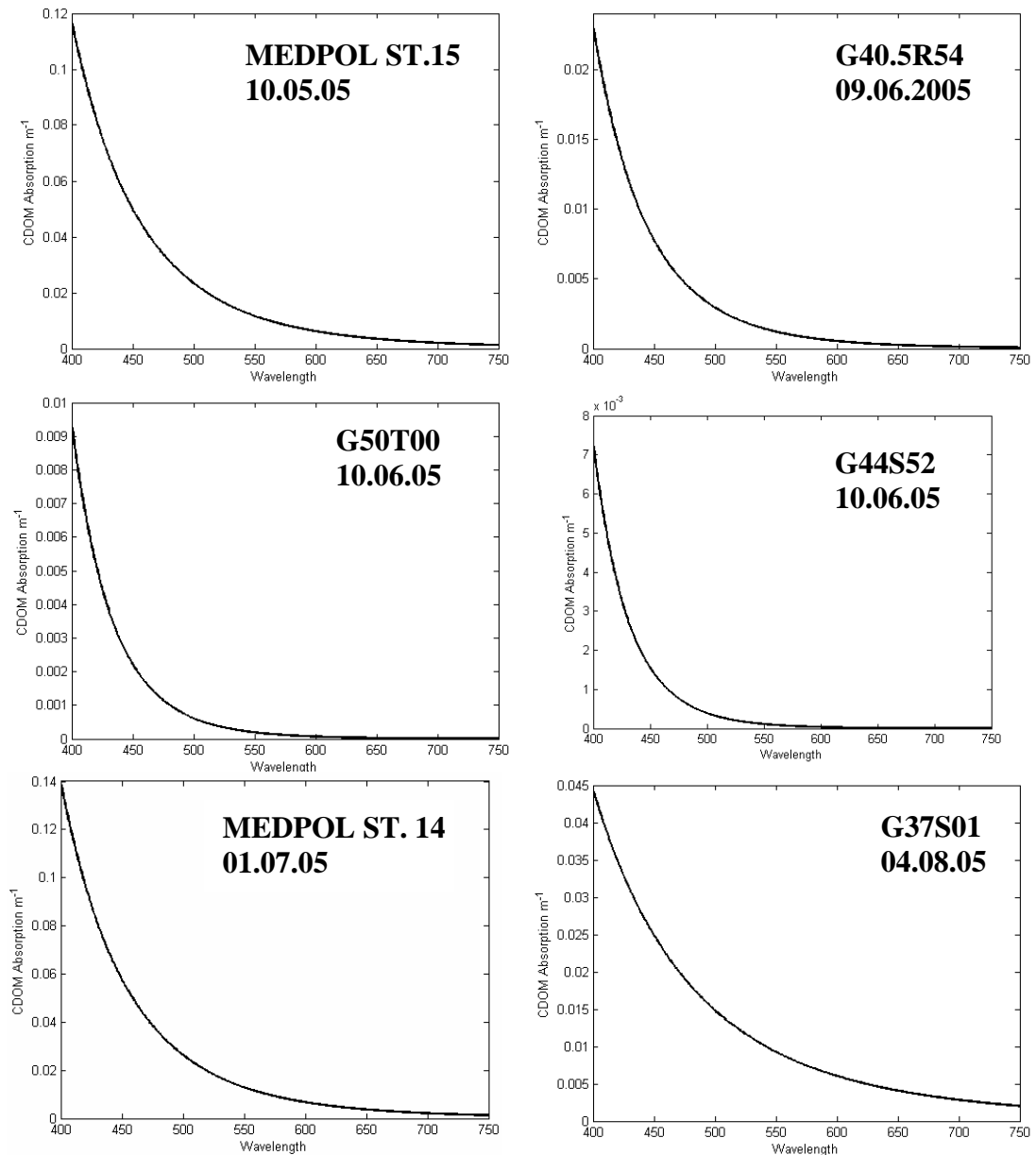
Figure 34: CDOM measurements from different stations and different periods from the North Eastern Mediterranean (see figure 4 for station locations and latitude and longitude values are given in table 4).
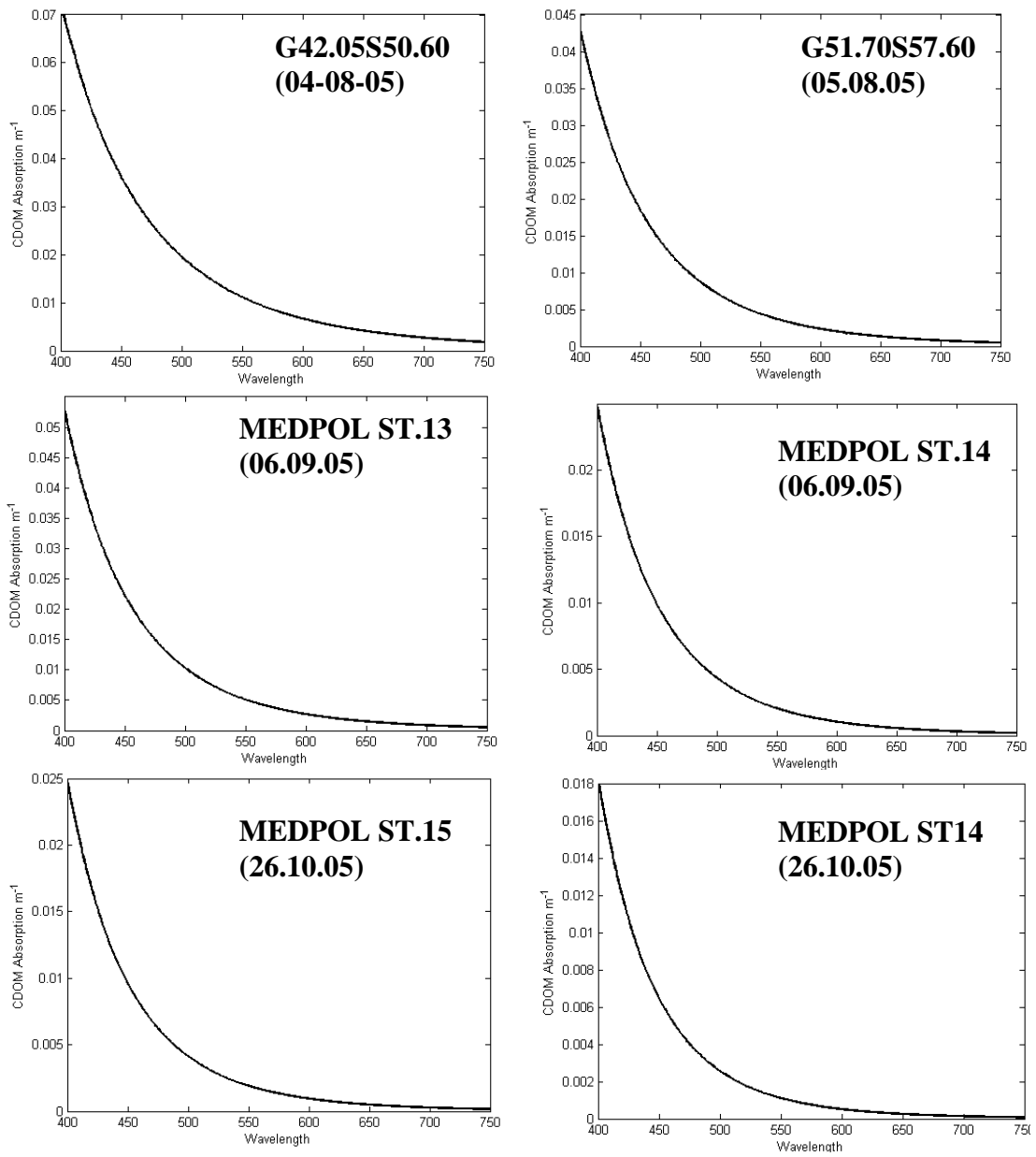
Figure 35: CDOM measurements from different stations and different periods from the North Eastern Mediterranean (see figure 4 for station locations and latitude and longitude values are given in table 4).

3.3.3 Spectral Irradiance Measurements

Distribution of the spectral irradiance, reflectance and diffuse attenuation coefficients are significantly changed from Western Black Sea to Mediterranean. Measurements in the relatively productive Western Black Sea coastal waters show that the spectral distribution of downward irradiances reached at maximum at 550 nm or at 530 nm, which indicates the high chlorophyll concentration (Figure 36, 37). The upward irradiance at the region shows similar variability with downward irradiance. Relatively high reflectance of 6 % in the green (550 nm) observed at station L20M30 as compared to 3 % reflectance at station L50P15 (see figure 3 for station locations and latitude and longitude values are given in table 4) (Figure 36, 37). It should be noted that these two stations were sampled with 10 days delay and changes in optical characteristics were expected. The downward diffusivity at surface exhibited a minimum value around 550 nm and 530 nm at stations L20M30 and L50P15 (see figure 3 for station locations and latitude and longitude values are given in table 4) respectively, at. It appears that the minimum value of the downward diffusivity shifted to higher wavelengths with increasing depth which can be attributed to the increase or stable in chlorophyll with depth (Figure 36, 37).

The station in the Marmara Sea display same characteristics as observations in the Western Black Sea as described above except very low reflectance (1.75 %) at surface (Figure 38). This may be due to the high anthropogenic input to the Marmara Sea which results in high absorbance of the light. The ocean color in the Western Black Sea was green and homogenous at upper 30 m (Figure 38).

Figure 36: Light measurements from West Black Sea station L20M30 (see figure 3 for station location and latitude and longitude values are given in table 4). Date: 16.06.01.

**Figure 37:** Light measurements from Western Black Sea station L50P15 (see figure 3 for station location and latitude and longitude values are given in table 4). Date: 26.05.01.

81
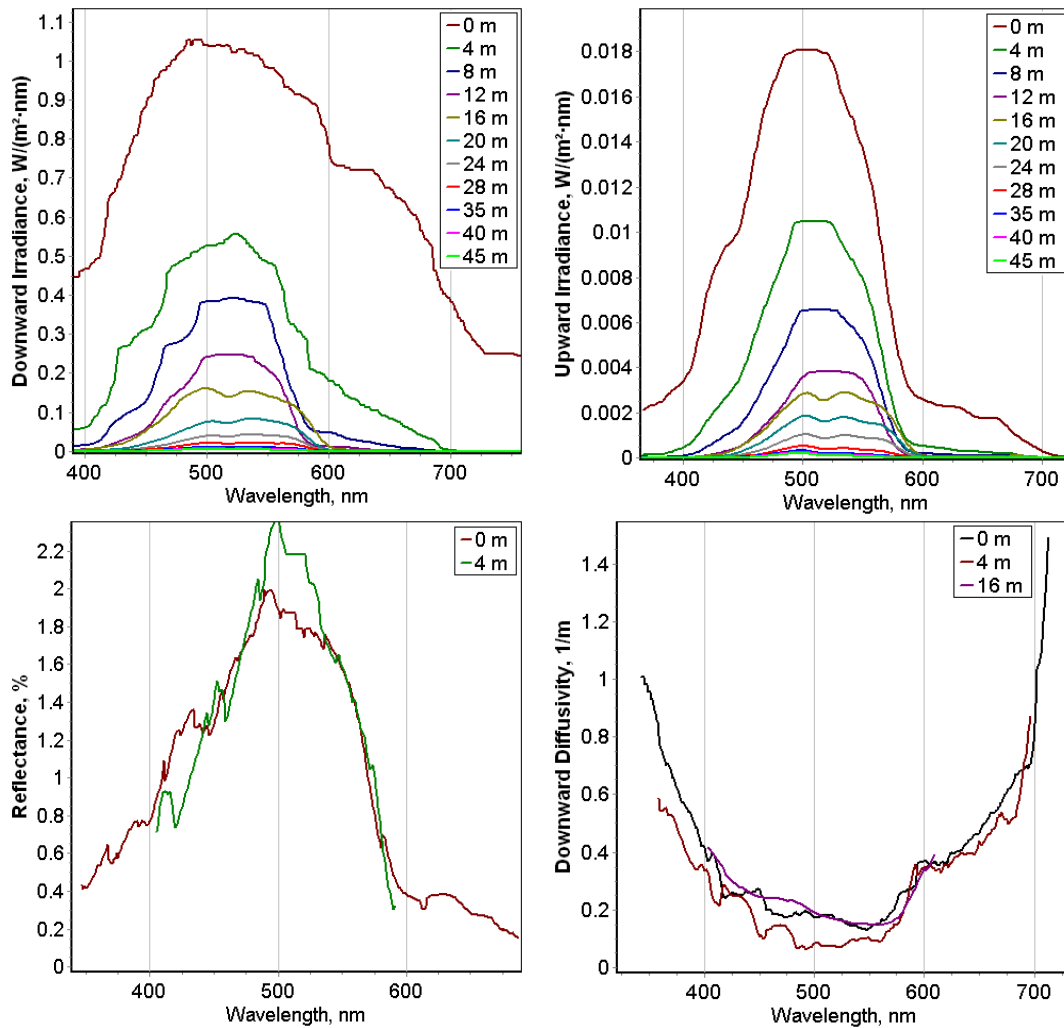
Figure 38: Light measurements from the Sea of Marmara station K50J34 (see figure 3 for station location and latitude and longitude values are given in table 4). Date: 24-06-01.

Spectral irradiance profiles changed in the Northern and the Southern Aegean Sea. Reflectance increases 5 % and 7.5% in the Northern and Southern Aegean, respectively which are greater than that measured in the Western Black Sea. The ocean color in the Aegean was blue. Reflectance maximum values are shifted towards shorter wavelengths in addition to the increasing. Another peculiarity in the spectral distribution of irradiance profiles and reflectance was the existence of the secondary peak or a shoulder at 410 nm (Figure 39, 40).

Figure 39: Light measurements from Northern Aegean Sea station; J37H35 (see figure 3 for station location and latitude and longitude values are given in table 4). Date: 25-06-01.

Figure 40: Light measurements from Southern Aegean Sea station; G35K35 (see figure 3 for station location and latitude and longitude values are given in table 4). Date: 28-06-01.

Characteristics of the spectral light field are fairly similar in the North Eastern Mediterranean and the Southern Aegean (Figure 41).

Irradiance and specially reflectance peaks were shifted during the winter in the North Eastern Mediterranean. The peaks occurred around 400-450 nm in July 2001 shifted towards 450 nm in December 2003 (Figure 42). All the stations visited in December 2003 were situated in the offshore waters, and showed similar spectral distribution. This shift from blue to blue-green can be attributed to the autumn bloom

observed in December 2003 and the surface chlorophyll values are two times higher than in July 2001 and in December 2003 (see Figure 17).

Figure 41: Light measurements from North Eastern Mediterranean Sea, station; F30Q30 (see figure 4 for station location and latitude and longitude values are given in table 4). Date: 03-07-01.
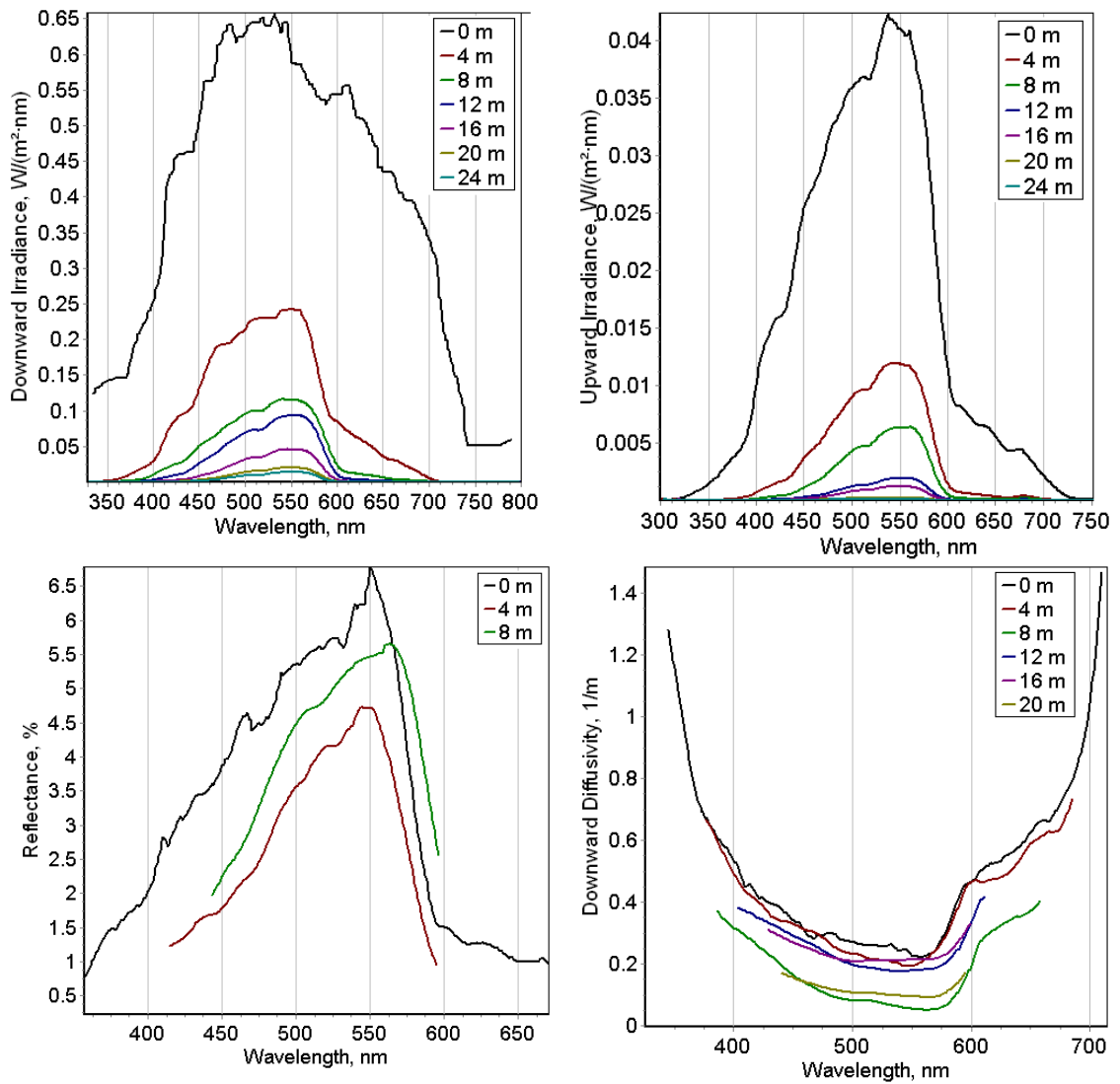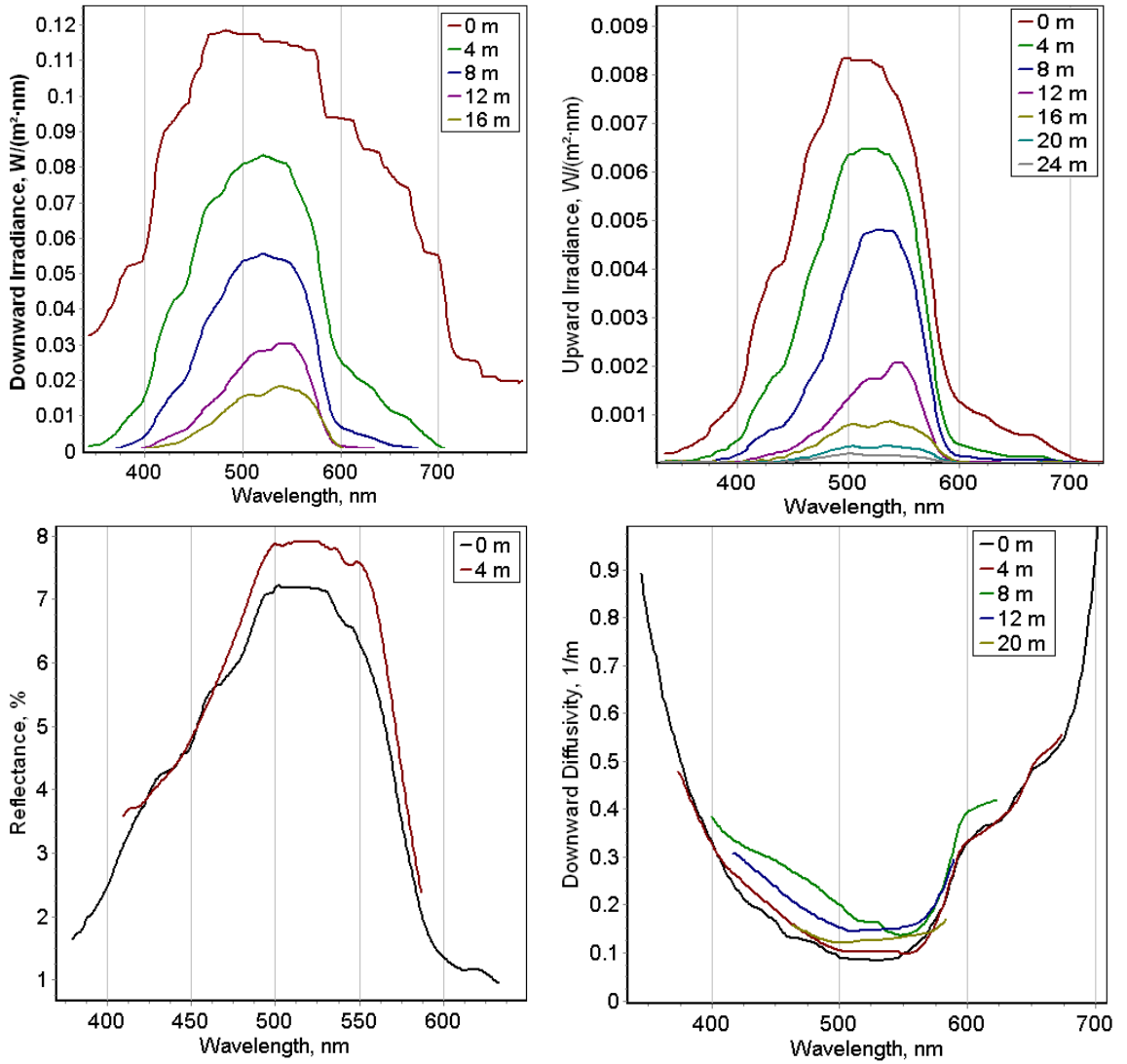
Figure 42: Light measurements from North Eastern Mediterranean, station; G00Q45 (see figure 3 for station location and latitude and longitude values are given in table 4). Date: 20-12-03.

The temporal variability of the spectral light field in the North Eastern Mediterranean is changed seasonally. However, only two periods were observed. Main difference between autumn-winter and summer-spring is the shifted reflectance peak from 450-550 nm (Figure 43) to 400-450 nm (Figure 44) from winter to summer (Figure 43, 44). This pattern is clearly demonstrated by the measurements in 2004 and 2005.

Figure 43: Light measurements from METU-IMS time series station (see figure 4 for station location and latitude and longitude values are given in table 4). Date: 16-03-04.
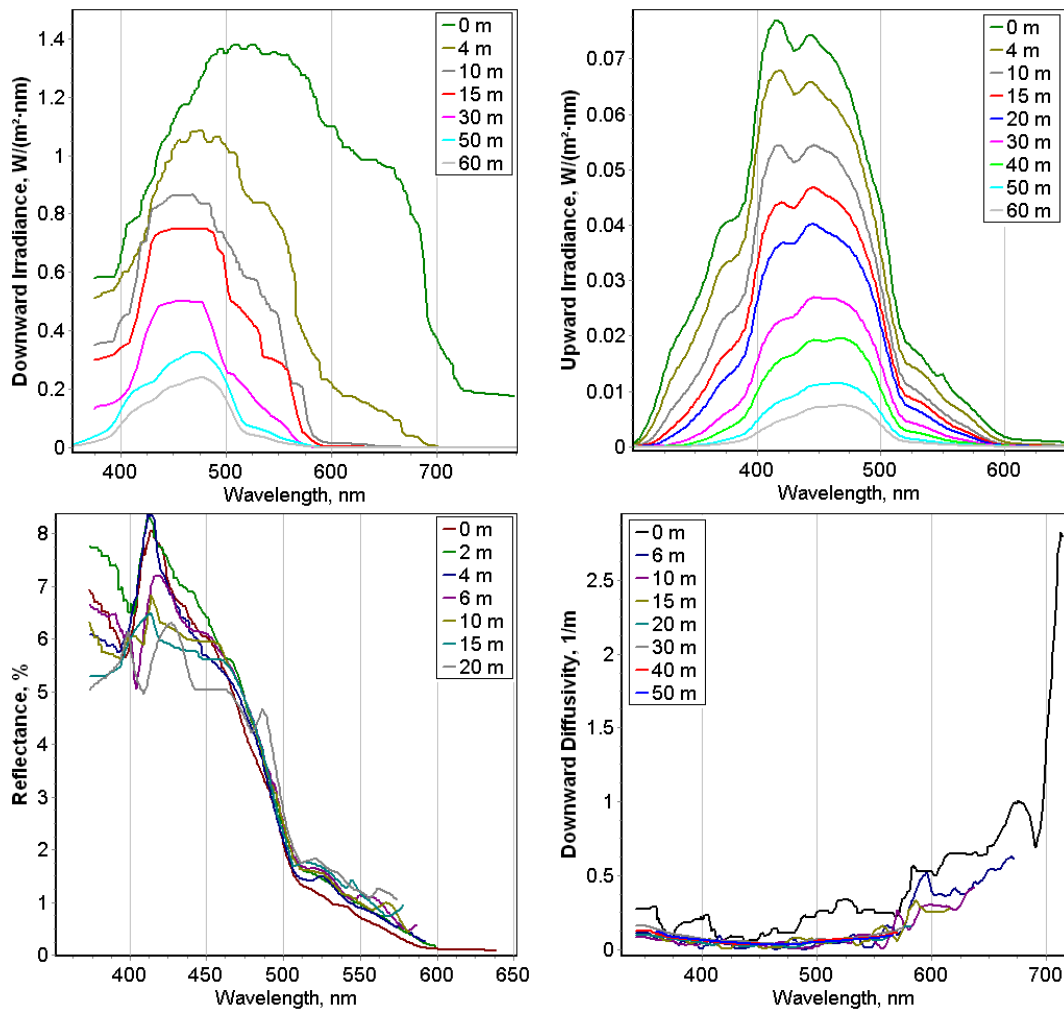
Figure 44: Light measurements from METU-IMS time series station (see figure 4 for station location and latitude and longitude values are given in table 4). Date: 19-07-04.

Winter summer differentiation has been observed, in 2005 measurements of the METU-IMS time series station. The measurements carried out in the METU-IMS time series station in 2005 clearly show the shift of the peak from 450-500 nm in winter to 400-450 nm in summer. During the winter period reflectance peak is situated at around 500 nm and the peak shifted in April (Figure 45, 46). After April until October, during the summer period position of the reflectance peak was stable around 400 nm (Figure 47). Reflectance peak started to shift at October (Figure 48).
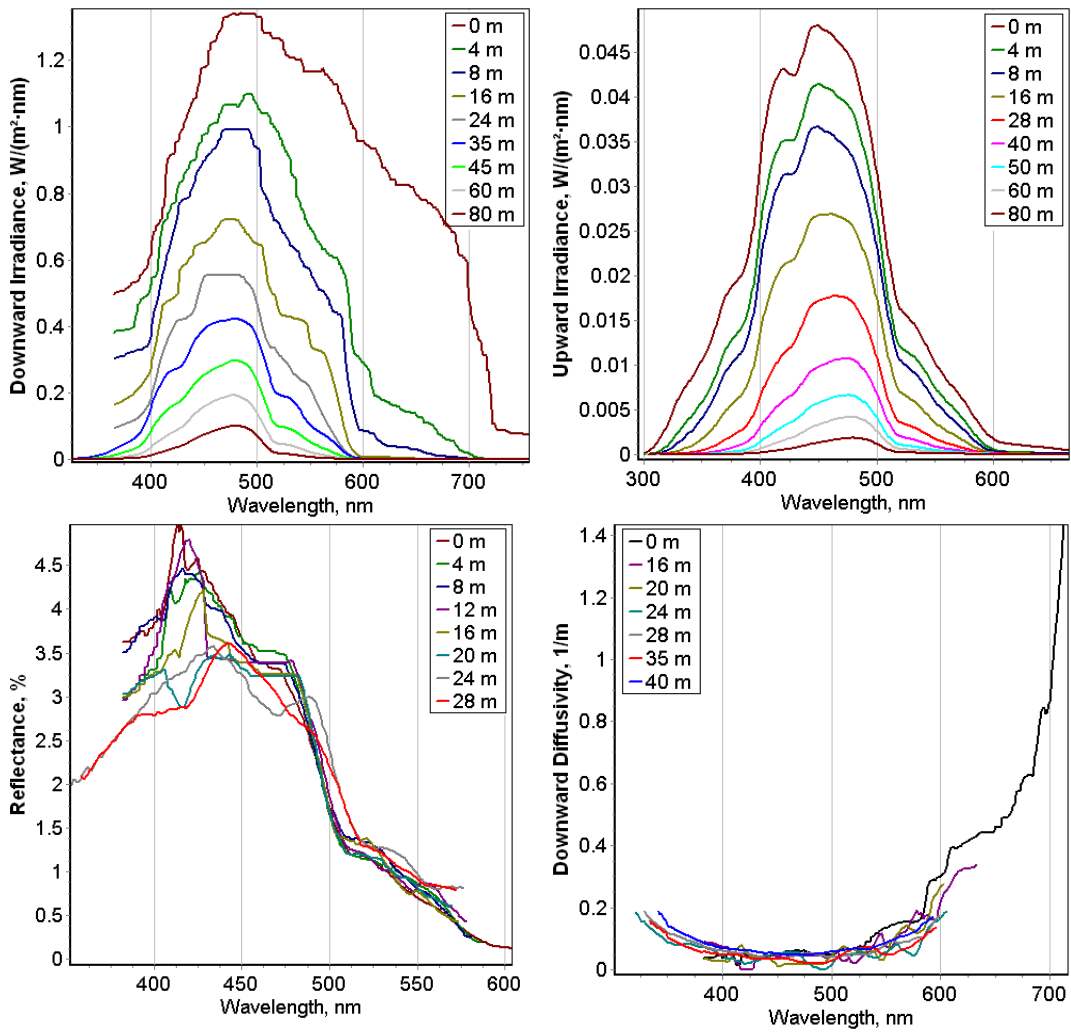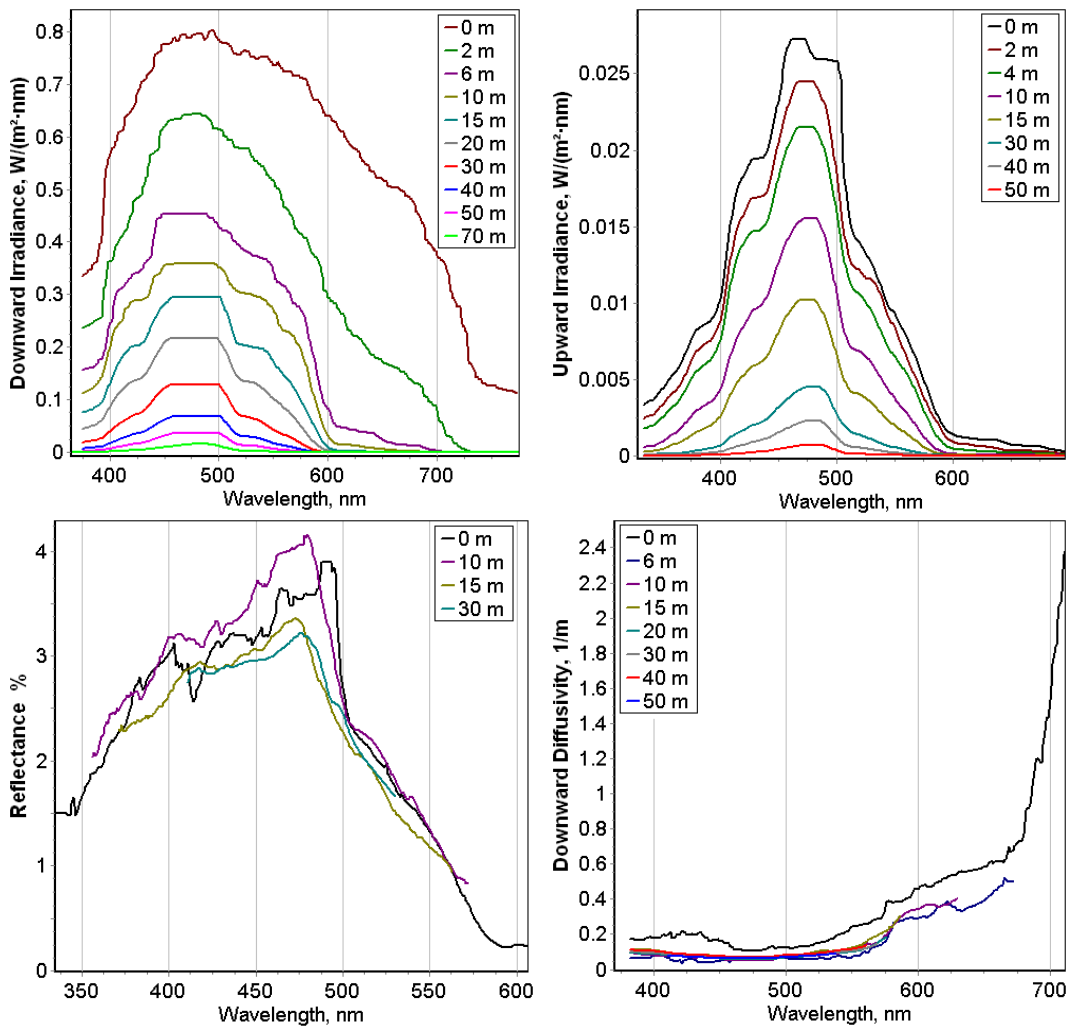
Figure 45: Light measurements from METU-IMS time series station (see figure 4 for station location and latitude and longitude values are given in table 4). Date: 10.02.05.
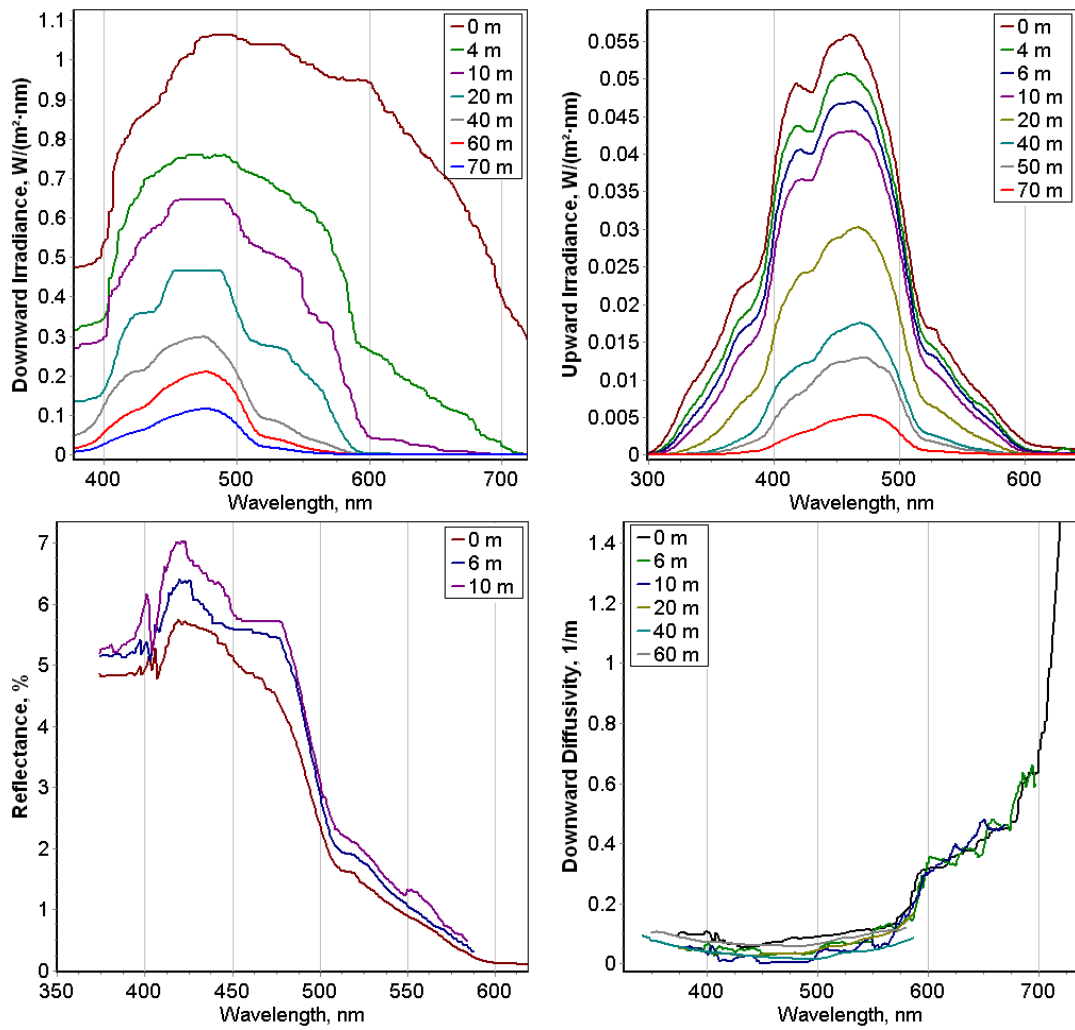
Figure 46: Light measurements from METU-IMS time series station (see figure 4 for station location and latitude and longitude values are given in table 4). Date: 21.04.05.
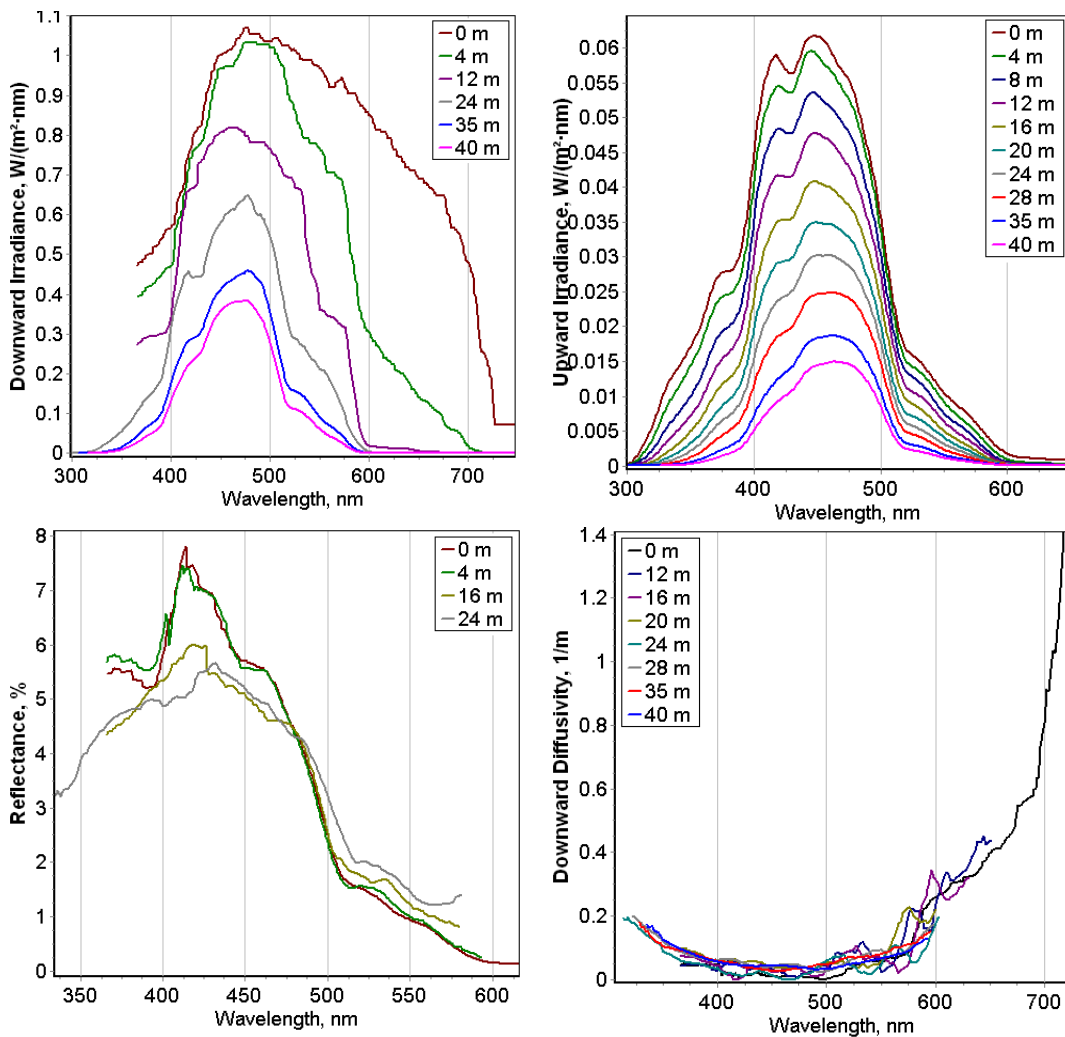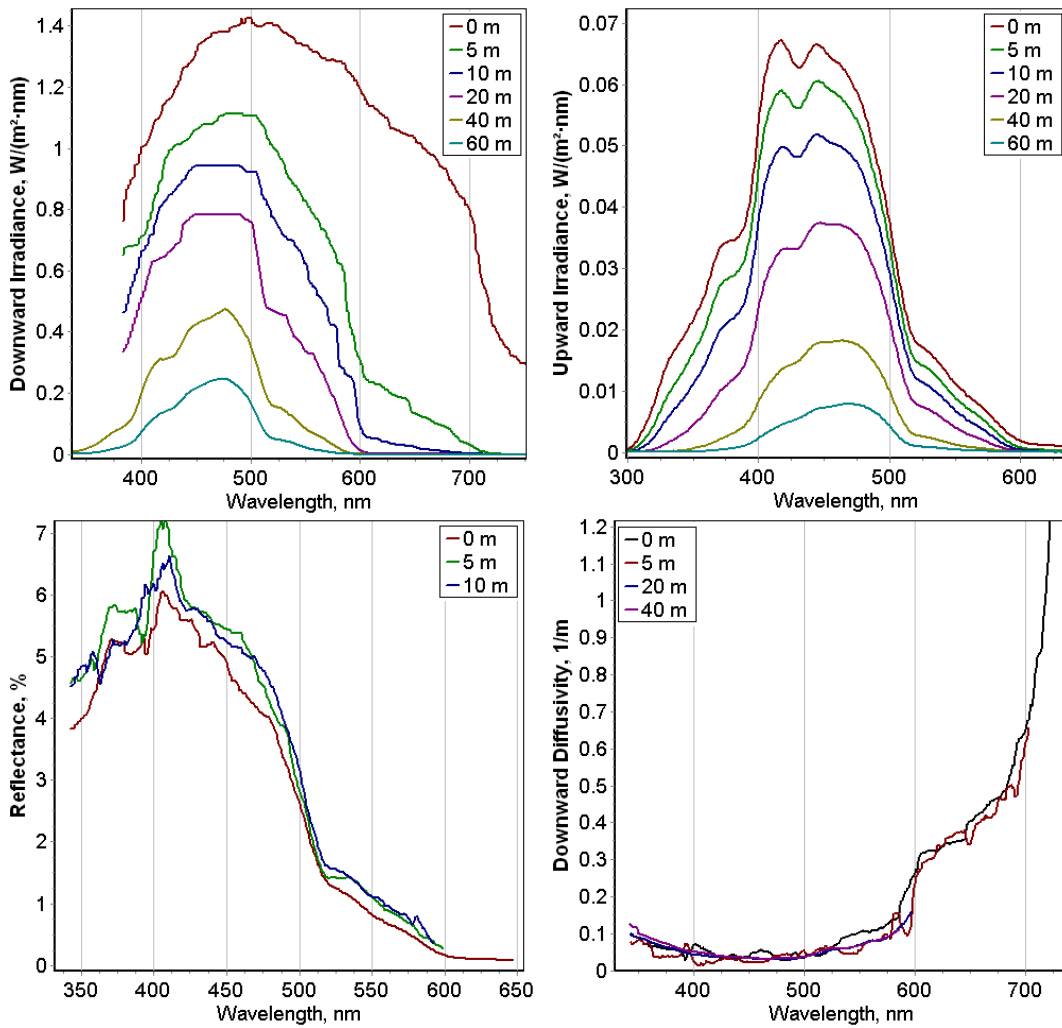
Figure 47: Light measurements from METU-IMS time series stations (see figure 4 for station location and latitude and longitude values are given in table 4). Date:02.07.05.
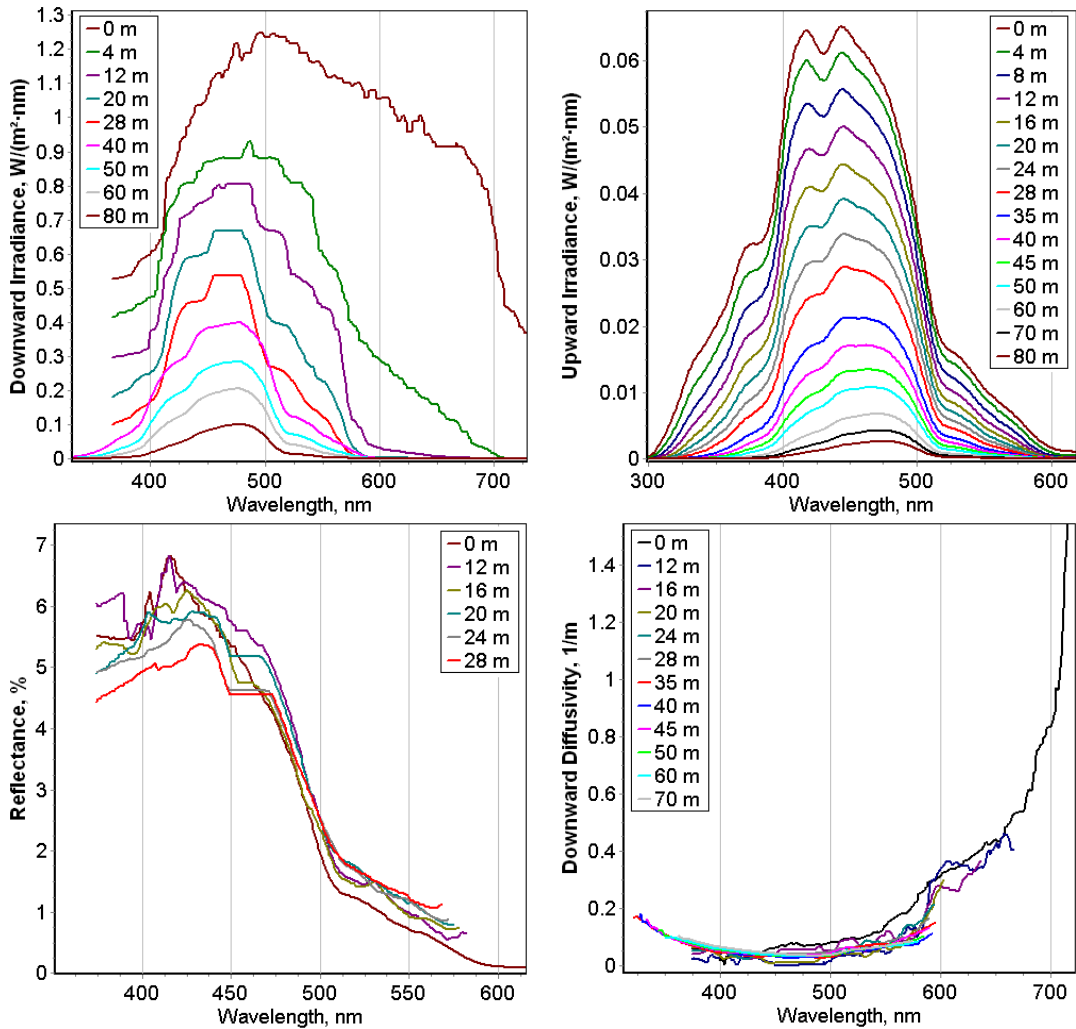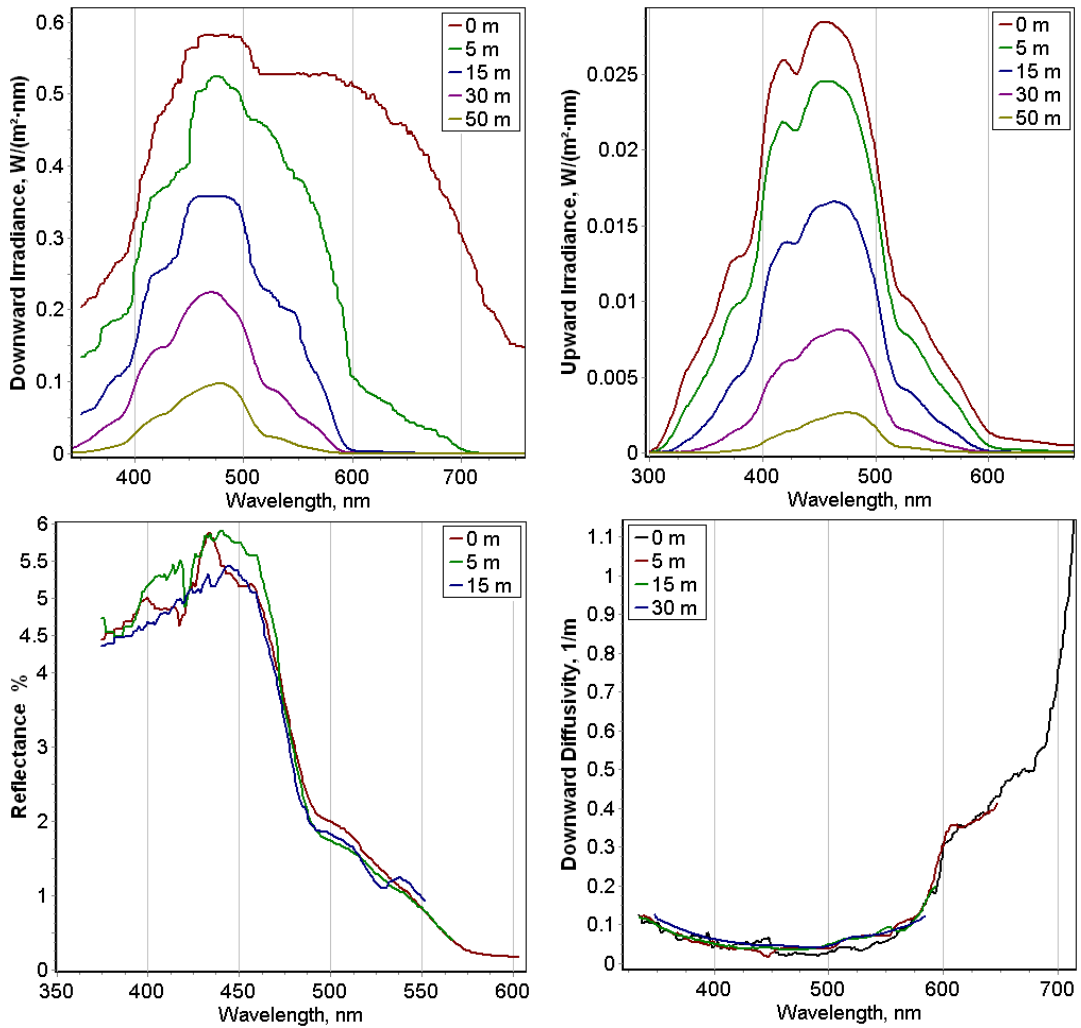
Figure 48: Light measurements from, METU-IMS time series station (see figure 4 for station location and latitude and longitude values are given in table 4). Date: 27.10.05.

The measurements carried out at coastal regions of the North Eastern Mediterranean showed similar spectral characteristics as the Western Black Sea. According to the measurements, the spectral characteristics in the different regions and periods in the offshore North Eastern Mediterranean did not differ significantly (Figure 49, 50). The reflectance peaks observed at the coastal regions were placed between 450-500 nm. In some cases a broaden reflectance peak may observed between 400 to 500 nm. In station G31S33.30 (see figure 4 for station locations and

latitude and longitude values are given in table 4 Date: 23.05.05) the reflectance peak broadened from 400 to 500 nm (Figure 51).
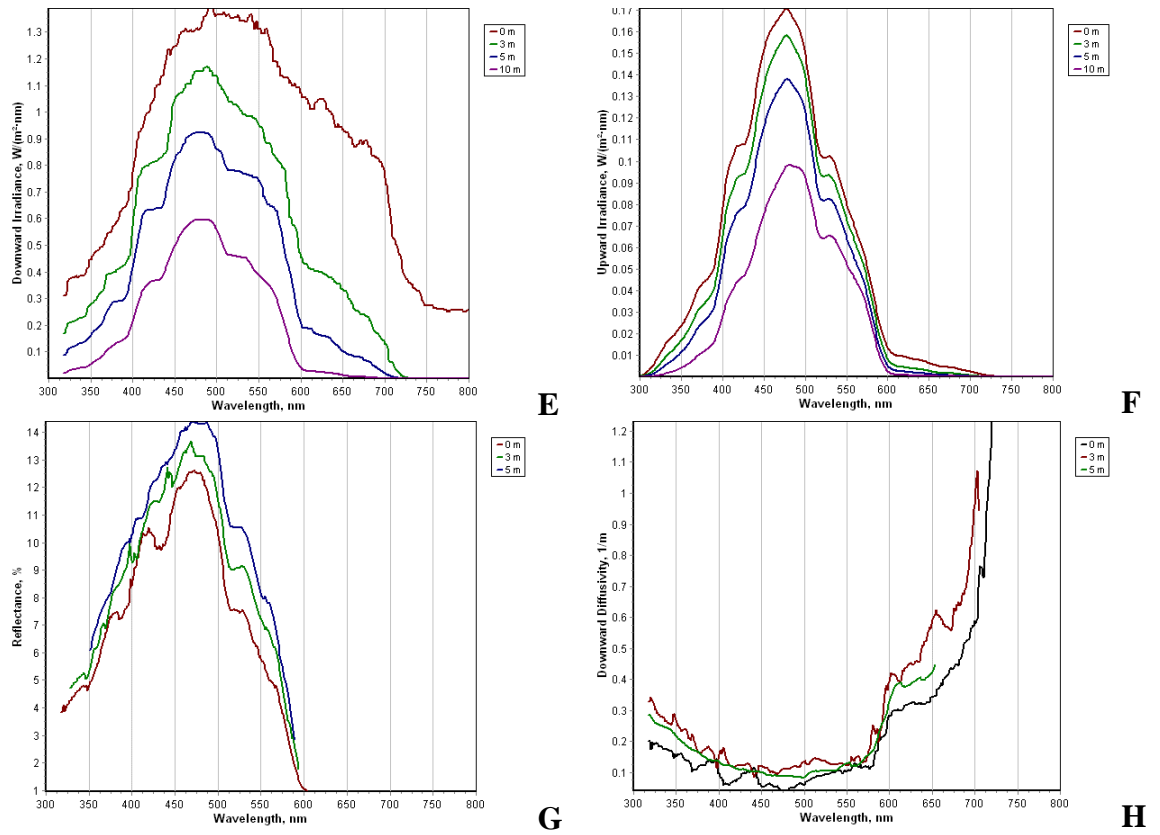
Figure 49: Light measurements from coastal North Eastern Mediterranean station; G33.41S13.61 (see figure 4 for station location and latitude and longitude values are given in table 4). Date: 04.08.05.
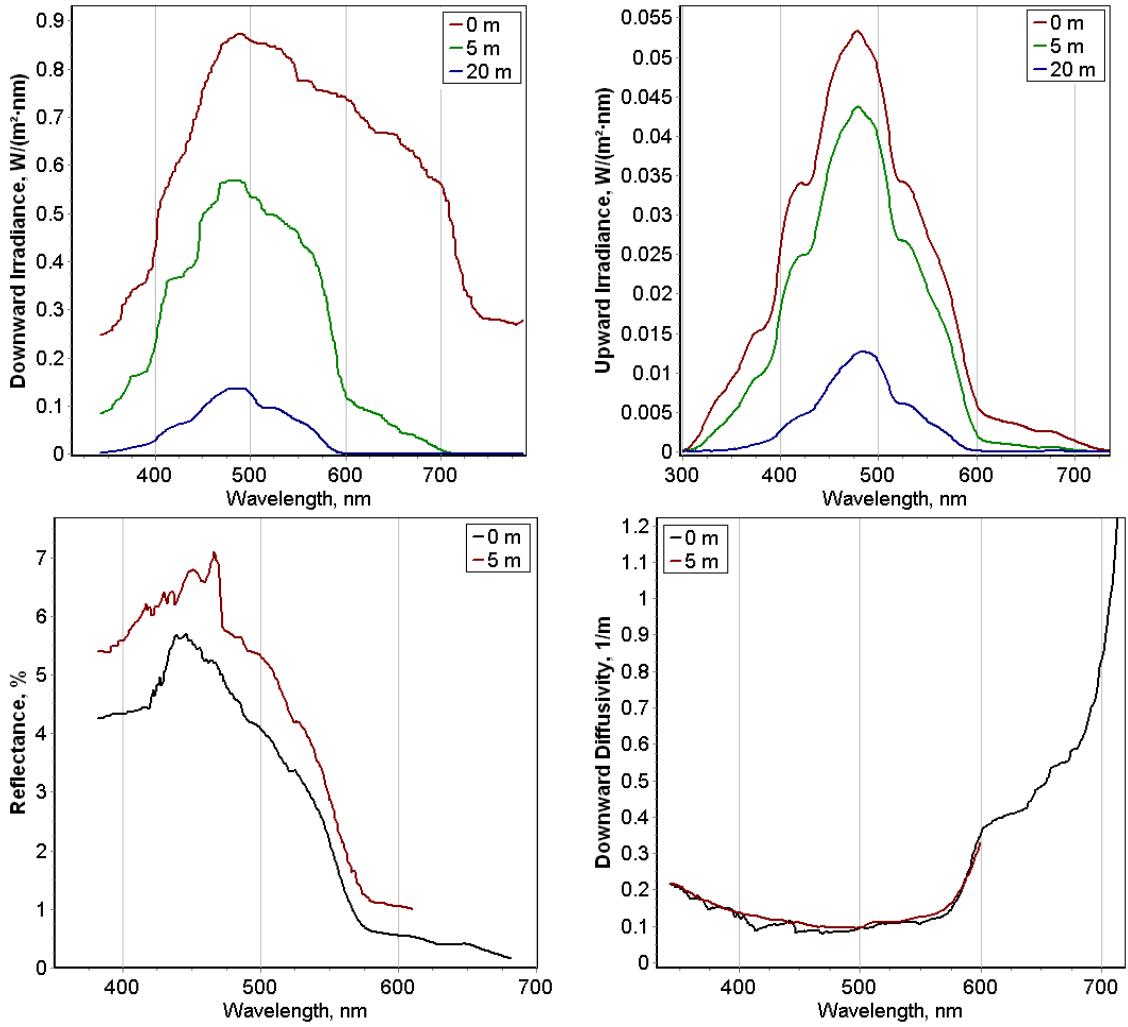
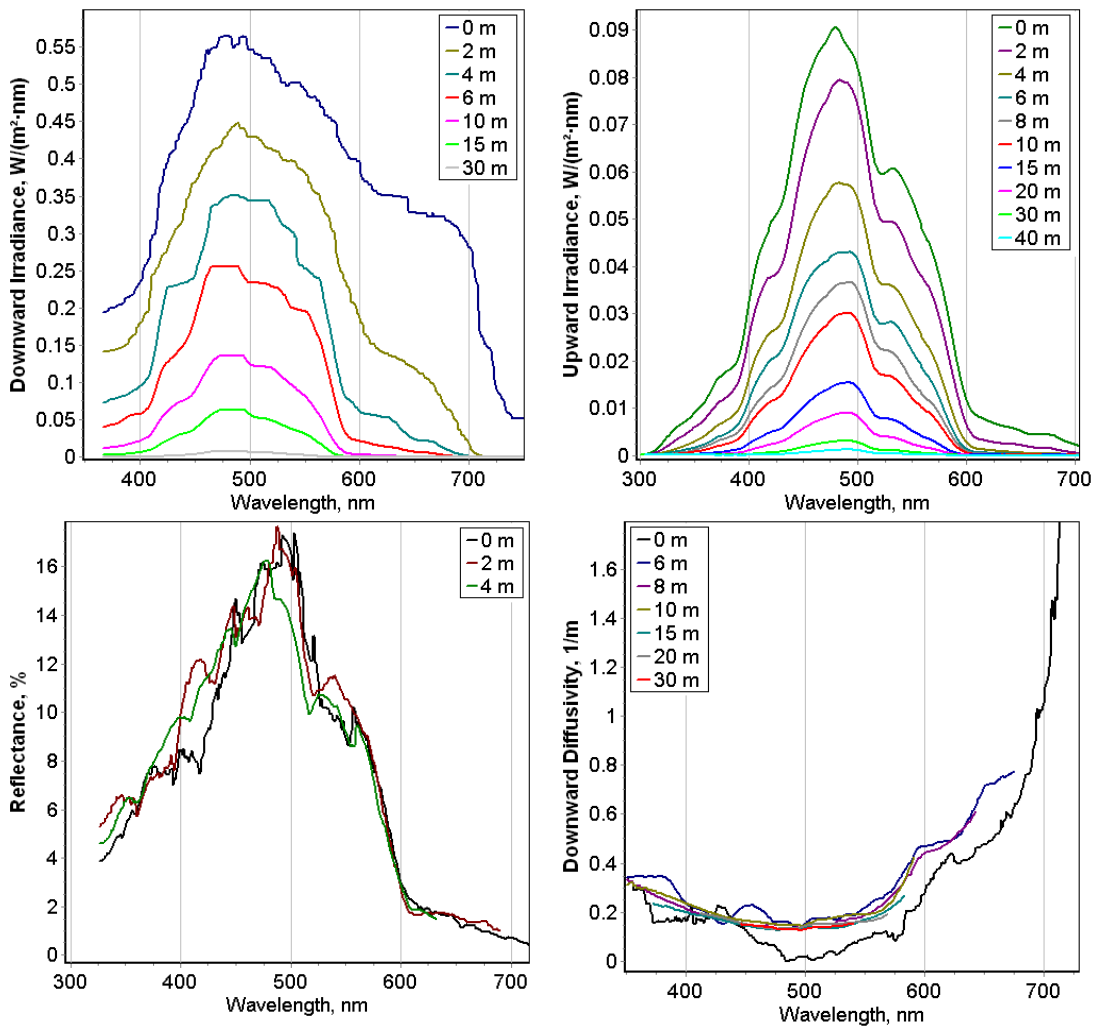**Figure 50:** Light measurements from coastal North Eastern Mediterranean station; Medpol.15 (see figure 4 for station location and latitude and longitude values are given in table 4) Date:26.10.05.
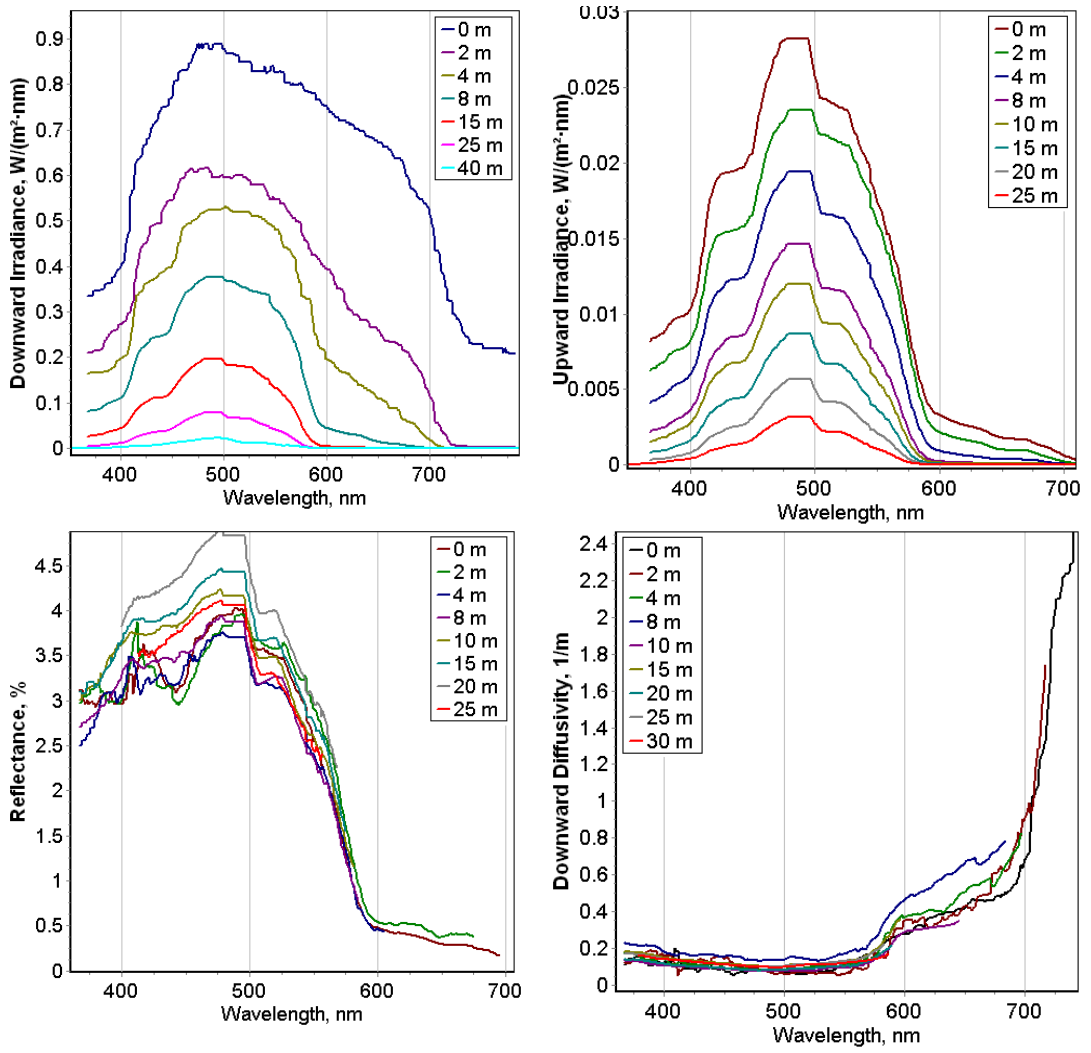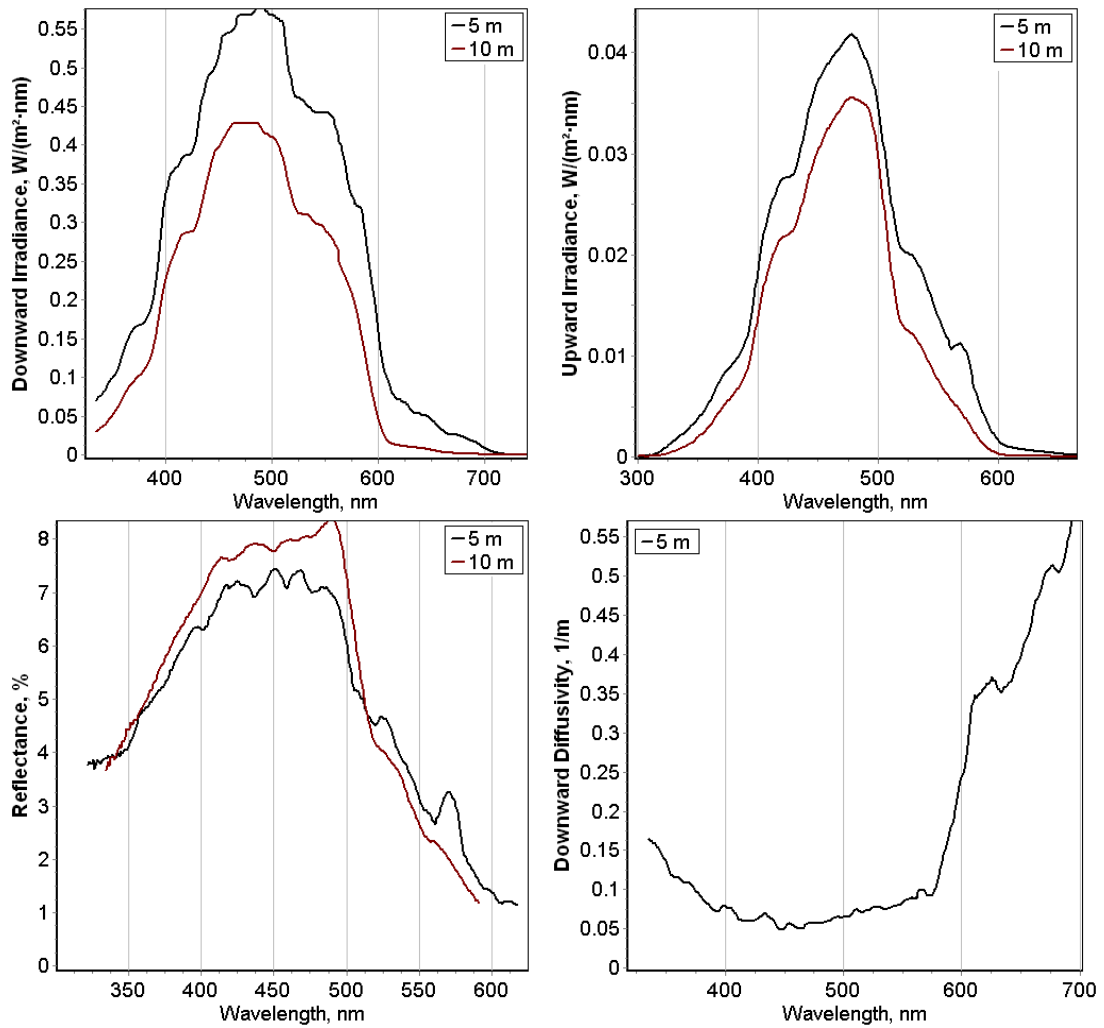
Figure 51: Light measurements from coastal North Eastern Mediterranean station; G31S33.30 (see figure 4 for station location and latitude and longitude values are given in table 4). Date:23.05.05.

Spectral characteristics of the North Eastern Mediterranean were very variable at the offshore depending on seasons and at the coastal regions, other parameters like anthropogenic impact and the phytoplankton concentration are controlling these properties. Although it is hard to compare these measurements qualitatively, the percentage of the reflected light in coastal regions is usually higher than at the offshore.

3.4. Pigment Measurements

The method used to analyze the samples is capable to differentiate 14 different pigments (Baelow et al., 1997). The temporal and spatial distribution of the pigments was determined. Two major regions can be differentiated according to pigment compositions, and concentrations:

a. Western Black Sea

b. Mediterranean Sea

The Western Black Sea region is dominated by fucoxanthin pigment, which is the indicator of the high diatom availability (Figure 52). The chlorophyll a, concentration in the Western Black Sea within sampling period was clearly higher than the Mediterranean, but divinyll chlorophyll was not detected in the Western Black Sea sampling stations. The mean chlorophyll-a, concentration in the Western Black Sea is 2 mg/m^3 (standard deviation = 2.29), and including divinyll chlorophyll-a. North Eastern Mediterranean mean chlorophyll-a was calculated as 0.26 mg/m^3 (standard deviation = 0.36).
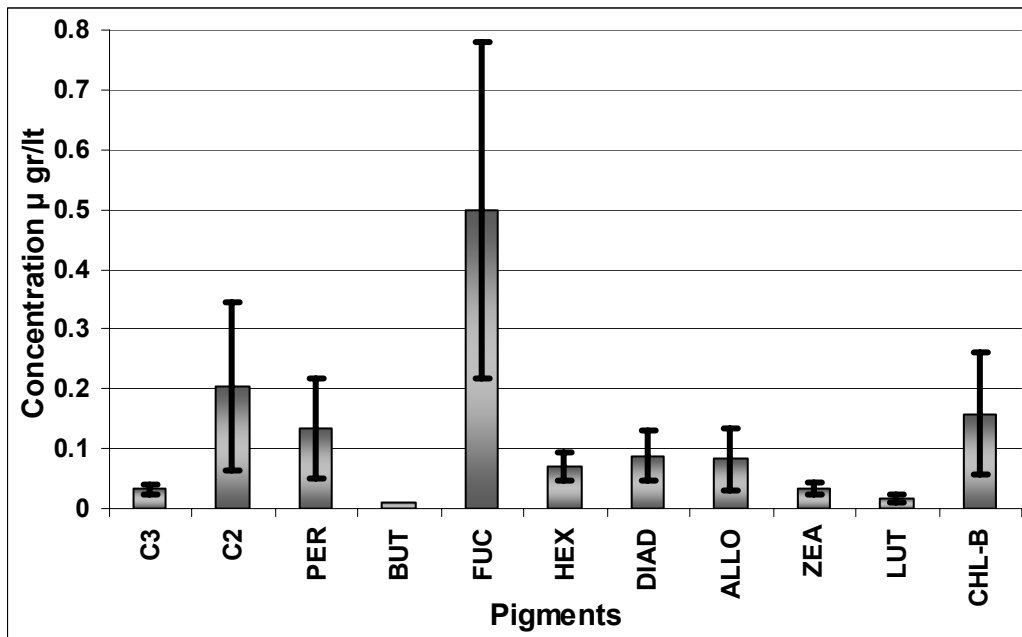
Figure 52: Mean Pigment concentration and composition in the Western Black Sea.

The North Eastern Mediterranean is known as an oligotrophic basin. However, relatively higher river input and shallow shelf areas are also present. Here, therefore, three regions were determined, instead of a single basin. These are:

a: Offshore North Eastern Mediterranean,

b: Coastal North Eastern Mediterranean,

c: İskenderun Bay.

These three sub basins are similar to each other in terms of pigment composition and ratios. However, there are considerable differences, in the total amount of the pigments. Chlorophyll a concentration in the İskenderun Bay, offshore North Eastern Mediterranean and coastal North Eastern Mediterranean are 0.19, 0.175, and 0.75 respectively. Highest chlorophyll-a concentration was observed in the coastal North Eastern Mediterranean where the samples were collected close to the estuaries and drainage of the cities. Zeaxanthin, chlorophyll-b, and divinyll chlorophyll-a, concentrations are higher than the other pigments found in the North Eastern Mediterranean. However, fucoxanthin, divinyll chlorophyll-a, and zeaxanthine are the highest pigments in the Coastal North Eastern Mediterranean, offshore of the North Eastern Mediterranean and İskenderun Bay respectively (Figure 53).
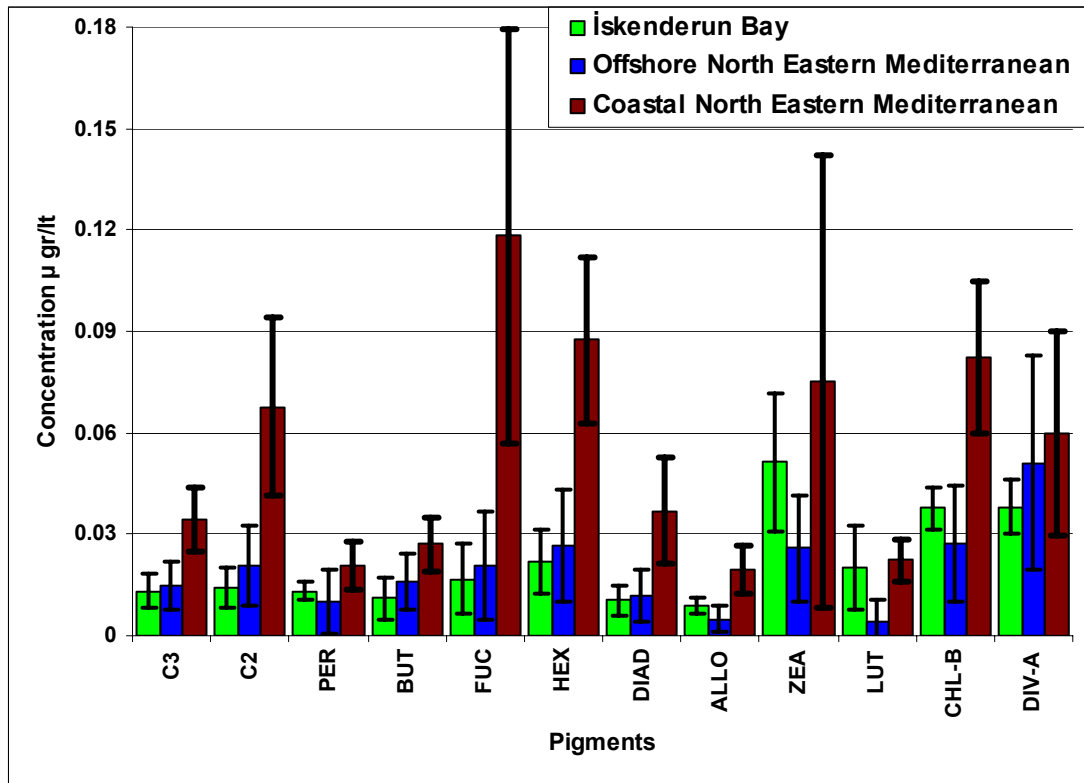
Figure 53: Pigment concentrations and compositions in the North Eastern Mediterranean sub regions chosen in this work.

3.4.1. Chemtax Analysis

HPLC measurements carried out in 2003 and 2005 at more than 100 stations revealed 14 different pigment types, determined using the method described in Barlow et al., (1997). The pigment types and the ratios are used to classify phytoplankton groups (Mackey et. al. 1996, 1997, Higgins and Mackey 2000, Suzuki et al., 2002). HPLC results were used to determine the percent contribution of the phytoplankton groups to the total chlorophyll-*a.*

HPLC results showed obvious difference between the Western Black Sea and the North Eastern Mediterranean Sea (Figure 52, 53). Regarding the Chemtax result, the Western Black Sea was dominated by the diatoms (Figure 54). The coastal and offshore differentiation in the Western Black Sea was not determined.
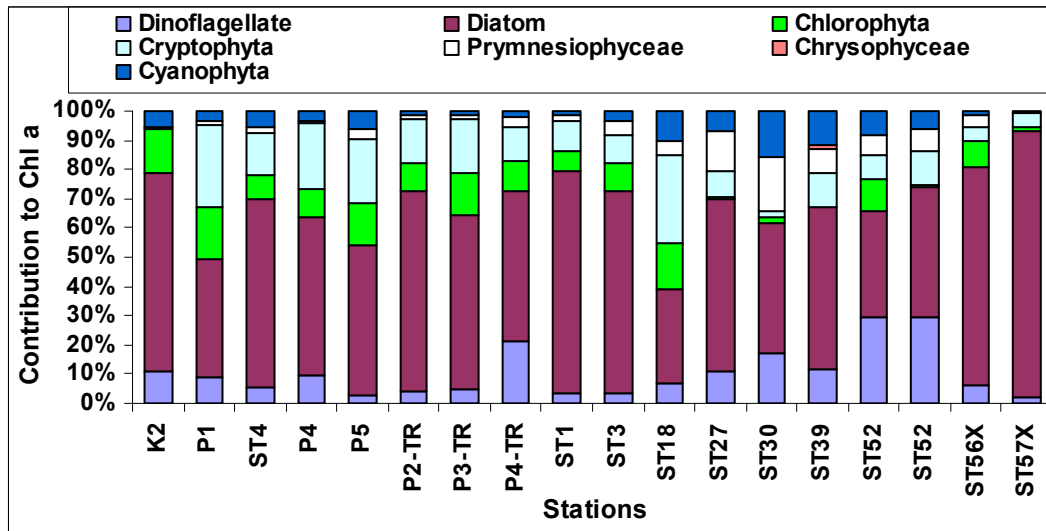
Figure 54: Phytoplankton groups and their contributions to the total chlorophyll-a concentration, in the Western Black Sea (Stations listed in Figure 54 can be seen see figure 4 for station locations and latitude and longitude values are given in table 4).

According to Chemtax analysis, the North Eastern Mediterranean can be considered as consisting of two distinct regions: the offshore and coastal region. Cyanophyta usually dominates offshore waters of the North Eastern Mediterranean. Other groups' contributions to the chlorophyll-a were not as much as the contribution by *Cyanophyta* (Figure 55). In the coastal stations, *Cyanophyta* contribution to the total chlorophyll-a is still high but not as much as the offshore stations (Figure 56).
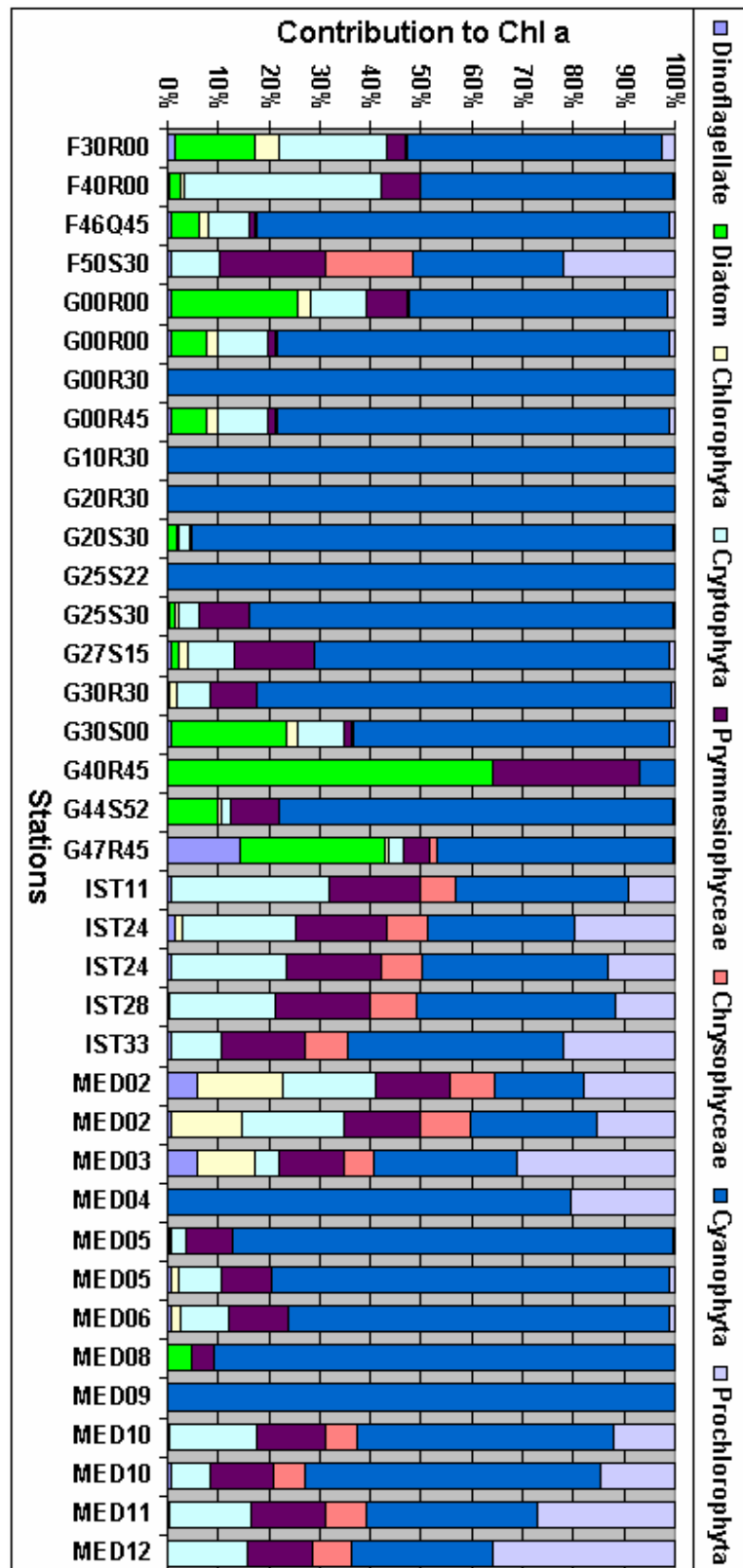
Figure 55: Phytoplankton groups and their contributions to the total chlorophyll-a concentration, in the offshore of the North Eastern Mediterranean (Stations listed in the figure 55, can be seen in figure 4 for station locations and latitude and longitude values are given in table 4).
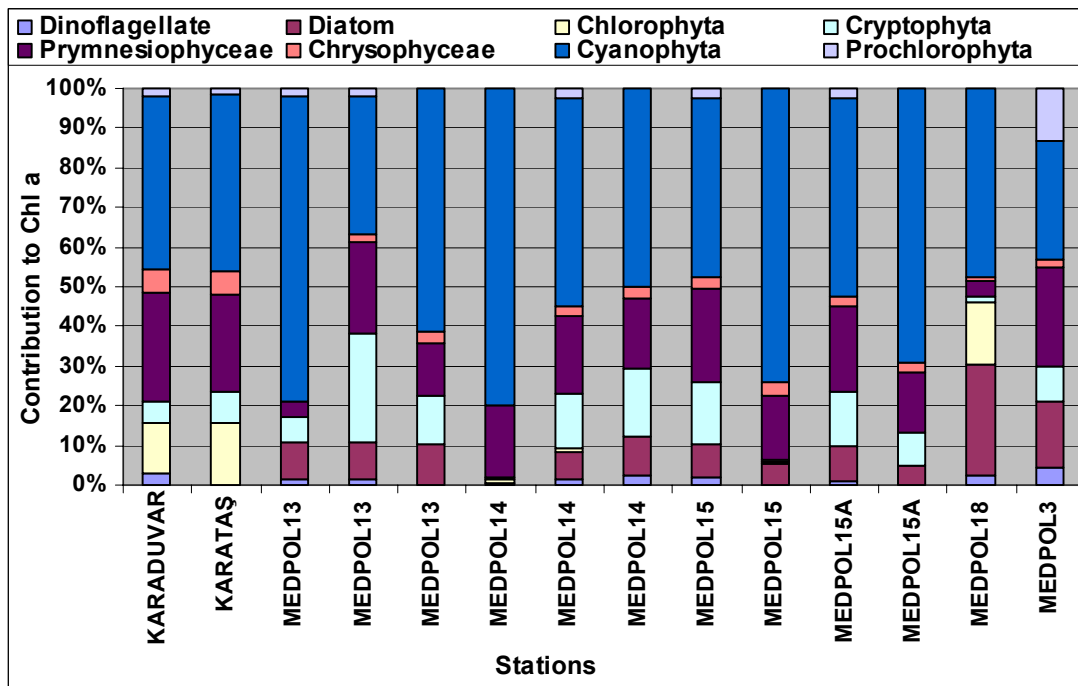
Figure 56: Phytoplankton groups and their contributions to the total chlorophyll-a concentration, in coastal North Eastern Mediterranean (Stations listed in figure 56 can be seen see figure 4 for station locations and latitude and longitude values are given in table 4).

The pigment compositions within the sampling regions did not vary significantly. However, some exceptions were observed. The mean ratios showed the difference between the North Eastern Mediterranean and the Western Black Sea. Diatoms dominate the Western Black Sea ecosystem during the sampling period (Figure 54). Prochlorophytes and chrysophytes were not detected in the Western Black Sea during the sampling period. High contribution of the cyanophyta to the chl-a, in the North Eastern Mediterranean ecosystem is the main difference. The North Eastern Mediterranean, offshore and coastal regions are not highly different from each other. The main differences are the higher prymnesiophyceae (nearly two times higher than the offshore) and lower cyanophyta contribution in the coastal regions than the offshore regions (Figure 57). The cyanophyta usually dominates the North Eastern Mediterranean ecosystem.
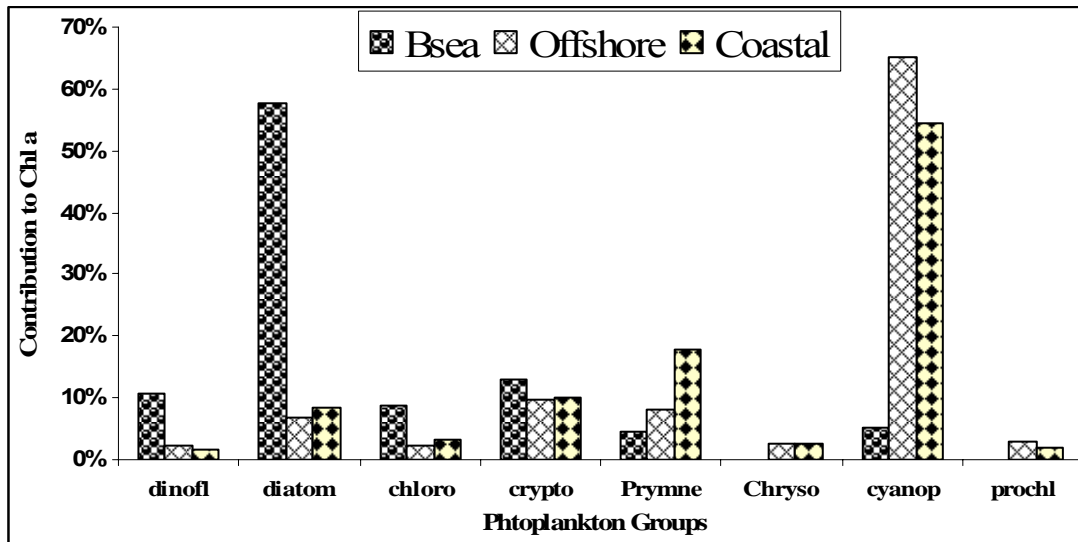
Figure 57: Comparison of the Phytoplankton groups' contribution to chlorophyll a in the three basins (Bsea: Western Black Sea, Offshore: North Eastern Mediterranean offshore, Coastal: North Eastern Mediterranean coastal).

3.5 Satellite Data

SeaWifs and MODIS (Aqua), satellites are utilized for the ocean color data. The 3x3 km squares were chosen from the satellite frames, which corresponded to sampling stations in study area. According to the station locations, frames were extracted from the corresponding days. However, quality of the data around the station was checked before extracting the remote sensing data. Data quality control was carried out by using data quality flags, included in the level 2 data. Cloudiness, sun glint, polarization, high solar and sensor zenith angles, high aerosol, and absorbing aerosol, were the main quality check parameters. Data points or frames contaminated with any of these flags were not used for the comparison. More than 100 frames were analyzed, but only 20 frames remained without contamination of any flag. Standard level 2 data products were extracted from both SeaWifs and MODIS appropriate frames. These parameters are given below (Table 7, 8).

Table 7: SeaWifs Level 2, standard products.

Parameter	Description	Unit
nLw_412	Normalized water-leaving radiance at 412 nm	$mW \cdot cm^{-2} \cdot \mu m^{-1} \cdot sr^{-1}$
nLw_443	Normalized water-leaving radiance at 443 nm	$mW \cdot cm^{-2} \cdot \mu m^{-1} \cdot sr^{-1}$
nLw_490	Normalized water-leaving radiance at 490 nm	$mW \cdot cm^{-2} \cdot \mu m^{-1} \cdot sr^{-1}1$
nLw_510	Normalized water-leaving radiance at 510 nm	$mW \cdot cm^{-2} \cdot \mu m^{-1} \cdot sr^{-1}$
nLw_555	Normalized water-leaving radiance at 555 nm	$mW \cdot cm^{-2} \cdot \mu m^{-1} \cdot sr^{-1}$
nLw_670	Normalized water-leaving radiance at 670 nm	$mW \cdot cm^{-2} \cdot \mu m^{-1} \cdot sr^{-1}$
Tau_865	Aerosol optical thickness at 865 nm	dimensionless
Eps_78	Epsilon of aerosol correction at 765 and 865 nm	dimensionless
Chlor_a	OC4 Chlorophyll a concentration	Mg/m^{-3}
K490	Diffuse attenuation coefficient at 490nm	m^{-1}
Ang_510	Angstrom coefficient 510-865 nm	dimensionless

Table 8: MODIS Level 2, standard products.

Parameter	Description	Unit
nLw_412	Normalized water-leaving radiance at 412 nm	$mW \cdot cm^{-2} \cdot \mu m^{-1} \cdot sr^{-1}$
nLw_443	Normalized water-leaving radiance at 443 nm	$mW \cdot cm^{-2} \cdot \mu m^{-1} \cdot sr^{-1}$
nLw_488	Normalized water-leaving radiance at 488 nm	$mW \cdot cm^{-2} \cdot \mu m^{-1} \cdot sr^{-1}1$
nLw_531	Normalized water-leaving radiance at 531 nm	$mW \cdot cm^{-2} \cdot \mu m^{-1} \cdot sr^{-1}$
nLw_551	Normalized water-leaving radiance at 551 nm	$mW \cdot cm^{-2} \cdot \mu m^{-1} \cdot sr^{-1}$
nLw_667	Normalized water-leaving radiance at 667 nm	$mW \cdot cm^{-2} \cdot \mu m^{-1} \cdot sr^{-1}$
Tau_869	Aerosol optical thickness at 869 nm	dimensionless
Eps_78	Epsilon of aerosol correction at 748 and 869	dimensionless
Chlor_a	OC3 Chlorophyll a concentration	Mg/m^{-3}
K490_D	Diffuse attenuation coefficient at 490nm m-1	m^{-1}
Ang_531	Angstrom coefficient, 531-869 nm	dimensionless
SST	Sea Surface Temperature - 11micron	degrees Celsius

The comparison of the SeaWifs and MODIS data with the in situ measurements and light measurements gave good agreement. Usually the trends in the reflectance and the water leaving radiance were parallel to each other. The seasonal and regional differences were clearly seen from both in situ and satellite data.

Radiance maximum in the Western Black Sea stations was mostly observed around 500 nm. Comparison of the in situ measurements with the remote sensing data was done with the light measurements taken in 2001 and SeaWifs remotely sensed data (Figure 58, 59, 60).
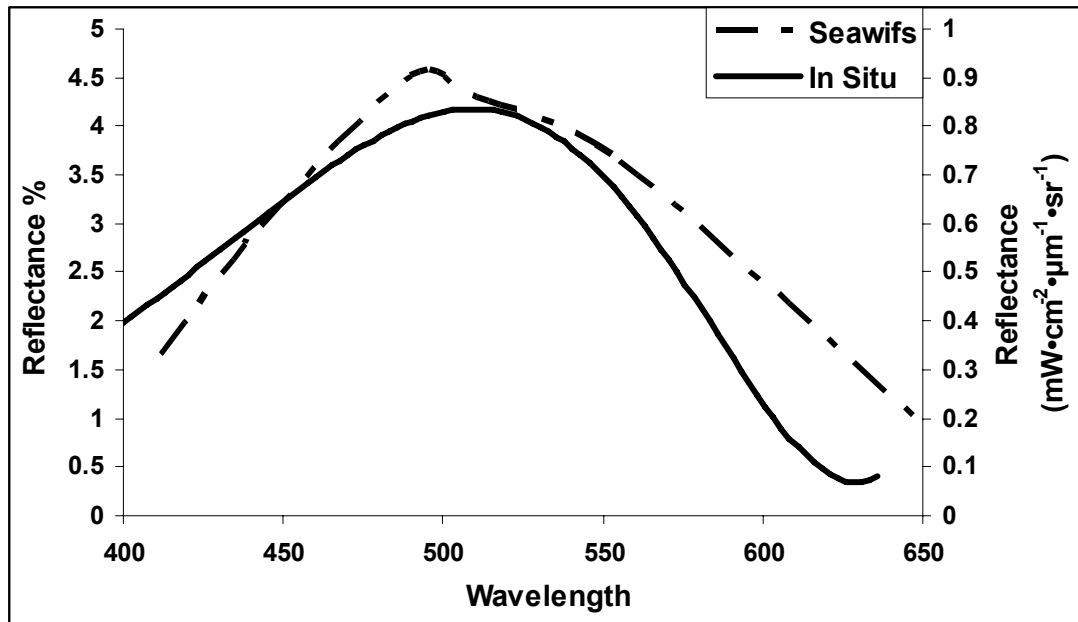
Figure 58: Comparison of the in situ (station: M30N45 see figure 3 for station location and latitude and longitude values are given in table 4) reflectance (percentage) and normalized water leaving radiances obtained from satellite (SeaWifs). Date: 25.05.01.
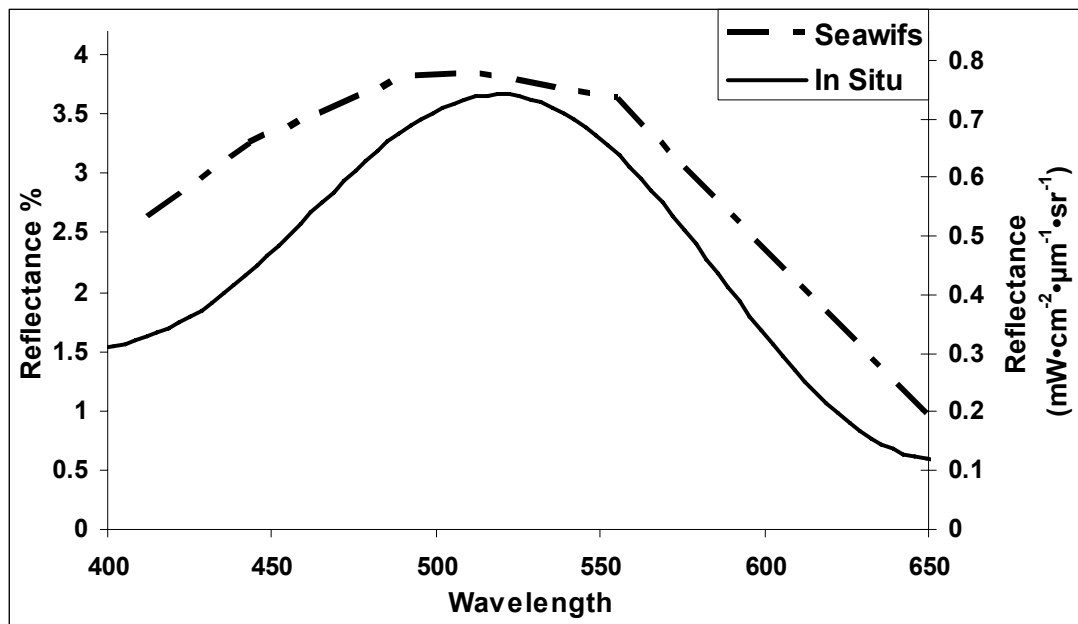
Figure 59: Comparison of the in situ (station L27L30 see figure 3 for station location and latitude and longitude values are given in table 4) reflectance (percentage) and normalize water leaving radiances obtained from satellite (SeaWifs). Date: 17-06-01.
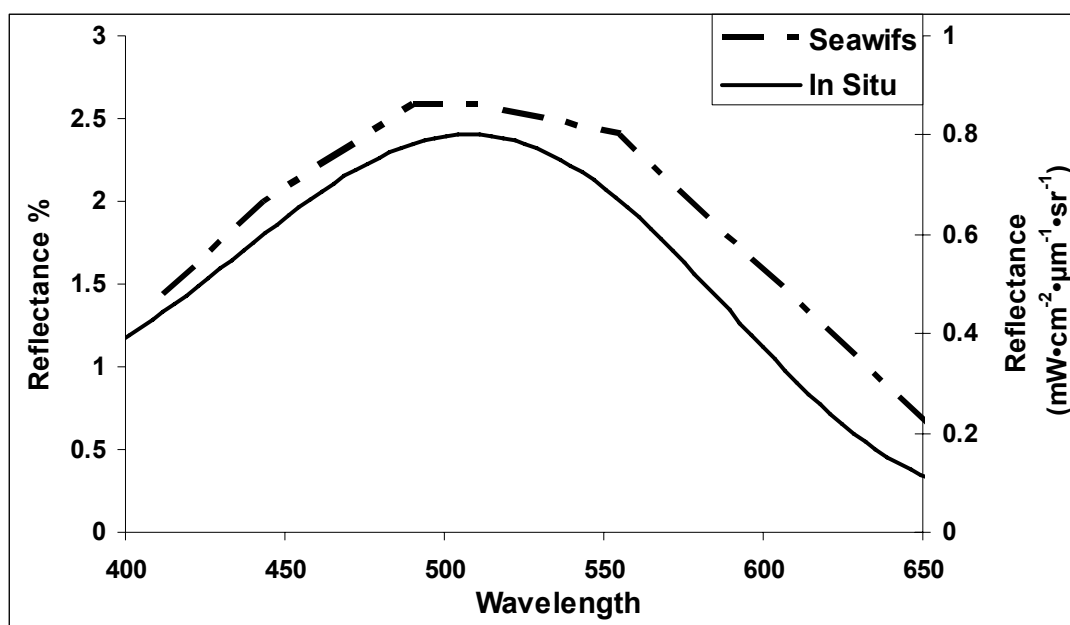
Figure 60: Comparison of the in situ (station: L44L39 see figure 3 for station location and latitude and longitude values are given in table 4) reflectance (percentage) and normalize water leaving radiances obtained from satellite (SeaWifs). Date: 18.06.01.

Comparison of the satellite data and in-situ measurements carried out in Aegean and Mediterranean Seas are rather complicated. Both SeaWifs and MODIS have no any ocean color bands lower than 412 nm wavelengths. Thus the peaks, which are close to 400 nm, are not really represented by the satellite measurements. However, if the peak is not very close to the 400 nm, tip of the peak and the maximum generated by the satellite data coincided (Figure 61, 62, 63).
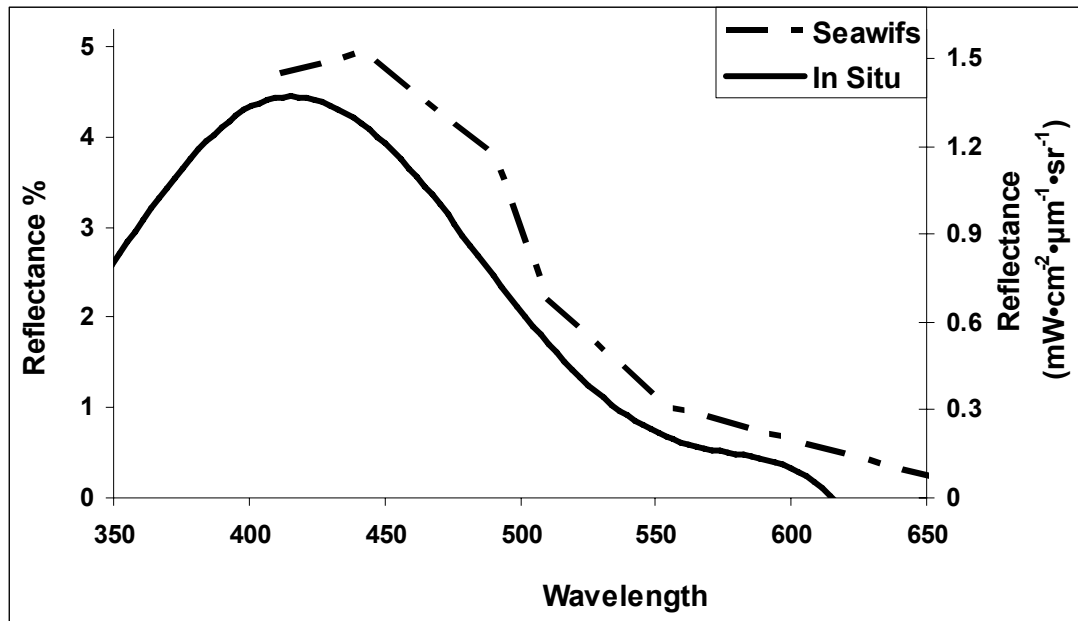
Figure 61: Comparison of the in situ (station: J37H35, see figure 3 for station location and latitude and longitude values are given in table 4) reflectance (percentage) and normalize water leaving radiances obtained from satellite (SeaWifs). Date: 25.06.01.
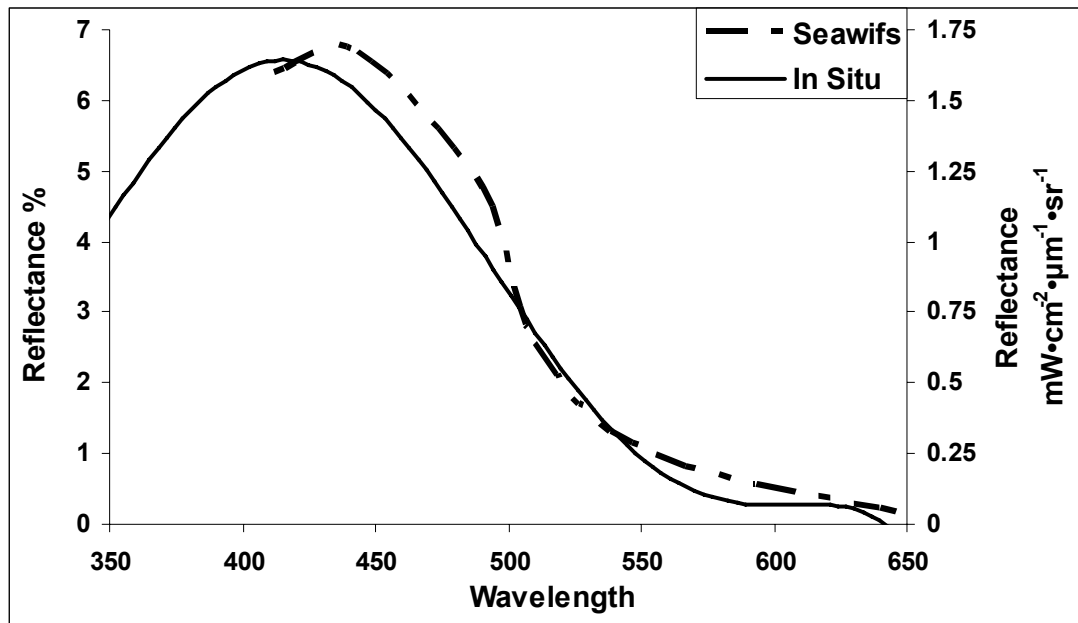
Figure 62: Comparison of the in situ (station: G35K35, see figure 3 for station location and latitude and longitude values are given in table 4) reflectance (percentage) and normalize water leaving radiances obtained from satellite (SeaWifs). Date: 28.06.01.
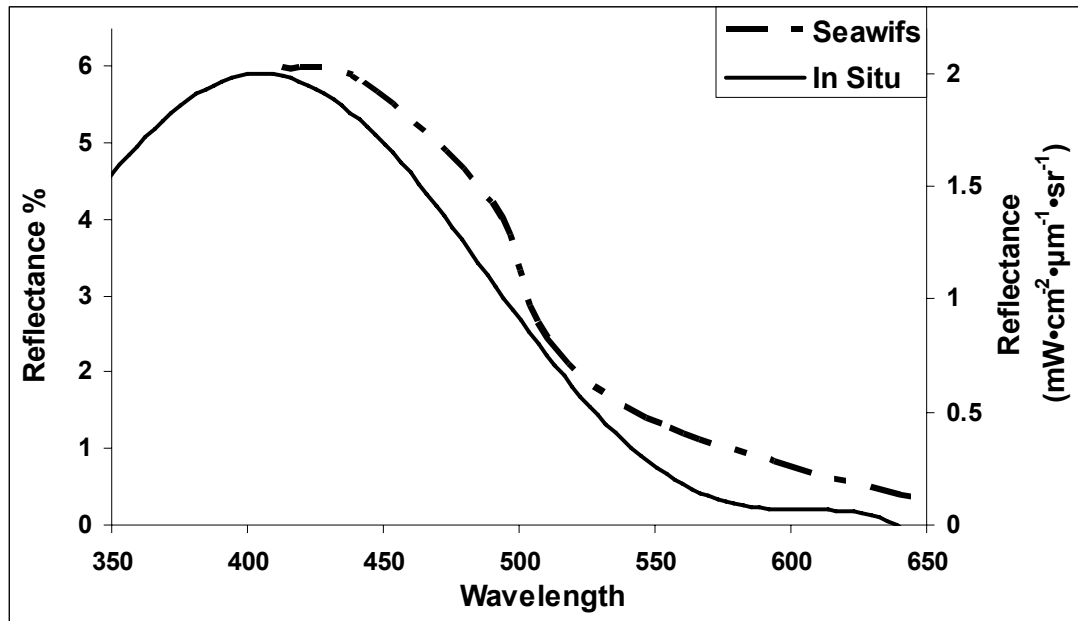
Figure 63: Comparison of the in situ (station: F30Q30, see figure 4 for station location and latitude and longitude values are given in table 4) reflectance (percentage) and normalize water leaving radiances obtained from satellite (SeaWifs). Date: 03.07.01.

In winter period radiance peak position in the North Eastern Mediterranean has changed. Satellite data represented the real situation much more correctly in the winter period, as the peak is moved close to or beyond 450 nm. However, if the reflectance peak occurred beyond 500 nm, satellite data may not match with the in situ measurements (Figure 64). Most of the samples were collected during 2004 and 2005. MODIS data was also available during this period and hence comparable with that of SeaWifs (until December 2004).

Usually, SeaWifs and MODIS normalized water leaving graphs were very similar, however in Figure 64, MODIS graph is more close to the in-situ measurement, in terms of peak position. Differentiation may arise from the different band numbers, in SeaWifs and MODIS sensors, and sensor zenith angle or pass time.
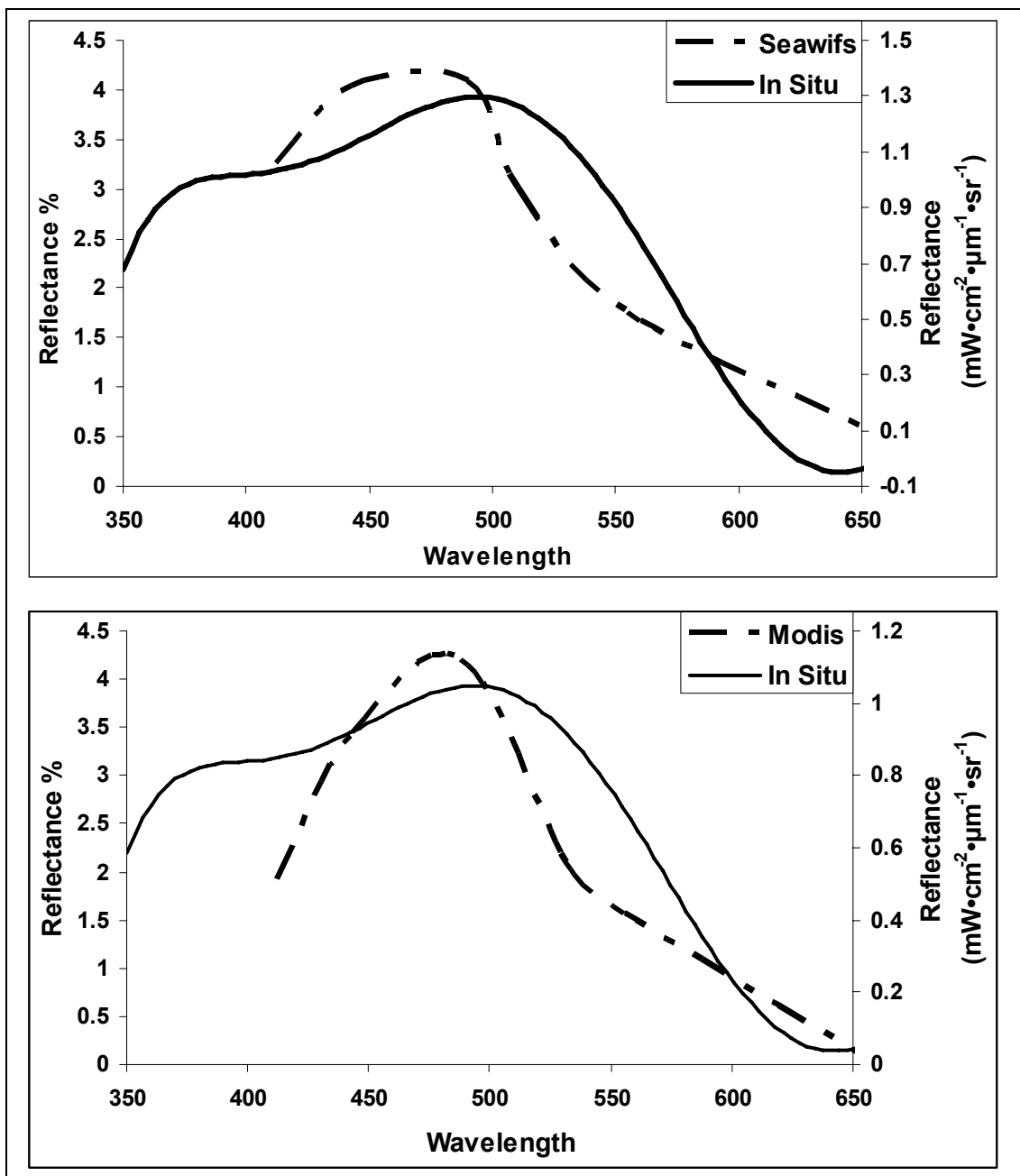
Figure 64: Comparison of the in situ (METU-IMS time series station see figure 4 for station location and latitude and longitude values are given in table 4) reflectance (percentage) and normalize water-leaving radiances obtained from satellites (SeaWifs; above) and (MODIS; below). Date: 16.03.04.

Reflectance peaks were very variable in terms of shape and location in different parts of the North Eastern Mediterranean. In Iskenderun Bay (station G40S57, see figure 4 for station locations and latitude and longitude values are given in table 4) a broad peak occurred between 400-475 nm, but the satellite data may not represent the starting peak very close to the 400 nm (Figure 65). In the coastal station (G40R30, see figure 4 for station locations and latitude and longitude values are given in table 4) of the North Eastern Mediterranean, a broad peak of reflectance is observed with the peak location around 420 nm. However, satellite reflectance peak occurred at 490 nm (Figure 66). At the offshore station (G23R45, see figure 4 for station locations and latitude and longitude values are given in table 4) both in situ and satellite reflectance were similar to each other (Figure 67).
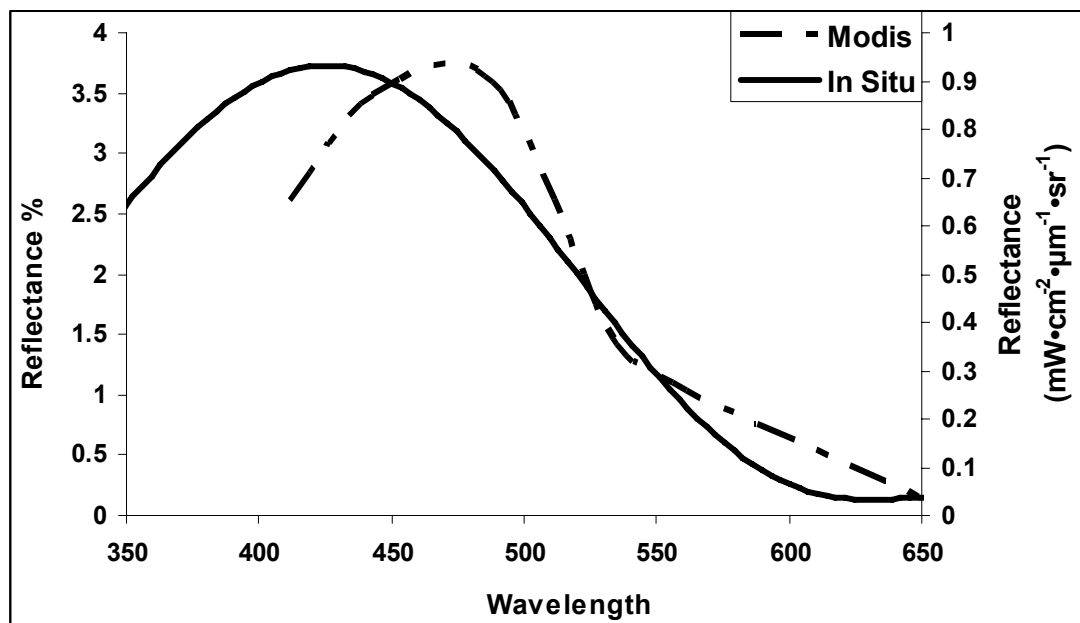
Figure 65: Comparison of the in situ (G40S57, see figure 4 for station location and latitude and longitude values are given in table 4) reflectance (percentage) and normalize water leaving radiances obtained from satellite (MODIS). Date: 18.09.04.
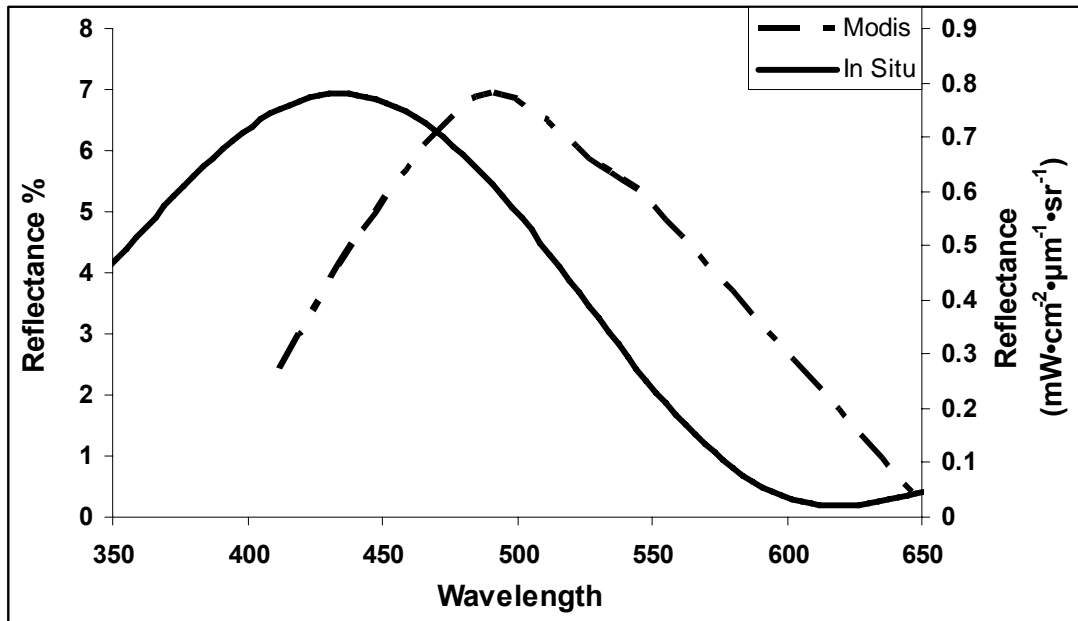
Figure 66: Comparison of the in situ (G40R30, see figure 4 for station locations and latitude and longitude values are given in table 4) reflectance (percentage) and normalize water leaving radiances obtained from satellite (MODIS). Date: 08.06.05.
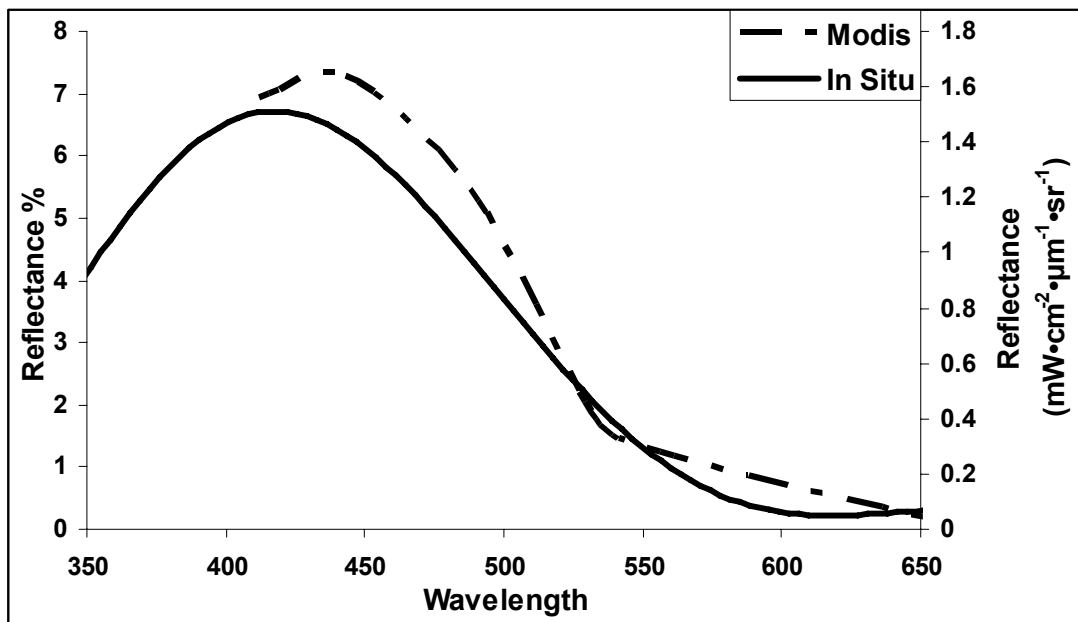
Figure 67: Comparison of the in situ (G23R45, see figure 4 for station locations and latitude and longitude values are given in table 4) reflectance (percentage) and normalize water leaving radiances obtained from satellite (MODIS). Date: 08.06.05.

4. DISCUSSION

This study was generally concentrated on the North Eastern Mediterranean, with a limited number of measurements in the other seas. Therefore, some insight was obtained regarding regional differences, although the seasonal variability for regions other than the NE Mediterranean was not sufficiently covered. Earlier studies in the region are limited. Some data exists for the Western Black Sea but does not cover all aspects of the bio-optics.

In order to obtain a meaningful evaluation of the results obtained in this study, comparison is made with the Western Mediterranean and Sargasso Sea.

4.1. Optical Classification of the Turkish Seas.

Classification of water bodies according to their optical properties is based on the clarity index of the water, known as the Jerlov Water Type (Jerlov 1976). The index assigns Type 1, Type 1 (upper 50 m), Type 1A, Type 1B, Type II and Type III for the parameterization of the water clarity. To simplify the notation, the water type is assigned an integer value from 1 to 5, where 1 represents the clearest and 5 the most turbid water. An additional type, denoted as "very clear water" type was introduced by Kraus (1972). Table 9 shows the parameters related to each of the water type.

Table 9: Jerlov water type classification and related parameters.

Jerlov Water Type	r	β_R	β_B
Very Clear Water	0.4	5	40
1	0.58	0.35	23
2	0.62	0.60	20
3	0.67	1	17
4	0.77	1.50	14
5	0.78	1.40	7.9

The classification of the water types is based on the parameters obtained from the light extinction coefficient model developed by Jerlov (1976):

$$I_k = I_0 \left[r * \exp(z/\beta_R) + (1-r)\exp(z/\beta_B) \right]$$

Where I_0 is the PAR Irradiance (measured spectral light integrated from 400 to 700 nm) at the surface, r is the fraction that is red, z is collection depth of the data, β_R is the penetration depth scale of red light, β_B is the penetration depth scale of blue light.

The light measurements carried out in the different regions of the Turkish seas are utilized to classify the waters according to Jerlov (1976). Light measured at the surface and within the water column is used to determine the water type. According to the measurements, the clear (type 1) and very clear water type characteristics were observed in the Mediterranean and the Aegean seas, and very turbid (type 5) waters in the Western Black Sea and the Marmara (Table 10).

Table 10: Water types in the Turkish waters (V.Clear = Very Clear).

REGION	STATION	r	β_R	β_B	DATE	Water Type
Black Sea	L20M30	0.815	1.651	7.252	16.06.01	5
Marmara	K50J34	0.820	4.454	10.18	24.06.01	5
North Aegean	J37H35	0.376	7.556	24.54	25.06.01	V. Clear
South Aegean	G35K35	0.162	1.594	21.79	28.06.01	V. Clear
N.E.Mediterranean	F30Q30	0.220	1.450	22.25	03.07.01	V. Clear
N.E.Mediterranean	METU-IMS	0.356	1.562	8.949	16.03.04	V. Clear
N.E.Mediterranean	METU-IMS	0.426	1.767	25.59	19.07.04	V. Clear
İskenderun Bay	G40S57	0.322	2.800	16.34	18.09.04	V. Clear
N.E.Mediterranean	METU-IMS	0.495	1.291	14.14	10.02.05	1
N.E.Mediterranean	METU-IMS	0.308	1.359	16.71	25.03.05	V. Clear
N.E.Mediterranean	METU-IMS	0.436	2.796	24.85	21.04.05	V. Clear
N.E.Mediterranean	METU-IMS	0.432	3.683	30.75	13.05.05	V. Clear
Coastal Med	G27S15	0.371	0.421	13.69	24.05.05	V. Clear
N.E.Mediterranean	METU-IMS	0.335	3.542	29.88	12.06.05	V. Clear
Coastal Med	medpol15a	0.561	1.870	17.05	01.07.05	1
N.E.Mediterranean	METU-IMS	0.404	2.542	26.76	02.07.05	V. Clear
N.E.Mediterranean	METU-IMS	0.339	5.073	26.38	27.11.05	1

Due to variability of the atmospheric and the sea conditions, the data used to calculate these parameters are very variable, therefore the results do not match well with the Jerlov's parameter numbers. These numbers change from region to region (Clayton and Simpson, 1977, Kirk 1994, and Arst et al., 2002). This problem is due to the different methodologies used to measure light and the ambient conditions, such as the solar zenith angle and cloudiness (Smith and Baker 1978, and Kirk 1994). Thus it was decided to base the classification on the values of both r and β_B, but here again β_R was highly variable and did not match the original Jerlov values.

Comparison of the basins according to the light measurements and the other parameters such as downward diffusivity provides additional information on the water type. Classification according to the optical properties is affected by the constituents within the water and water itself (Smith and Baker 1978, Baker and Smith 1982, Kirk 1994, Stramski et al., 2004). For a better understanding of the

measured data, other parameters affecting the light absorption, reflection and scattering have to be interpreted to improve the classification.

The Jerlov values show two water bodies with very different characteristics for the seas surrounding Turkey. The regional differences are determined by the results and interpretations of the light measurements carried out in 2001. Nearly all the basins (Including the Western Black Sea, Marmara, Aegean Sea and the North Eastern Mediterranean Sea were covered within a relatively short period.

The incoming light spectrum, measured in the first few meters, is the surface downward irradiance (Smith and Baker 1978). Surface downward irradiance was not variable in the entire region. The only major difference occurred between the Western Black Sea and the other Basins. This difference was related with the measurement time (atmospheric conditions were hazy and partly cloudy) and changed only the magnitude of the spectrum (Figure 68). Incoming solar radiation is very stable especially between the visible ranges (Thuillier 1998). The near infra red and ultra violet part of the spectrum disappear within the first few centimeters. Thus the shape of spectrum in these regions is very low and the spectrum resembles a top pressed bell, although some spikes and peaks do occur. Possible reasons for these fluctuations are the ambient light, movement of the ship or the sea surface conditions (mainly waves or white caps). One common peak appears between 450 and 500 nm, except in the Western Black Sea. This part of the spectrum in the Western Black Sea is flat.
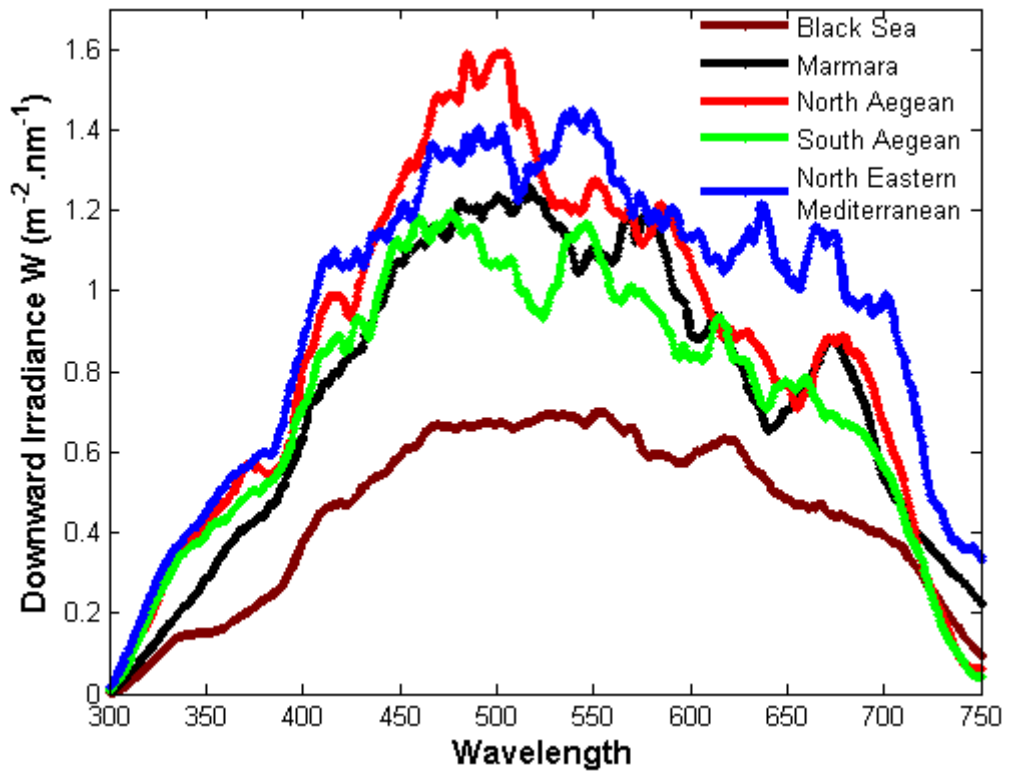
Figure 68: Downward Irradiance values between 300-750 nm measured in 2001 from different regions.

The shape and the magnitude of the upward irradiance spectrum are dependent on the absorbing agents in the water column (Karen and Smith 1982, Sathyendranath 2000, and Starmski et al., 2004). The shape of the spectrum depends on the constituent concentration and composition in the water. In the North Eastern Mediterranean and the Aegean Seas, blue light is not absorbed at the surface, thus indicating low chlorophyll concentration (Jeffrey et al., 1997, Starmski et al., 2004). In the North Eastern Mediterranean Sea a twin peak is observed between 400 and 450 nm. On the other hand broad peaks occur in the Western Black Sea and in the Sea of Marmara between 450 to 600 nm. The absorption of the light around 400 - 450 nm is the reason of this shape. The absorption of the light within this range is attributed to high phytoplankton concentrations (Baker and Smith 1982, Kirk 1994, and Felix 2002) (Figure 69).
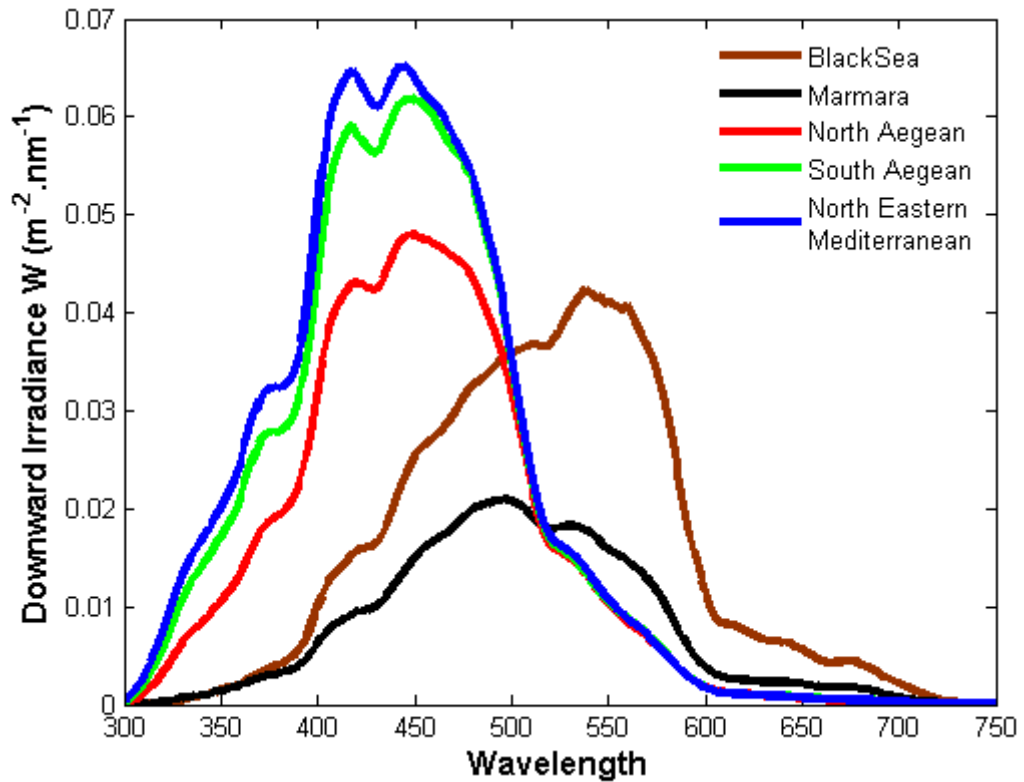
Figure 69: Upward irradiance values between 300-750 nm measured in 2001 from different regions.

Reflectance is the ratio of the downward to upward irradiance. In this study, it is given as a percentage. The reflectance spectrum shapes are similar to the upward irradiance spectrums. The reflection peak in the North Eastern Mediterranean and the Aegean Sea is located between 400 and 450 nm. However, for the Western Black Sea and the Sea of Marmara, this peak is moved towards 450 nm, and to 500 nm in the Western Black Sea, indicating that the Western Black Sea and the Sea of Marmara are greener than the Mediterranean. In the North Eastern Mediterranean, relatively no light is reflected beyond 500 nm (Figure 70). The peak locations are identical as given in Sancak et al., (2005). These stations are located in the offshore regions, hence anthropogenic influence is negligible. Thus the controlling mechanisms of the optical properties are due essentially to the phytoplankton composition and their concentration.
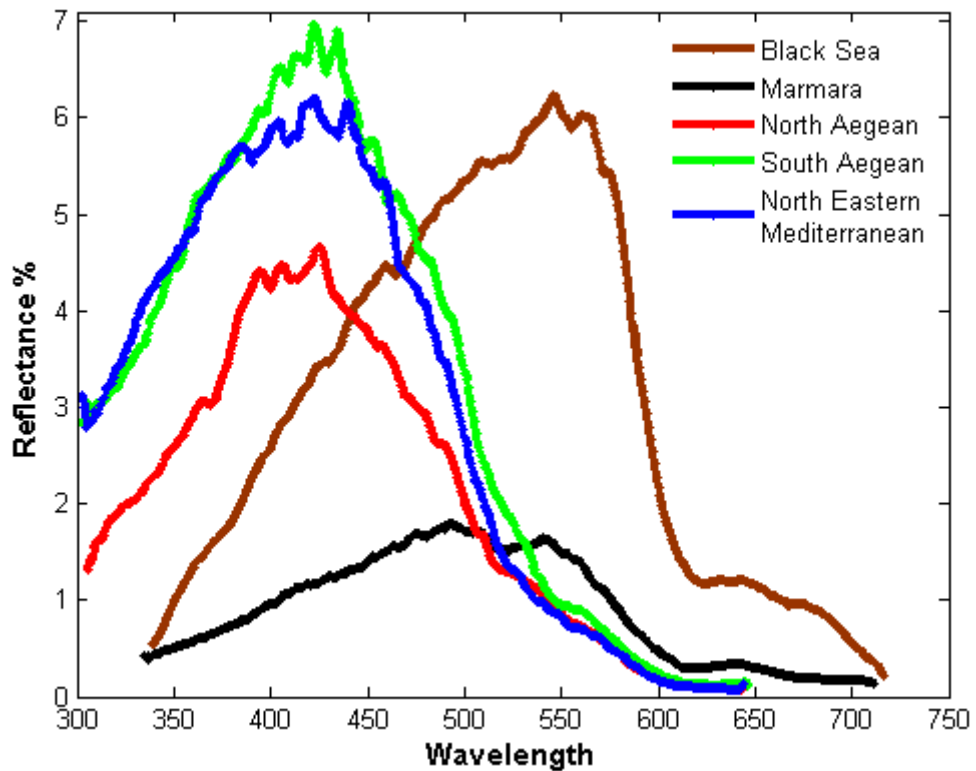
Figure 70: Reflectance values between 300-750 nm measured in 2001 from different regions.

The diffusivity of light through the water column is dependent on both the constituents and the water itself. Diffusivity, K_d, is classified in the apparent optical properties (or quasi-inherent properties) (Baker and Smith 1982, Kirk 1994, and Mobley 1995). The diffusivity can be defined by the loss of light from surface to the discrete depths. The differences between the basins are clearly seen, Table 10. The diffusivity graphs show two different regions. High diffusive attenuation coefficients are observed in the Western Black Sea and the Sea of Marmara, as the Jerlov numbers indicate in Table 10. The U shaped curve imply that the infra red and ultra violet or shorter wavelengths until 400 nm disappear at the surface. Related to the increase in the chlorophyll concentration, a broad attenuation bump is centered at 430 nm in the North Aegean. In the South Aegean and the North Eastern Mediterranean, the attenuation minimum moves from 450 to 560 nm both in Western

Black Sea and Marmara. In-vivo fluorescence of the chlorophyll a flattens the sharp increase of the coefficients between 640-670 nm within range of 550 nm to 700 nm (Western Black Sea, Marmara, and North Eastern Mediterranean) (Baker and Smith 1982). The flat shape of the North Eastern Mediterranean and the Aegean downward diffusivity curves are typical to the low chlorophyll concentration waters (Figure 71). Similar results have been found by Williams et al (1995) in the sub-arctic, Ignatiades (1998) in the Creatan Sea, Stambler (2005) in the northern Red Sea the Gulf of Eilat.
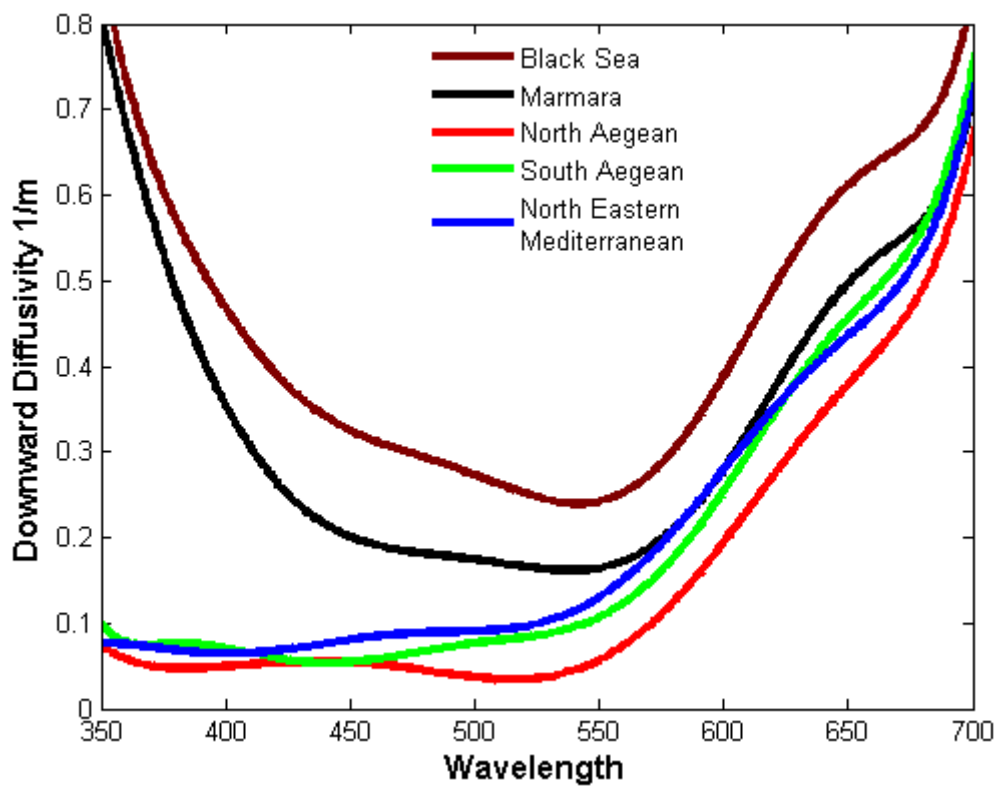
Figure 71: Downward diffusivity coefficients from 300 nm to 750 nm derived from measurements in 2001 from different regions.

The optical properties of the water are controlled by the biogenic and non-biogenic constituents (Kirk 1994, Mobley 1995, Sathyendranath. ed. 2000). Besides the water itself, biogenic constituents are the most important parameters in the offshore waters and also in some coastal waters, where mixing is not strong, and away from the river or anthropogenic input. The living and non-living fractions of the biogenic constituents are evaluated separately (Kirk 1994, Mobley 1995, Sathyendranath 2000, Stramski et al., 2004).

CDOM is a very important parameter, which absorbs light at shorter wavelengths (usually beyond 450 nm) (Bricaud et al., 1981, Kirk 1994, Sathyendranath 2000, Stedmon et al., 2000, Hensell and Carlson 2001, Siegel et al., 2002). The dynamics of the CDOM are briefly explained in Hensell and Carlson (2001). The main source of the CDOM is the degradation of the terrestrial and marine plants (Kirk 1994, Sathyendranath .ed. 2000, Stedmon et al., 2000, Hensell and Carlson 2001, Siegel et al., 2002). Therefore, CDOM formation is dependent only upon the phytoplankton activities, in regions away from anthropogenic inputs. CDOM distribution is highest in the Western Black Sea and Sea of Marmara, and decreases through North Aegean, to North Eastern Mediterranean (Figure 72). The effect of the CDOM absorption in the Western Black Sea and the Sea of Marmara is clearly seen at the shorter wavelengths in the downward diffusivity also (Figure 71). However, no effect occurred in the same regions of the Aegean and the North Eastern Mediterranean on the diffusivity coefficients. According to CDOM measurements values higher than the 0.2 m^{-1} at λ=400 nm can be taken to indicate turbid water and Jerlov type 5. The mean Western Black Sea measurements are always higher than this value (Figure 30). Kowalczuk et al., (2005) found similar results in Baltic Sea. However in Labrador Sea, values were measured 10 times lower than the Western Black Sea (Cota et al., 2003).
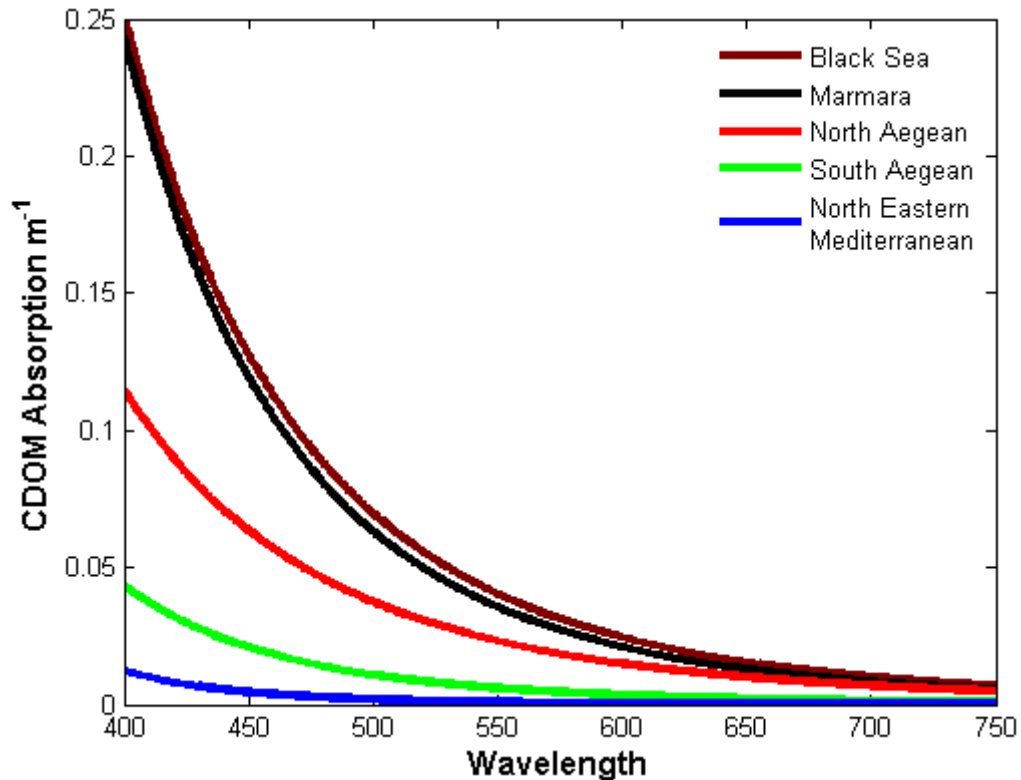
Figure 72: CDOM Absorption coefficients, from different regions between 400 nm to 750 nm.

Particles both scatter and absorb light, whereas CDOM only absorbs the light. This concept is in question, because CDOM has in fact a particle size (Ogawa and Tanoue 2003). Therefore, some authors, for example, Sathyendranath (2000), and Stramski et al (2004), claim that the high concentration of CDOM contributes to the scattering also. In this study the scattering is not taken into account, because the scattering measurements can be done either in laboratory conditions or by using very advanced instruments (Stramski et al., 2004). Particles contribution to the total absorption is based on its composition (Garver et al., 1994, Stramski and Mobley. 1997, Sathyendranath 2000, Morel 2001, Stramski et al., 2004).

The particle absorption measurements show the same sequence as CDOM. The highest absorption coefficients were measured at the Western Black Sea. Unfortunately no samples were taken from the Sea of Marmara, but the particle

absorption coefficients in Marmara are similar to the Western Black Sea (Sancak et al., 2005). Due to the phytoplankton, a peak occurred at 675 nm, and shape of the absorption spectra reflects phytoplankton absorption features. If the phytoplankton concentration is not high enough, the detritus absorption features dominated the spectra as in the North Eastern Mediterranean (2001) (Figure 73). Absorption characteristics of the regions in the sampling area differed from each other, both in shape, and magnitudes (Figure 73). Shape and magnitude of the spectra are very dependent on the particle composition (Kirk 1994, Morel and Maritorena 2001, and Stramski et al., 2004). The comparison given on Figure 73 is generated from offshore stations, where the waters are accepted as case 1. Thus the differences between the spectra are attributed to different phytoplankton group activities and concentrations (Figure 52, 53). Different phytoplankton groups have different absorption characteristics, which effect the shape of the total absorption spectra (Figure 74, 75, 76, 77) (Bidigare et al., 1989, Allali et al., 1997, Gomez et al., 1995 and 2001, Jeffrey et al., 1997, Devred et al., 2006).
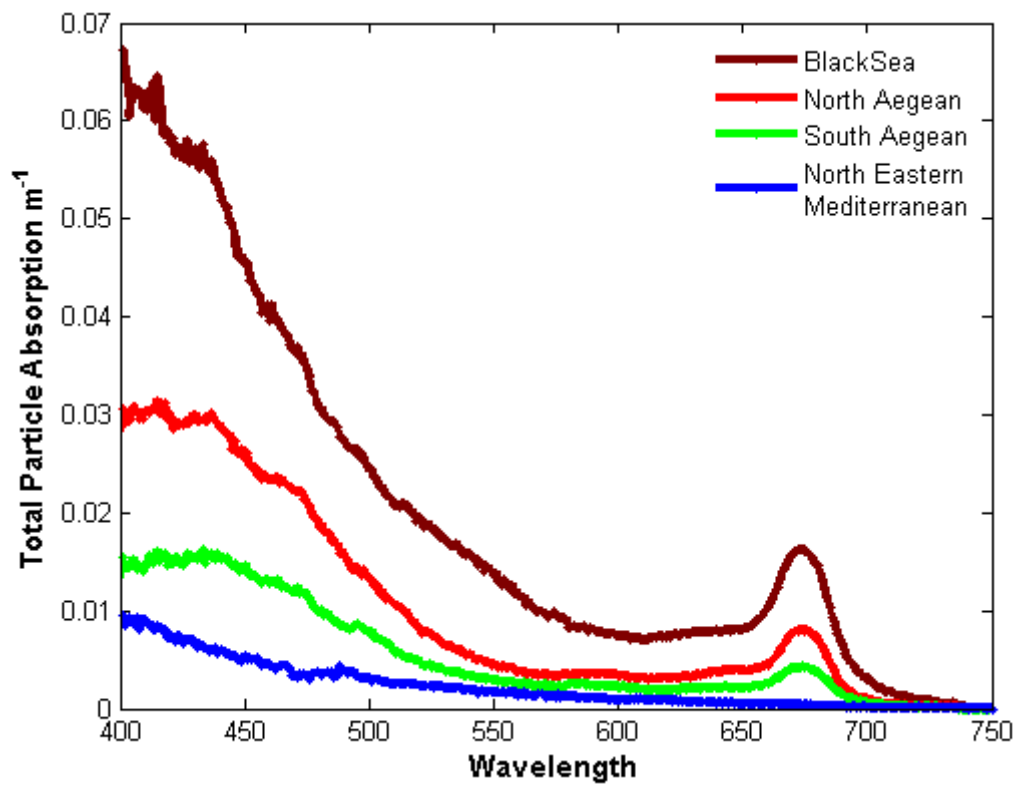
Figure 73: Comparison of the total particle absorption coefficients, from different regions between 400 nm to 750 nm.
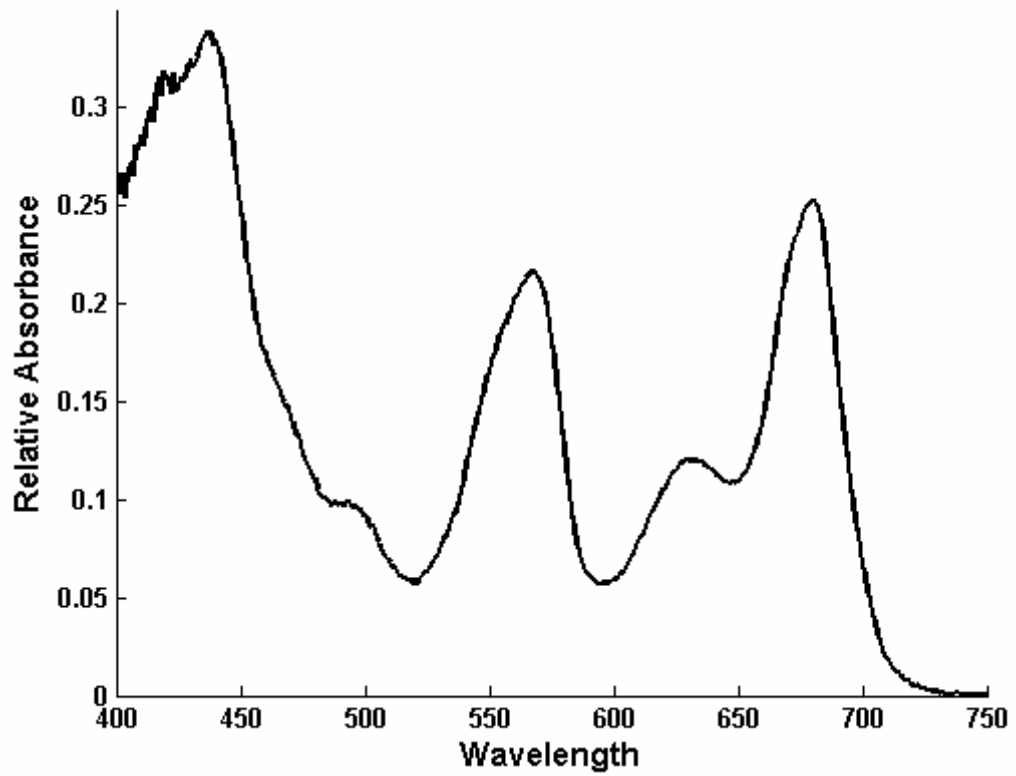
Figure 74: Relative absorbance of the Cyanophyta (*Synechococcus spp*).
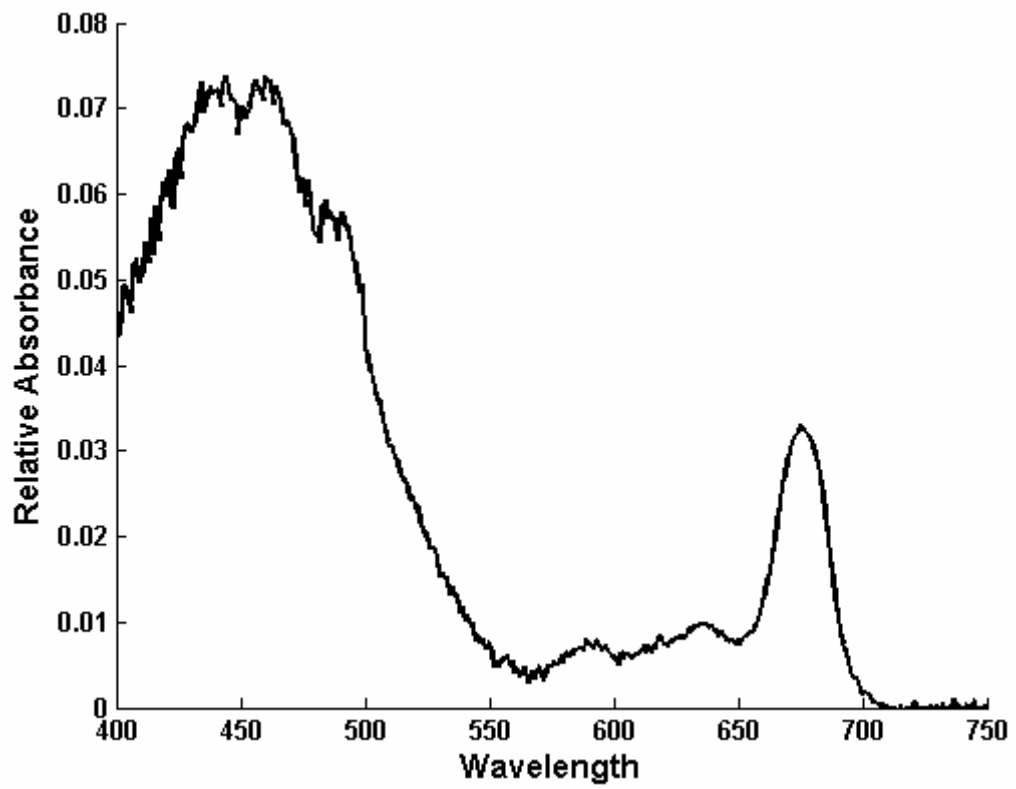
Figure 75: Relative absorbance of the *Emiliania huxleyi* (non motile).
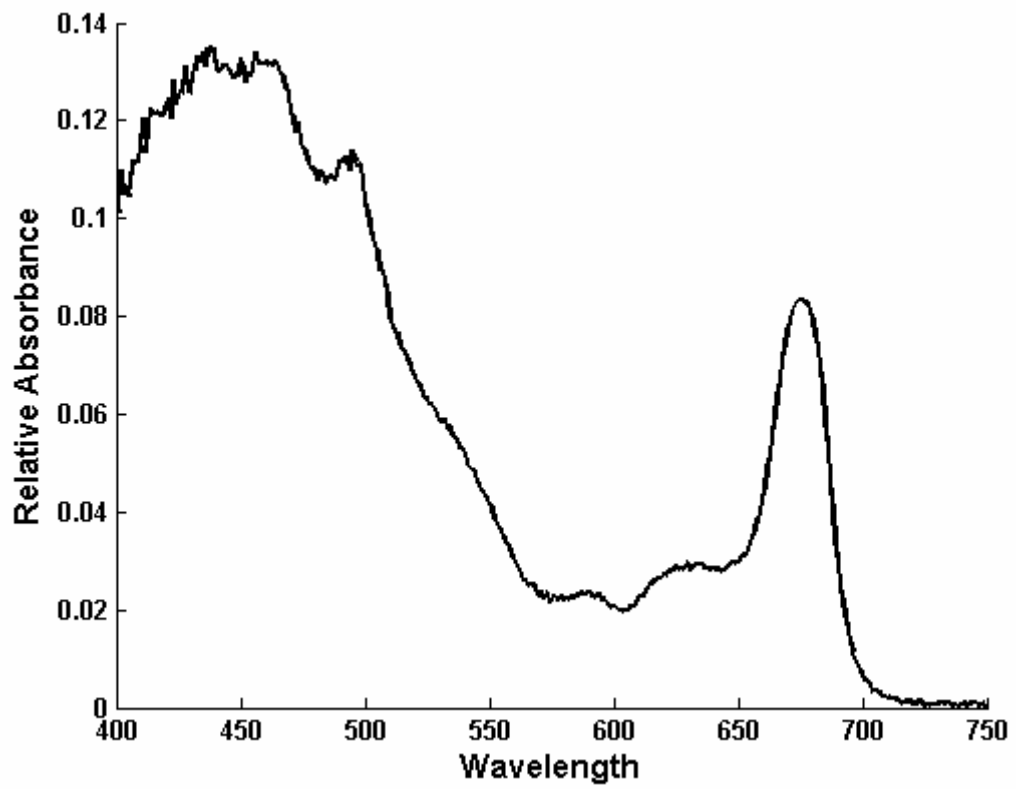
Figure 76: Relative absorbance of the dinoflagellate (*Prorocentrum calcitrans*).
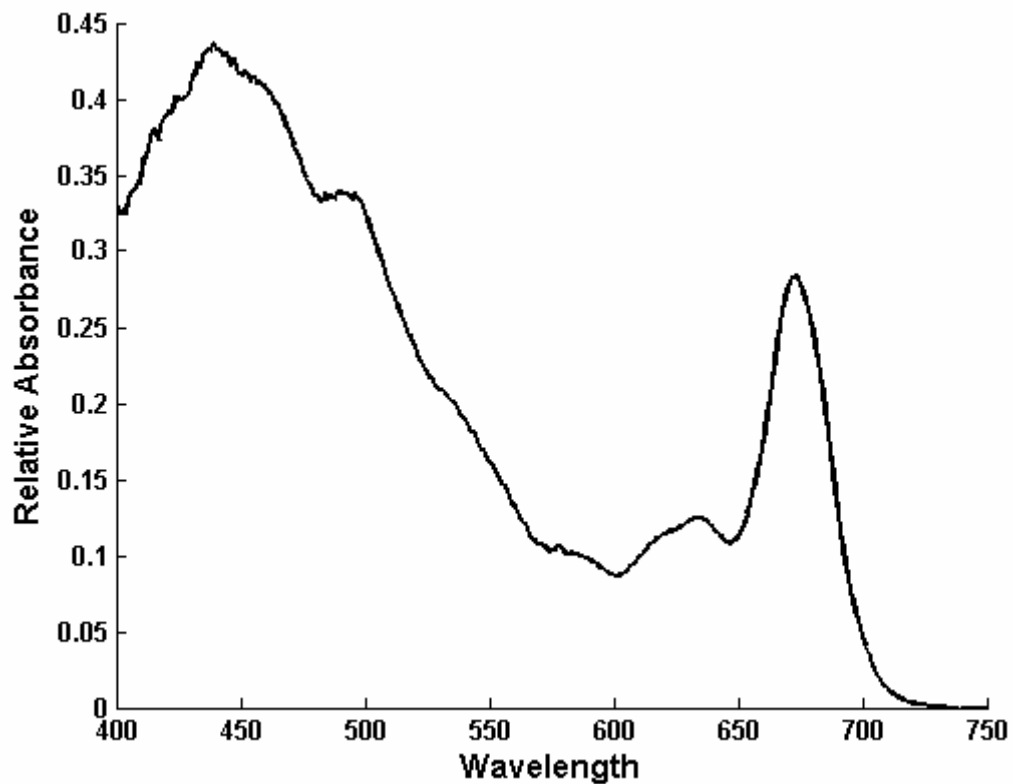
Figure 77: Relative absorbance of the diatom (Isolated from North Eastern Mediterranean by Dr. Zahit Uysal).

Temporal variability of the optical properties and the time dependent changes were studied at the METU-IMS time series station. The downward irradiance within the year fluctuated in the intensity of irradiance. The shape of the spectra did not change much (Figure 78). Ambient light conditions, like cloudiness, solar zenith angle and sampling conditions, such as rolling of the ship are possible reasons of the fluctuation of the downward irradiance at the surface.
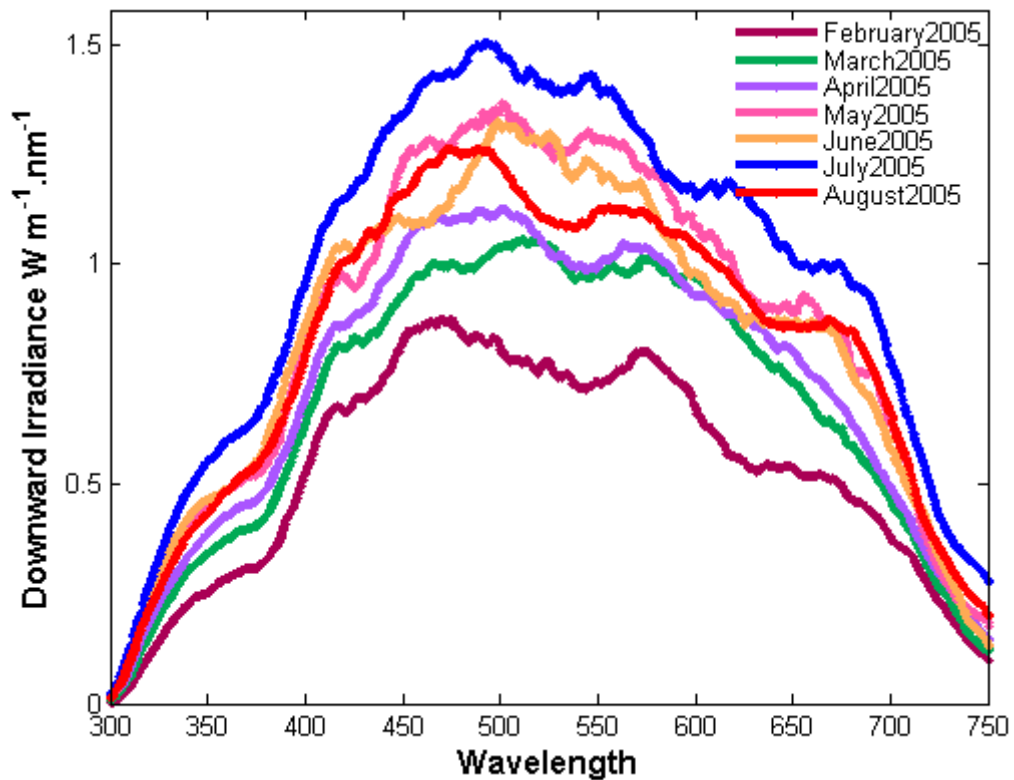
Figure 78: Comparison of downward irradiance values between 300-750 nm measured between February 2005 and November 2005 at the METU-IMS time series station (see figure 4 for station location and latitude and longitude values are given in table 4).

Shape and magnitude of the upward irradiance were highly variable within the sampling period. At the beginning of the year (February 2005) the spectra showed a broad peak centered at 470 nm with two bumps centered at 420 and 520 nm. The broad peak began to narrow and the bump at 420 nm started rising in March. Development of new bumps at the 370 and 520 nm appeared as two shoulders. The magnitude of the rising bump from March became a secondary peak and the broad peak at the 440 nm narrowed in April. From May to August, the shape of the spectra is not changed much. Two peaks centered at 420 and 440 nm are observed during this period, while the shoulders at the 320 and 520 nm are continued to exist (Figure 79).
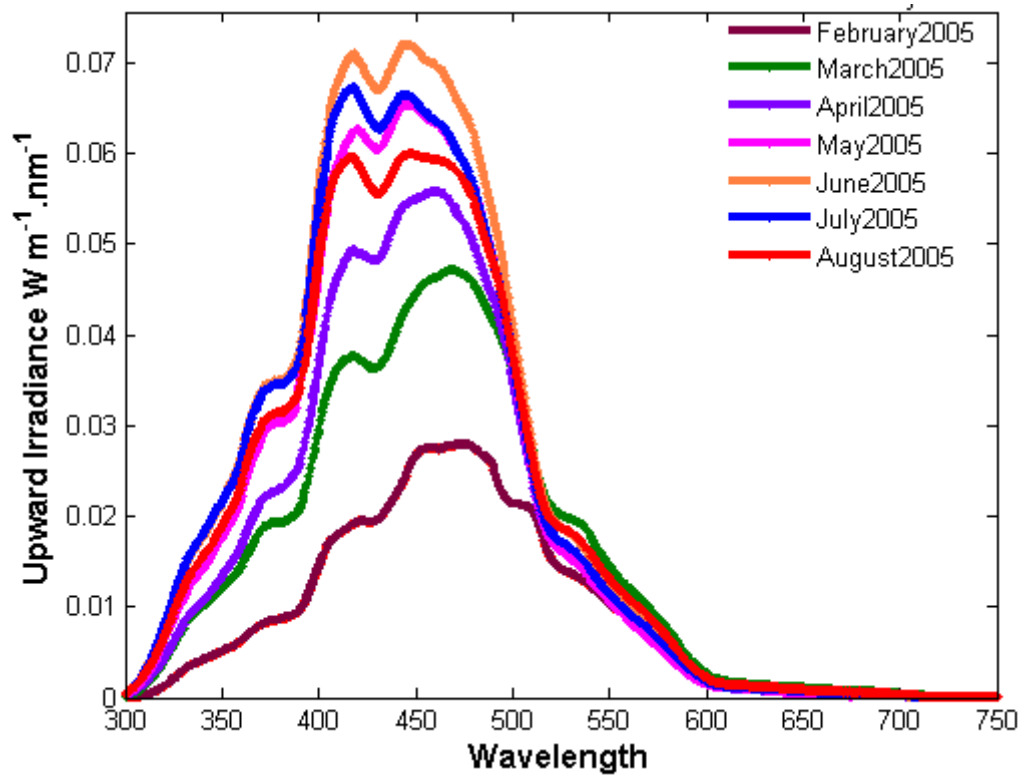
Figure 79: Up ward Irradiance values between 300-750 nm measured between February 2005 and November 2005 at METU-IMS time series station (see figure 4 for station location and latitude and longitude values are given in table 4).

The calculated reflectance shapes are very close to each other. The main differences between the reflectance values are the extended shape of the spectra in winter (February) at 500 nm and a secondary bump around 375 nm. In March and April, two broad peaks centered at 375 and 440 nm occurred. A sharp peak around 420 nm with a smaller peak at 375 nm occurred in May. During the summer period, a broadened shaped spectra is observed. August is differentiated from other months with a single peak occurred around 400 nm. In general, autumn and winter peaks extended to the 450 to 500 nm, where the summer and spring peaks are located between 400 and 450 nm (Figure 80).
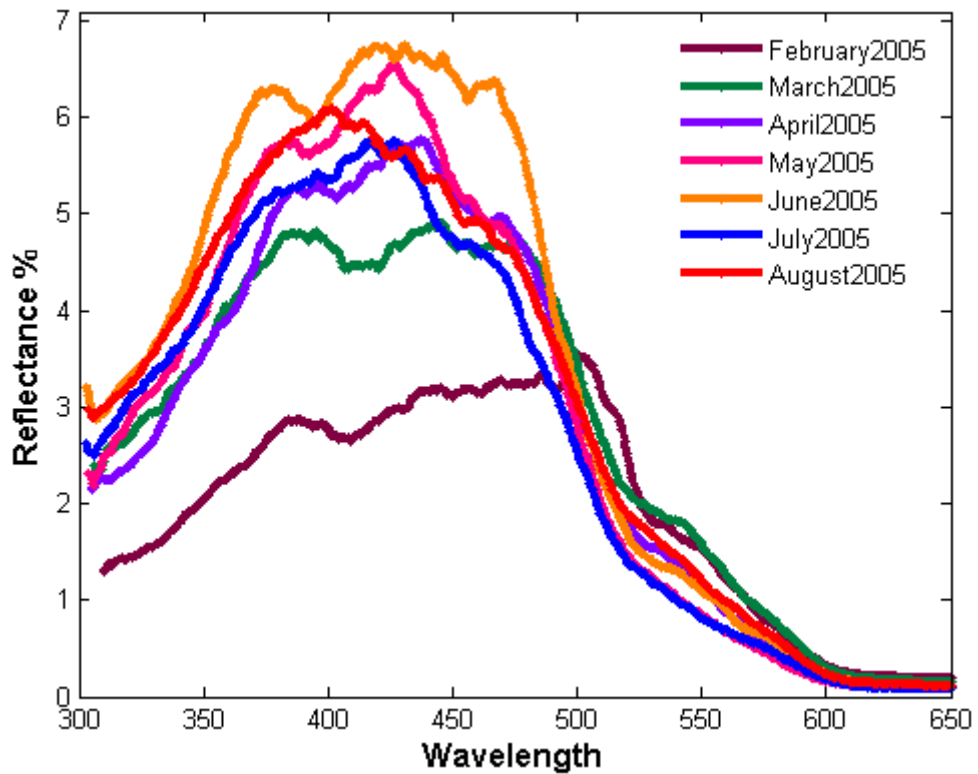
Figure 80: Reflectance values at METU-IMS time series station (see figure 4 for station location and latitude and longitude values are given in table 4) between 300-750 nm calculated from irradiance measurements.

Downward diffusivity varied temporally. Almost identical curves are observed in February and April. The February curve is similar to the Western Black Sea downward diffusivity curves (Figure 71). Very strong absorption occurred between 400 and 500 nm. In April, strong absorption occurred until 400 nm and is followed by a gradual increase until 500 nm. The shape and magnitude of the curves in the rest of the months were the same (Figure 81).
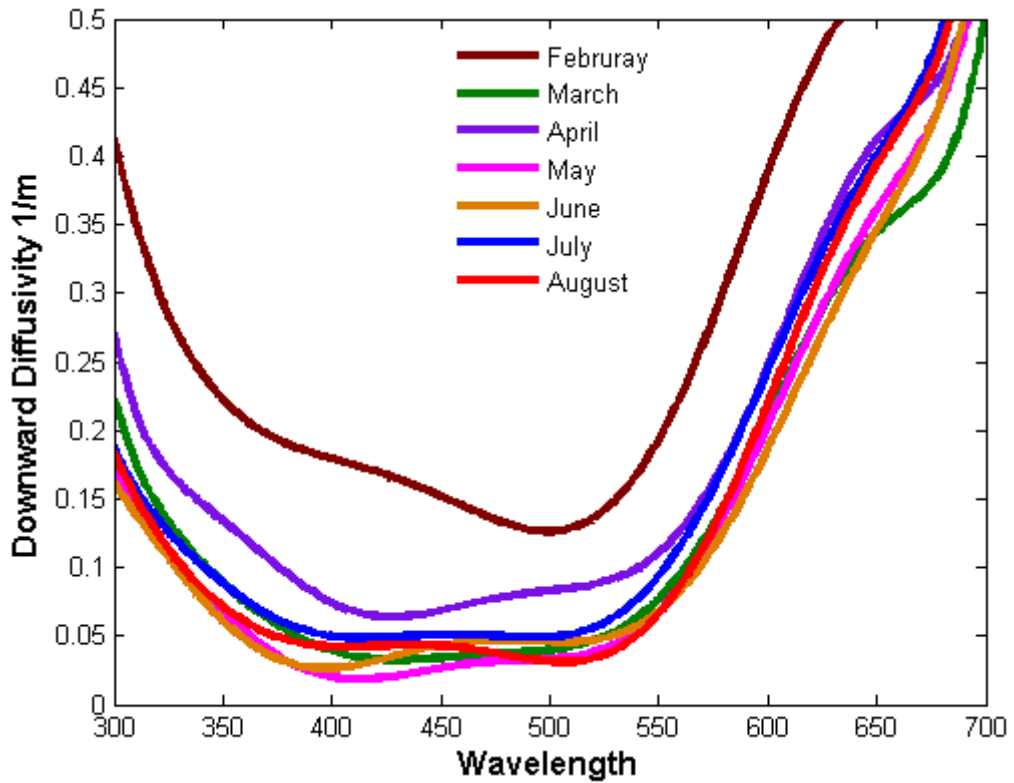
Figure 81: Downward Diffusivity coefficients at METU-IMS time series station (see figure 4 for station location and latitude and longitude values are given in table 4) between 300-700 nm, calculated from irradiance measurements.

The similar reflectance and downward diffusivities do not give clear information about the bio-optical processes within the sampling period. CDOM results obtained at the METU-IMS time series station during the sampling period showed that the highest CDOM absorption coefficients were measured in February, which is not included in Figure 82, because it is too high. The second highest values were detected in April. Thus, it is clear that the higher CDOM values cause the higher diffusivity coefficients (Figure 81) (Baker and Smith 1982, Sathyendranath 2000, Morel 2001, Stramski et al., 2004). Highest values of the CDOM were measured in March, April and May. However, in June the values were too low to plot on the graph (Figure 82). Possible reasons of these low values are the photo oxidation of CDOM to optically inactive forms and low phytoplanktonic activities

(Nelson et al., 1998, Siegel et al., 2002). Extremely low values in June are attributed to both photo oxidation and low chlorophyll (phytoplankton) concentration (Figure 83).
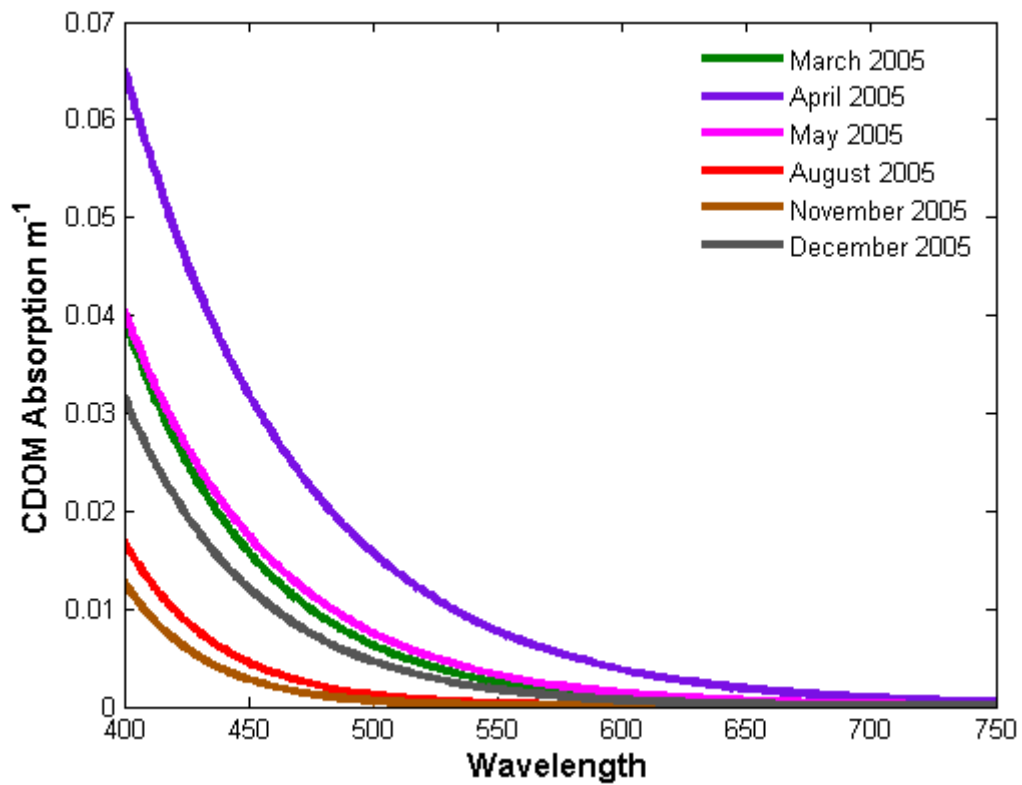
Figure 82: Temporal variability of the CDOM absorption coefficients in the METU-IMS time series station (see figure 4 for station location and latitude and longitude values are given in table 4).
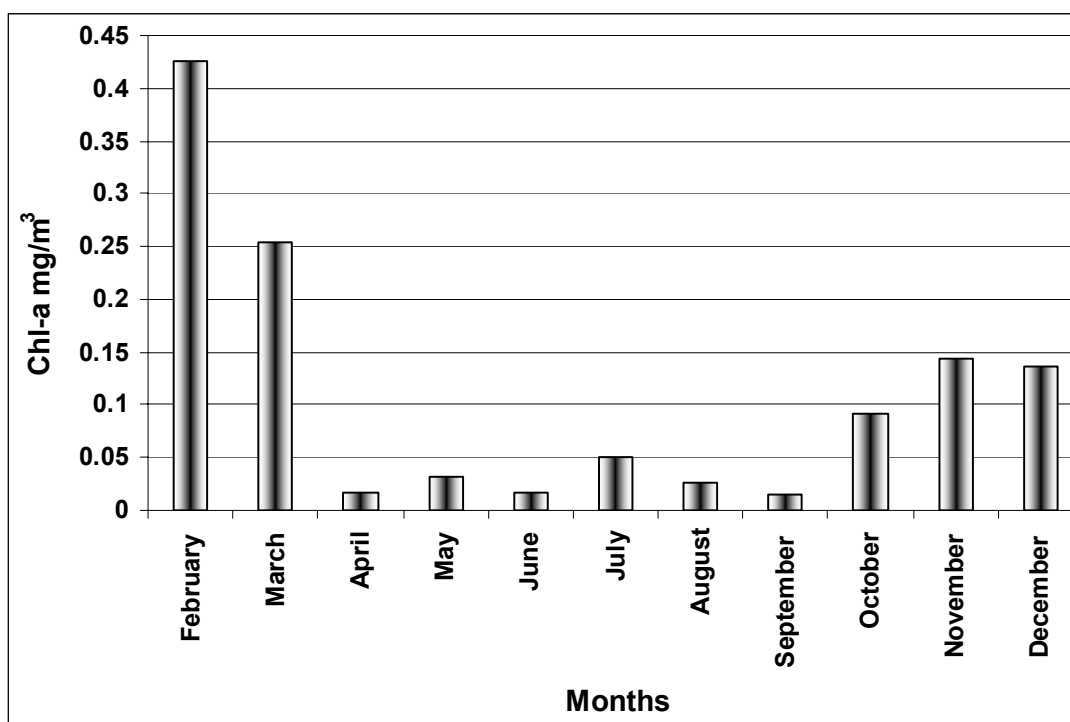
Figure 83: Monthly, chlorophyll a (including divinyll chlorophyll a) concentration at the METU-IMS time series station in 2005 (see figure 4 for station location and latitude and longitude values are given in table 4).

However, in July higher values are only attributed to higher phytoplankton (chlorophyll concentration). But CDOM absorption was lower than winter and spring period even though the chlorophyll concentration was higher than in April and May. Therefore, the photo oxidation of CDOM in this period controlled the CDOM absorption coefficients. CDOM absorption in August started to decrease, continuing through September, and increased afterwards, except in November (Figure 33). In this connection, high CDOM absorption period was between March and May, followed by low CDOM absorption period until September, and again increased afterwards. Thus, at the end of the winter, CDOM values remained the same or even higher than the winter values (e.g. April) (Figure 82).

Temporal variability of the particle absorption coefficients at the METU-IMS time series station did not co varies with the CDOM absorption coefficients, except in the winter season period. This indicates the phytoplankton activity controls the

bio-optical processes. Highest particle absorption coefficients are found in February and November, followed by March, July and August respectively. The lowest values occurred in April, May and June respectively (Figure 27, Figure 84). Contrary to CDOM, particle absorption measurements are dependent on the particle composition in the water. Concerning the METU-IMS time series station, particle composition depends on the phytoplankton activity, because of its offshore location. However, every phytoplankton group has different absorption characteristics (Allali et al., 1997, Bricaud et al., 1998, Babin and Stramski 2002, Barlow et al., 2002, Cleveland and Weidemann 1993, Cota et al., 2000, Devered et al., 2006, Gomez et al., 1995, 2001, Hoepffner and Sathyendranath 1993, Mitchell et al., 2000, 2002, Moore et al., 1995). Hence it is possible to get different absorption coefficients, even similar concentration of chlorophyll a. In spite of this, general trend of the chlorophyll a concentration and particle absorption coefficients are coherent.
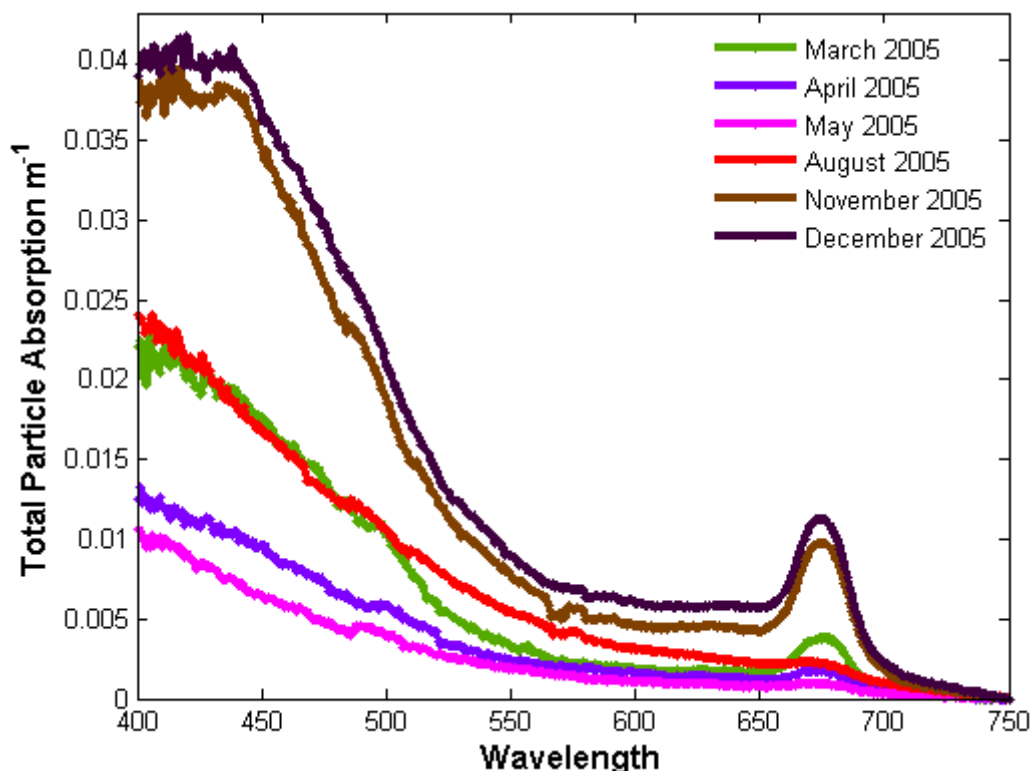
Figure 84: Temporal variability of the total particle absorption coefficients in the METU-IMS time series station (see figure 4 for station location and latitude and longitude values are given in table 4).

CDOM and particle absorption dynamics are implied the biogeochemical cycle in the basin. Higher chlorophyll concentration in the region is observed during the winter period when the stratification through the water column disappeared. After the bloom period, CDOM values start increasing and reach the maximum in April, and particle absorption coefficients are very low. This may be evidence of the degradation of winter bloom products. This degradation started in April and ended in June. Decreasing of the particle absorption and chlorophyll concentrations support this degradation process, for locations relatively far from anthropogenic sources (Figure 82, 83, 84). From July onwards, a slight increase is observed in all parameters including CDOM, particle absorptions and chlorophyll a concentration. The winter increase began in October. The stratified water column in summer limited or blocked the mixing, limiting the production. Until early winter, regenerated production should take place. Mixing, in early winter, brought deep waters to surface and allowed new production.

The optical properties of seawater are controlled both by phytoplankton activities, as in the North Eastern Mediterranean, and anthropogenic input, as in the coastal Western Black Sea. The measurements in the North Eastern Mediterranean showed that the light penetration is quite high, and even the absorption is very close to the pure water value (Figures 81, 85). While the constituents do not change much seasonally, two main seasonal changes are observed. Higher chlorophyll concentration occurred in late autumn and winter period and lower chlorophyll concentration occurred in the spring-summer period (Figure 84).
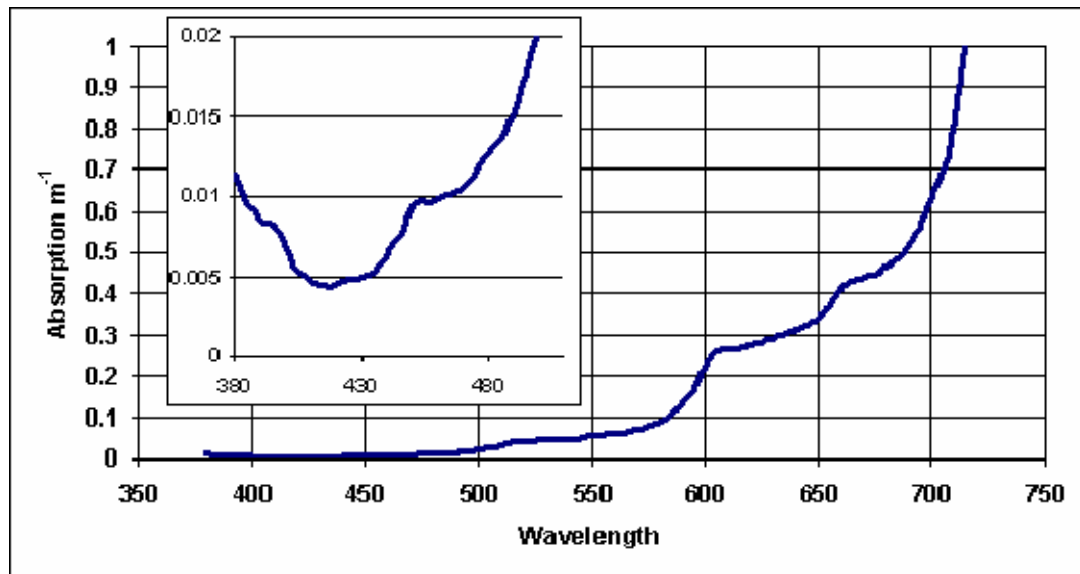
Figure 85: Pure water absorption coefficients between 380 and 720 nm, and a detail between 380nm and 500 nm (Redrawn from Pop and Fry 1997).

The irradiance measurements did not indicate any particular features by its self. The down welling irradiance measured at the surface is very similar to absolute solar irradiance, which showed the correctness of the measurements (Figure 78, 86).
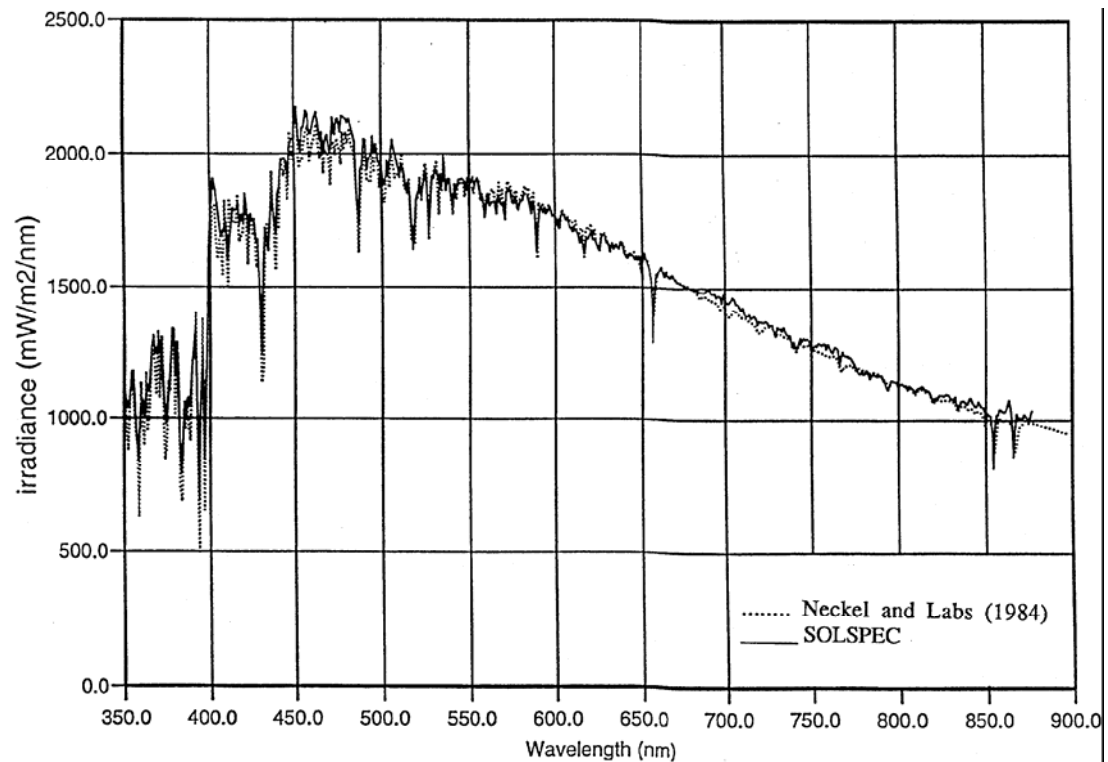
Figure 86: Absolute solar spectral irradiance from the SOLSPEC/ATLAS 1 spectrometer displayed together with the spectrum of Neckel and Labs (1984) measured at the Jungfraujoch (Thuillier et al., 1998).

4.2. HPLC Measurements and "Chemtax" Analysis

Regional differences according to the pigment measurements and Chemtax are determined. Temporal variability and the community structure of the phytoplankton in the water column is the main parameter which influences the optical properties. The temporal variability of the phytoplankton groups at the METU-IMS time series station (see figure 4 for station locations and latitude and longitude values are given in table 4) is separated in two periods (Figure 87):

1: Cyanophyta dominated
2: Mix
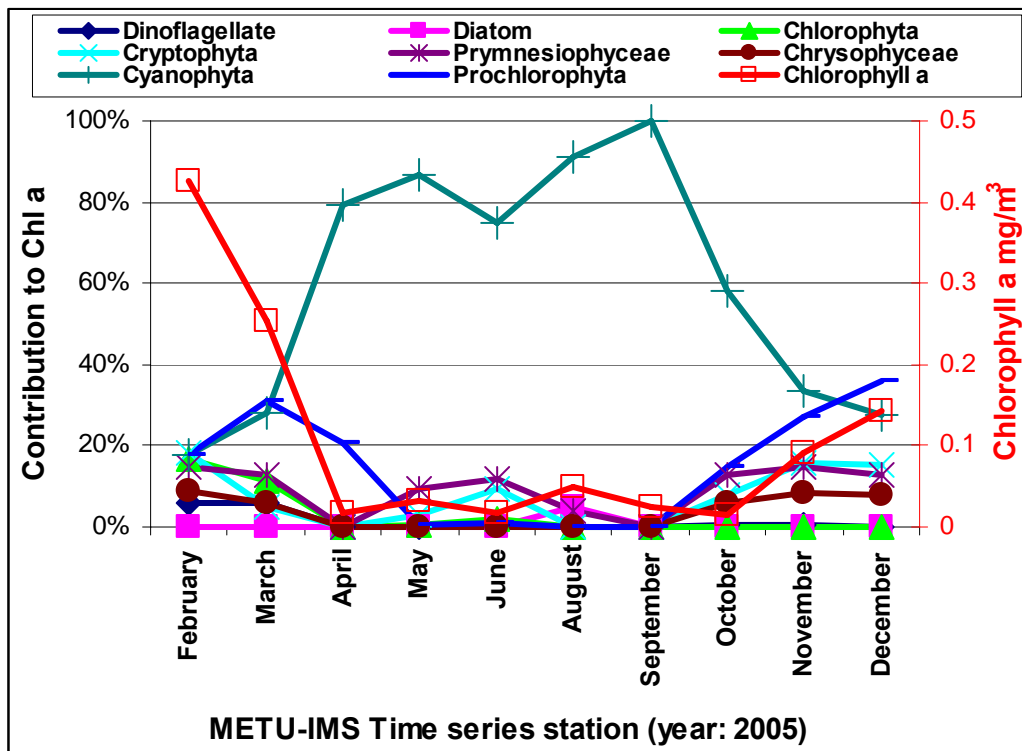
Figure 87: Temporal variability of the phytoplankton groups' contribution to total chlorophyll a and chlorophyll a concentration in METU-IMS time series station (see figure 4 for station location and latitude and longitude values are given in table 4) in 2005.

Cyanophyta is dominant in the North Eastern Mediterranean Basin (Figure 55, 56, 57). The basin is well known for its oligotrophic character (Dolan et al., 1999, Krom et al., 2005, Zohary et al., 2005) and the Cyanophyta, according to the results obtained from Chemtax, controls the oligotrophy. During the oligotrophic phase Cynophyta has contributed to the chlorophyll a around 80%. Similar results were found by Vidussi et al., (2000) and Dolan et al., (1999) from Western and Eastern Mediterranean. The advantage of the Cyanophyta over other groups is its low requirement on phosphorus (Bertilsson et al., 2003).

The results from these analyses are supported by the particle and CDOM absorption measurements. Two periods have been observed according to both measurements. An inverse relation between the Cynophyta and the chlorophyll a concentration has been found (Figure 88). All high chlorophyll concentrations

occurred whenever other groups contributed to the total chlorophyll a production. These periods coincided with autumn and winter.
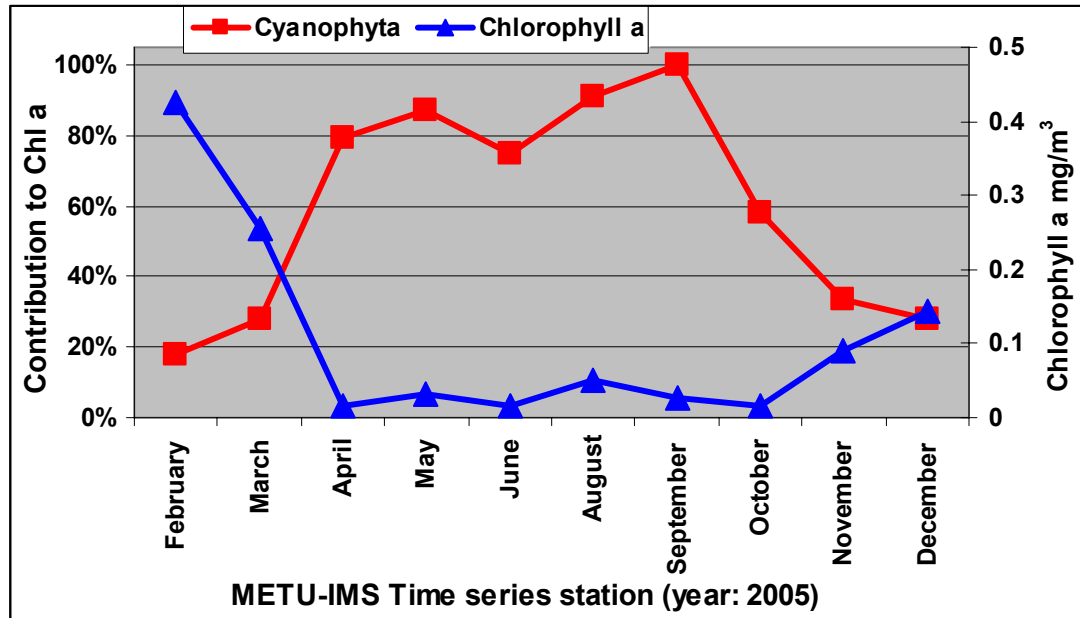
Figure 88: Relationship between Cynophyta and total chlorophyll a concentration between February to December 2005.

5. SUMMARY and CONCLUSIONS

This study focuses on investigating the variability of the optical properties in the Mediterranean, specifically the spectral characteristics of the optical properties and the relation between the in-situ and satellite measured properties.

SeaWiFS and MODIS derived chlorophyll data obtained during the time period where the data were coexistent (2002-2004) gave consistent results. Thus, data from both sensors are used to establish temporal continuity.

High temporal and spatial variability is observed in the optical properties of the two basins. The Western Black Sea and the North Eastern Mediterranean Seas are two typical examples of the Case I and the Case II waters, respectively. Seasonal variations were the dominating features that effect bio-optical characteristics of the North Eastern Mediterranean. Optical classification of the water types Western Black Sea, Marmara and the North Eastern Mediterranean and Aegean Seas, based on the Jerlov model shows that the Mediterranean has clear and very clear water type characteristics and the Western Black Sea and the Marmara waters are turbid (Type 5).

Chlorophyll a and phytoplankton group composition are the main components controlling the optical properties in Turkish offshore waters. Anthropogenic impact on the optical properties is not observed. In the North Eastern Mediterranean, seasonal variability can be divided in two main periods: the higher chlorophyll concentration period in late autumn and winter and the spring summer period where the chlorophyll concentration is very limited. Cyanophyta group dominates (80%) the low concentration period. Chlorophyll concentrations show increase with increased mixing in late autumn.

Absorption from yellow substance (or so-called CDOM) does not optically dominate the North Eastern Mediterranean allowing accurate estimation of pigment concentrations by remote sensing methods. Phytoplanktonic activities are controlled by the optical characteristics usually. However, similar to April 2005, degradation occurred with relatively high CDOM absorption coefficients after the winter blooms. The present study contributes towards an understanding of the bio-optical characteristics of the waters surrounding Turkey and suggests that the ability to develop algorithms for the estimation of pigment concentrations by remote sensing requires further studies. This study gives information on the relation between phytoplankton concentration and composition, and the optical properties which can be used to study primary production estimations, ecosystem modeling, microbial loop and satellite oceanography.

HPLC measurements show that the diatoms are the main group in the ecosystem, whereas in North Eastern Mediterranean *Cyanophyta* dominates. Phytoplankton group compositions in the offshore and coastal regions of the North Eastern Mediterranean do not show considerable difference. The main differences are the higher *Prymnesiophyceae* (nearly two times higher than the offshore) and lower *Cyanophyta* contribution in the coastal regions compared to offshore regions.

The general properties and characteristics of the study area and the temporal variability observed in the METU-IMS time series station can be summarized as follows (Table 11).

Table 11: General bio-optical properties of the sampling region and temporal variability observed in METU-IMS time series station.

REGIONAL VARIABILITIES

REGION/PARAMETER	PA (PEAK)	PA PEAK MAGNITUDE	PA (PHYTO-PEAK)	PHYTO-PEAK MAGNITUDE	PHYTO-PEAK-DETRITUS 400NM	% Phytoplankton Absorption at 440 nm	CDOM (400NM)	REFLECT PEAK	DOMINANT PHYTO-GROUP	JERLOV TYPE	MEAN CHL A	STD DEV
OFFSHORE BLACK SEA	420,440	0.04	420,440	0.027	0.012	69	0.25	450-550	DIATOMS	5	2.025	2.3
COASTAL BLACK SEA	440	0.19	440	0.18	0.06	59	0.25	450-550	DIATOMS	5	2.025	2.3
SEA OF MARMARA							0.25	450-550		5		
AEGEAN SEA	NO PEAK	0.02	420,440	0.008	0.008	48	0.1	400-450		V.CLEAR		
OFFSHORE MED. SEA	NO PEAK		420,440	0.008	0.012	48	0.043	400-450	CYANOPHYTA	V.CLEAR	0.175	0.18
COASTAL MED. SEA	420	0.07	440	0.027	0.04	45.7	0.02	400-500	CYANOPHYTA	1	0.752	0.66
ISKENDERUN BAY	420,440	0.01	420,440	0.01	0.02	36.4	0.038	400-450	CYANOPHYTA	V.CLEAR	0.192	0.135

TEMPORAL VARIABILITIES — METU-IMS T.SERIES

MONTHS/PARAMETER	PA (PEAK)	PA PEAK MAGNITUDE	PA (PHYTO-PEAK)	PHYTO-PEAK MAGNITUDE	PHYTO-PEAK-DETRITUS 400NM	% Phytoplankton Absorption at 440 nm	CDOM (400NM)	REFLECT PEAK	DOMINANT PHYTO-GROUP	JERLOV TYPE	CHL A
FEBRUARY	FLAT 440	0.034	440,470	0.011	0.025170	34.3	Very High	450-500	Mix	1	0.40
MARCH	FLAT 420	0.022	440	0.0109	0.012477	53.5	0.039	400-450	Prochl,Cyano	V.CLEAR	0.25
APRIL	LINEER 400	0.013	FLAT	0.006	0.006628	60.8	0.065	400-450	Cyano	V.CLEAR	0.01
MAY	LINEER 400	0.01	416	0.003	0.006994	33.1	0.04	420	Cyano	V.CLEAR	0.02
JUNE	LINEER 400	0.0085	420	0.005	0.003474	59.1	Very Low	410	Cyano	V.CLEAR	0.02
JULY	LINEER 400	0.024	420,440	0.0057	0.017818	28.8	0.033	410		V.CLEAR	0.05
AUGUST	LINEER 400	0.023	412,430,440	0.0047	0.017395	23.7	0.0165	410	Cyano	V.CLEAR	0.03
SEPTEMBER	LINEER 400	0.035	420,440	0.009	0.026783	33.1	0.00086	400-450	Cyano	V.CLEAR	0.01
OCTOBER	405,418,440	0.037	420,440	0.018	0.020187	53.9	0.055	400-450	Cyano	V.CLEAR	0.09
NOVEMBER	415,440	0.039	440	0.02	0.022989	52.0	0.0127	400-500	Mix	1	0.14
DECEMBER	420,440	0.041	440	0.023	0.023122	57.6	0.0316	400-500	Mix	1	0.14

REFERENCES

Allali K, Annick Bricaud, and Herve Claustre. 1997. Spatial variations in the chlorophyll-specific absorption coefficients of phytoplankton and photo synthetically active pigments in the equatorial Pacific. JGR. Vol. 102. No. C6 . 12413-12423.

Arst H, V. I. Haltrin, and R. A. Arnone. 2002. Informative Water Layer, Determined by Attenuation Depth, in Water Bodies of Different Turbidity. OCEANS 2002 MTS-IEEE Proceedings, vol.4.

Babin M., and Dariusz Stramski. 2002. Light absorption by aquatic particles in the near-infrared spectral region. (Notes) Limnol. Oceanog. 47 (3). 911-915.

Baker K. S., and Raymond C. Smith. 1982. Bi-optical classification and model of natural waters 2. Limnol. Oceanog.., 27(3), 1982.

Barlow R.G., Cummings D.G., Gibb S.W., 1997. Improved resolution of mono- and divinyl chlorophylls a and b and zeaxanthin and lutein in phytoplankton extracts using reverse phase C-8 HPLC. Mar. Ecol. Prog. Ser. 161. 303-307.

Barlow R.G., J. Aiken, P.M. Holligan, D.G. Cummings, S. Maritorena, S. Hooker. 2002. Phytoplankton pigment and absorption characteristics along meridional transects in the Atlantic Ocean. Deep-Sea Research I 47, 637–660.

Behrenfeld M.J., Falkowski, P.G., 1997. Photosynthetic rates derived from satellite-based chlorophyll concentration. Limnology and Oceanography 42. 1-20.

Bertilsson S. and O. Berglund D. M. Karl. 2003. Elemental composition of marine Prochlorococcus and Synechococcus: Implications for the ecological stoichiometry of the sea. Lim. Ocean., 48 (5), 1721-1731.

Bethoux J. P., Morin, P., Chaumery, C., Connan, O., Gentili, B., & Ruiz- Pino, D. 1998. Nutrients in the Mediterranean Sea, mass balance and statistical analysis of concentrations with respect to environmental change. Marine Chemistry, 63, 155-169.

Bethoux J. P., and Gentili, B. (1999). Functioning of the Mediterranean Sea: past and present changes related to freshwater input and climate changes. Journal of Marine Systems, 19, 33– 47.

Bidigare R. R., Morrow, J. H., and Kiefer, D. A., 1989, Derivative analysis of spectral absorption by photosynthetic pigments in the western Sargasso Sea. Journal of Marine Research, 47, 323-341.

Bowers D. G., Kratzer, J. R. Morrison, S. D. Smith, Tett, W. Walne and Wild-Allen. 2001. On the calibration and use of in situ ocean colour measurements for monitoring algal blooms. 2001. Int. j. remote sensing, vol. 22, no. 2 & 3, 359-368.

Bricaud A., Morel, A., & Prieur, L. 1981. Absorption by dissolved organic matter of the sea (yellow substance) in the UV and visible domains. Limnology and Oceanography, 26, 43-53.

Bricaud A., E. Bosc, and D. Antoine. 2002. Algal biomass and sea surface temperature in the Mediterranean Basin, Intercomparison of data from various sensors, and implications for primary production estimates," Remote Sens. Env. 81, 163-178.

Bricaud A., A. Morel, M. Babin, K. Allali, and H. Claustre. 1998Variations of light absorption by suspended particles with chlorophyll a concentration in oceanic (case 1) waters: Analysis and implications for bio-optical models, J. Geophys. Res., 103, 31,033-31,044.

Brown C. W. and G. P. Podesda. 1997. Remote Sensing of Coccolithophore Blooms in the Western South Atlantic Ocean. 1997. REMOTE SENS. ENVIRON. 60:83-91.

Butler W. L., and Hopkins, D. W., 1970. Higher derivative analysis of complex absorption spectra. Photochemistry and Photobiology, 12, 439-450.

Chen Z., Curran, P. J., and Hansom, J. D., 1992. Derivative reflectance spectroscopy to estimate suspended sediment concentration. Remote Sensing of Environment, 40, 67-77.

Clayton A. Paulson and James J. Simpson. 1977. Irradiance measurements in the upper ocean. Journal of Physical Oceanography. Vol. 7. 952-956.

Cleveland J.S., and A.D. Weidemann, 1993. Quantifying absorption by aquatic particles: A multiple scattering correction for glass-fiber filters. Limnology and Oceanography. 38, 1321-1327.

Cota Glenn F., W. Glen Harrison, Trevor Platt, Shubha Sathyendranath, and Venetia Stuart. 2000. Bio-optical properties of the Labrador Sea. Journal of Geophysical Research, VOL. 108, NO. C7, 3228.

Cunningham A., 1996, Variability of in vivo chlorophyll fluorescence and its implications for instrument development in bio-optical oceanography. Scientia Marina, 60, 309-315.

Demetriades-Shah T. H., Steven, M. T., and Clark, J. A., 1990, High-resolution derivative spectra in remote sensing. Remote Sensing of Environment, 33, 55-64.

Devred E E., S. Sathyendranath, V. Stuart, H. Maass, O. Ulloa and T. Platt . 2006 A two component model of phytoplankton absorption in the open ocean: Theory and applications, J. Geophys. Res., 111, C03011, doi: 10.1029/2005Jc002880.

Dolan J.R., Vidussi, F., Claustre, H. 1999. Planktonic ciliates in the Mediterranean Sea: longitudinal trends. Deep-Sea Research I 46, 2025-2039.

Ediger D., and Ayşen Y. 1996. Characteristics of deep chlorophyll maximum in the Northeastern Mediterranean with respect to environmental conditions. Journal of Marine Systems, 9, 291-303 pp.

Ediger, V., Ş. T. Beşiktepe, M. Okyar, D. Tezcan. 2005. Kilikya-Adana Baseninin batimetrik ve morfolojik özelliklerinin araştırılması. (Proje: YDABÇAG-102Y111). O.D.T.Ü. , Deniz Bilimleri Enstitüsü, Erdemli, Eylül, 2005, 27pages. (In-Turkish).

Faust M. A., and Norris, K. H., 1985, In vivo spectrophotometric analysis of photosyntheticpigments in natural populations of phytoplankton. Limnology and Oceanography, 30, 1316-1322.

Figueroa Felix L. 2002. Bio-optical characteristics of Gerlache and Bransfield Strait waters during an Antarctic summer cruise. Deep-Sea Research II 49 675-691.

Garver S., D. A. Siegel, and B. G. Mitchell. 1994. Variability in near-surface particulate absorption spectra: What can a satellite ocean color imager see Limnol. Ocean. 39, 1349-1367, 1994.

Gieskes W. W. C., 1991, Algal pigments fingerprints: clue to taxon-specific abundance, productivity and degradation of phytoplankton in sea and oceans. In Particle Analysis in Oceanography, edited by S. Demers (Berlin: Springer-Verlag). 61-99.

Gomez Aguirre R., Boxall, S. R., and Weeks, A. R., 1995, Identification of algal pigments using high order derivatives. Proceedings of the International Symposium on Quantitative Remote Sensing for Science and Applications, Florence, Italy, 10–14 July 1995 (IGARSS'95) (Florence: IEEE), vol. 3. 2084-2086.

Gomez Aguirre R., A. R. Weeks and S. R. Boxall. 2001. The identification of phytoplankton pigments from absorption spectra. Int. J. Remote Sensing, vol. 22, no. 2 & 3. 315–338.

Goodin D. G., Han, L., Fraser, R. N., Rundquist, D. C., and Stebbins, W. A., 1993, Analysis of suspended solids in water using remotely sensed high resolution derivative spectra. Photogrammetric Engineering and Remote Sensing, 59, 505–510.

Gordon H. R., and Morel, A., 1983, Remote assessment of ocean colour for interpretation of satellite visible imagery. Lecture Notes in Coastal and Estuarine Studies, Vol. 4 (Berlin: Springer-Verlag).

Gordon H. R. 1994. Modeling and simulating radiative transfer in the ocean. 13-15. In R. W. Spirit-ad, K. L. Carder, and M. J. Perry [eds.], Ocean optics. Oxford Univ. Press.1994.

Gulyayev S. A., and Litvin, F. F., 1970, First and second derivatives of the absorption spectrum of chlorophyll and associated pigments in cells of higher plants and algae at 20°C. Biofisika, 15, 701–712.

Habbane J., M. Dubois, M. I. EL-Sabh and P. Larouche.1998. Empirical algorithm using SeaWiFS hyperspectral bands: a simple test int. Technical note M., Int. J. remote sensing, vol. 19, no:11, 2161-2169.

Hansell Dennis A. and Craig A. Carlson. 2001. Marine Dissolved Organic Matter and the Carbon Cycle. SPECIAL ISSUE – JGOFS 41. Oceanography • Vol. 14 • No. 4/2001. Oceanography, Volume 14, Number 4, a quarterly journal of The Oceanography Society.

Hedges J.I. 2002. Why dissolved organics matter. In: Hansell, D.A., Carlson, C.A. (Eds.), Biogeochemistry of Marine Dissolved Organic Matter. Academic Press, San Diego. 1-33.

Higgins H. W. and Mackey, D. J. 2000. Algal class abundances in the western Equatorial Pacific under ENSO and non-ENSO conditions. Deep-Sea Research, 47: 1461-1483.

Hoepffner N and Shubha Sathyendranath 1992. Bio-optical characteristics of coastal waters: Absorption spectra of phytoplankton and pigment distribution in the western North Atlantic. Lim. Ocean., 37(8). 1660-1679.

Hoepffner N., and Shubha Sathyendranath 1993. Determination of the major groups of phytoplankton pigments from the absorption spectra of total particulate matter, J. Geophysical Res., 98. 22,789-22,803.

Jeffrey S.W., Mantoura R.F.C., Wright S.W. 1997. Phytoplankton pigments in Oceanography: guidlines to modern methods. UNESCO, Paris.

Jerlov N G., and Nielsen E S, 1974, "Optical Aspects of Oceanography", Academic Press, UK

Jerlov N.G., 1976. Marine Optics. Elsevier, Amsterdam.

Kirk J.T.O., 1994. Light and Photosynthesis in Aquatic Ecosystems, 2nd Edition. Cambridge University Press, Cambridge, 509 pages.

Kishino M., M. Takahashi, N. Okami and S. Ichimura. 1985. Estimation of the spectral absorption coefficients of phytoplankton in the sea. Bull. Mar. Sci., 37, 634-642.

Kishino M. 1995. Interrelationships between light and phytoplankton in the sea. Pp. 73-92. From: Richard W. Spinard, Kendall L. Carder, and Mary Jane Perry. Ocean Optics. Oxford monographs on geology and geophysics; no. 25). Oxford University Press, Inc. ISBN 0-19-506843-2. 283 pages.

Kowalczuk Piotr, Joanna Ston´-Egiert, William J. Cooper, Robert F. Whitehead, Michael J. Durako. 2005.Characterization of chromophoric dissolved organic matter (CDOM) in the Baltic Sea by excitation emission matrix fluorescence spectroscopy. Marine Chemistry 96. 273-292.

Krom M.D., Thingstad, T.F., Carbo, P., Drakopoulos, P., Fileman, T.W., Flaten, G.A.F., Groom., S., Herut, B., Kitidis, V., Kress, N., Law., C.S., Liddicoat, M.I., Mantoura, R.F.C., Pasternak, A., Pitta, P., Polychronaki, T., Psarra, S., Rassoulzadegan, F., Skjoldal, E.F., Spyres, G., Tanaka, T., Tselepides, A., Wassmann, P., Wexels-Riser, C, Woodward,
E.M.S., Zodiatis, G., Zohary, T. 2005. Overview of the CYCLOPS P addition Lagrangian experiment in the Eastern Mediterranean. Deep-Sea Research II, 52. 2879-2896.

Lamperta B. Queguinerc, T. Labasque, A. Pichon, N. Lebreton. 2002. Spatial variability of phytoplankton composition and biomass on the eastern continental shelf of the Bay of Biscay (north-east Atlantic Ocean). Evidence for a bloom of Emiliania huxleyi (Prymnesiophyceae) in spring 1998. 2002. Continental Shelf Research 22. 1225-1247.

Loisel H., and A. Morel. 1998. Light scattering and chlorophyll concentration in case 1 waters: A reexamination, Limnol. Oceanogr., 43, 847-858.

Longhurst. Alan, Shubha Sathyendranath, Trevor Platt and Carla caverhill. 1995. An estimate of global primary production in the ocean from satellite radiometer data. Journal of Plankton Research. Vol 17 no.6. 1245-1271.

Mackey M. D, D.Mackey, H. W. Higgins, S. W. Wright. 1996. CHEMTAX— a program for estimating class abundances from chemical markers: application to HPLC measurements of phytoplankton . Mar Ecol Prog Ser. Vol. 144: 265-283.

Mackey M. D., Higgins, H. W., Mackey, D. J. and Wright, S. W. (1997). CHEMTAX user's manual: a program for estimating class abundances from chemical markers - application to HPLC measurements of phytoplankton pigments. Report. Marine Laboratories. CSIRO Australia, (229): 41pages.

Mantoura R.F.C., Llewellyn C.A., 1983. The rapid determination of algal chlorophyll and carotenoid pigments and their breakdown products in natural waters by reverse-phase high performanse liquid chromatography. Analyt. Chim. Acta 151: 297-314.

McKee, D., Cunningham, A., and Jones, K. 1999. Simultaneous measurements of fluorescence and beam attenuation: instrument characterisation and interpretation of signals from stratified coastal water. Estuarine, Coastal and Shelf Science, 48. 51-58.

Mitchell B. G., and Dale A. Kiefer. 1988. Chlorophyll a specific absorption and fluorescence excitation spectra for light-limited phytoplankton. Deep Sea Research, Vol 35, No. 5. 639-663.

Mitchell B.G., Holm-Hansen, O. 1991. Bio-optical properties of Antarctica peninsula waters: differentiation from temperature ocean models. Deep-Sea Research II 38. 1009-1028.

Mitchell B. G., Annick Bricaud, Kendall Carder, Joan Cleveland, Giovanni Ferrari, Rick Gould, 1Mati Kahru, Motoaki Kishino, Helmut Maske, Tiffany Moisan, Lisa Moore, Norman Nelson, Dave Phinney, Rick Reynolds, Heidi Sosik, Dariusz Stramski, Stelvio Tassan, Charles Trees, Alan Weidemann, John Wieland and Anthony Vodacek. 2000. Determination of spectral absorption coefficients of particles, dissolved material and phytoplankton for discrete water samples. pp 125-153. From: Giulietta S. Fargion and James L. Mueller. (Eds). 2000. Ocean Optics Protocols For Satellite Ocean Color Sensor validation, Revision 2. Center for Hydro-Optics and Remote Sensing. NASA/TM-2000-209966. San Diego, State University, San Diego, California. National Aeronautical and Space administration. Goddard Space Flight Space Center Greenbelt, Maryland 20771.

Mitchell B G., Mati Kahru, John Wielland, and Malgorzata Stramska.2002. Determination of spectral, dissolved material and phytoplankton for discrete water samples. From: Mueller, J.L. and G.S. Fargion,[Eds.]: Ocean Optics Protocols for Satellite Ocean Color Sensor Validation, Revision 3. NASA Tech. Memo. 2002-210004, NASA Goddard Space Flight Center, Greenbelt, Maryland, 308 pages.

Mobley C. D. (1995). The Optical Properties of Water. In M. Bass, E. W. Van Stryland, D. R. Williams, & W. L. Wolf (Eds.), Handbook of Optics. Fundamentals, Techniques, and Design (Vol. I, pp. 43.3–43.56). New York: McGraw-Hill.

Mobley Curtis D., Dariusz Stramski , W. Paulbissett, and Emmanuel Boss. Optical Modeling of Ocean Water. Is the Case 1 - Case 2 Classification Still Useful? Oceanography. Volume 17, Number 2.

Moore L.R., Goericke, R., Chisholm, S.W., 1995. Comparative physiology of Synechococcus and Prochlorococcus:influence of light and temperature on growth, pigments, fluorescence and absorptive properties. Marine Ecology Progress Series 116, 259-275.

Morel A. and L. Prieur. 1977. "Analysis of variations in ocean color," Limn. Ocean. Vol. 22, no. 4. 709–722.

Morel A.1994. Optics from the single cell to the mesoscale. (pp: 93-106) From: Richard W. Spinard, Kendall L. Carder, and Mary Jane Perry. Ocean Optics. Oxford monographs on geology and geophysics; no. 25). Oxford University Press, Inc. ISBN 0-19-506843-2. 283 pages.

Morel A and Stephane Maritorena. 2001. Bio-optical properties of oceanic waters: A reappraisal. Journal of Geophysical Research, Vol. 106, No. C4. 7163-7180.

Mueller J.L., and G.S. Fargion,[Eds.], 2002: Ocean Optics Protocols for Satellite Ocean Color Sensor Validation, Revision 3. NASA Tech. Memo. 2002-210004, NASA Goddard Space Flight Center, Greenbelt, Maryland, 308 pages.

Mueller J. L., Giulietta S. Fargion and Charles R. McClain, Editors. 2003. Ocean Optics Protocols fr Satellite Ocean Color Sensor Validation, Revision 4, Volume VI: Special Topics in Ocean Optics Protocols and Appendices. NASA/TM-2003-211621/Rev4-Vol.VI. 141 pages.

Neckel H. and Labs, D. 1984. Solar Phys. 90, 205.

Nelson N. B., D. A. Siegel, and A. F. Michaels. 1998. Seasonal dynamics of colored dissolved material in the Sargasso Sea, Deep Sea Res., Part I, 45, 931-957.

Nezlin N., P. 2000. Remote-sensing studies of seasonal variations of surface chlorophyll-*a* concentration in the Black Sea. Satellites, Oceanography and Society. Ed. David Halpern. 257-271.

O'Reilly J. E., Maritorena, S., O'Brien, M. C., Siegel, D. A., Toole, D., Mitchell, B. G., Kahru, M., Chavez, F. P., Strutton, P., Cota, G. F., Hooker, S. B., McClain, C. R., Carder, K. L., Muller-Karger, F. E., Harding, L., Magnuson, A., Phinney, D., Moore, G. F., Aiken, J., Arrigo, K. R., Letelier, R., & Culver, M. 2000. Ocean color chlorophyll a algorithms for SeaWiFS, OC2 and OC4: version 4. In: S. B. Hooker, & E. R. Firestone (Eds.), SeaWiFS Postlaunch Technical Report Series, NASA Technical Memorandum 2000, 206892, Vol. 11. Greenbelt, Maryland: NASA Goddard Space Flight Center.

Ogawa H., and Eiichiro Tanoue. 2003. Dissolved Organic Matter in Oceanic Waters. Journal of Oceanofraphy, Vol. 59. 129-147.

Platt T., and Shubha Sathyendranath. 1988. Oceanic Primary Production: Estimation by Remote Sensing at Local and Regional Scales. Science. Vol. 241. 1613-1619.

Platt, T., Caverhill, C., Sathyendranath, S., 1991. Basin-scale estimates of oceanic primary production by remote sensing: the North Atlantic. Journal of Geophysical Research 96. 15147-15159.

Pope R. M., and E. S. Fry. 1997. Absorption spectrum (380-700 nm) of pure water, II, Integrating cavity measurements, Appl. Opt., 36. 8710-8723.

Preisendorfer R. W 1961. Application of radiative transfer theory to light measurements in the sea 1961; Report 10, International Union for Geodesy and Geophysics. 11-29.

Sancak S., Sukru T. Besiktepe, Aysen Yilmaz, Michael Lee and Robert Frouin. 2005. Evaluation of SeaWiFS chlorophyll-a in the Black and Mediterranean Seas. International Journal of Remote Sensing. Vol. 26, No: 10 2045-2060.

Sathyendranath S., Trevor Platt, Edward P. W. Horne, William G. Harrison, Osvaldo Ulloa, Richard Outerbridge and Nicolas Hoepffener. 1991. Estimation of new production in the ocean by compound remote sensing. Nature. Vol 353. 129-133.

Sathyendranath S. (ed). 2000. IOCCG Remote Sensing of Ocean Colour in Coastal and Other Optically-Complex, Waters. Reports of the International Ocean-Colour Coordinating Group, No. 3, IOCCG, Dartmouth, Canada.

Siegel D. A., S. Maritorena, N. B. Nelson, D. A. Hansell, and M. Lorenzi-Kayser. 2002. Global distribution and dynamics of colored dissolved and detrital organic materials. J. Geophys. Res., 107(C12), 3228, doi:10.1029/2001JC000965.

Smith C. Raymond and Karen S. Baker. 1978. Optical properties of natural waters[1]. 1978. Limnology and Oceanography. V. 23(2). 260-267.

Sogandares F. M., and E. S. Fry. 1997. Absorption spectrum (340–640 nm) of pure water, I, Photothermal measurements, Appl. Opt., 33. 8699-8709.

Srokosz M.A. 2000. Biological Oceanography by Remote Sensing in Encyclopedia of Analytical Chemistry. R.A. Meyers (Ed.) 8506–8533.

Stambler N., Lovengreen, C., Tilzer, M.N., 1997. The underwater light field in the Bellinghausen and Admudsen Seas (Antarctica). Hydrobiologia 344, 41–56.

Stramski D., and Curtis D. Mobley. 1997. Effects of microbial particles on oceanic optics: A database of single-particle optical properties. Lim. Ocean. 42(3). 538-549.

Stramski D., Emmanuel Boss, Darek Bogucki, Kenneth J. Voss. Review. 2004. The role of seawater constituents in light backscattering in the ocean. Progress in Oceanography 61. 27-56.

Stedmon C.A., Markager, S., and Kaas, H. 2000. Optical Properties and Signatures of Chromophoric Dissolved Organic Matter (CDOM) in Danish Coastal Waters. Estuarine, Coastal and Shelf Science 51: 267-278.

Stewart Robert H. 2006. Introduction to Physical Oceanography Department of Oceanography. Texas A & M University Copyright 2006 September 2006 Edition.

Strickland J.D.H. and T.R. Parsons. 1972. (2nd Edition) A practical handbook of sea-water analysis. J. Fish. Res. Bd. Canada. 167: 311 pages.

Subramaniama A., Carpenter, E.J., Falkowski, P.G., 1999. Optical properties of the marine diazotrophic cyanobacteria Trichodesmium spp.; IIFa reflectance model for remote-sensing. Limnology and Oceanography 44. 618-627.

Subramaniama A., Christopher W. Brownb, Raleigh R. Hoodc, Edward J. Carpenterd, Douglas G. Caponea. Detecting Trichodesmium blooms in SeaWiFS imagery. 2002. Deep-Sea Research II 49. 107-121.

Suzuki K., Motoaki Kishino, Kousei Sasaoka, Sei-Ichi Saitoh And Toshiro Saino. 1998. Chlorophyll-Specific Absorption Coefficients and Pigments of Phytoplankton off Sanriku, Northwestern North Pacific Journal of Oceanography, Vol. 54. 517-526.

Suzuki K., Chie Minami, Hongbin Liu and Toshiro Saino. 2002. Temporal and spatial patterns of chemotaxonomic algal pigments in the subarctic Pacific and the Bering Sea during the early summer of 1999. Deep Sea Research Part II: Topical Studies in Oceanography Volume 49, Issues 24-25, 2002, Pages 5685-5704.

Thomas G.E.and K.Stamnes. 1999. Radiative transfer in the atmosphere and oceans. Cambridge University Press, Cambridge. 517 pages.

Thuillier G., Michelherse Paul C. Simon, Dietrich Labs, Holger Mandel, Didier Gillotay and Thomas Foujols., 1998. The Visible Solar Spectral Irradiance From 350 To 850 Nm As Measured By The Solspec Spectrometer During The Atlas I Mission. Solar Physics 177: 41–61, 1998. (Paper presented at the SOLERS22 International Workshop, held at the National Solar Observatory, Sacramento Peak, Sunspot, New Mexico, USA, (June 17–21, 1996).

Verdaguer Christina Vidal. 1995. Bio-Optical Characteristics of the Mediterranean and the Black Sea. Msc. Thesis in Marine Sciences. METU-IMS, İçel Turkey.

Williams C. Howard, Rob Davies-Colley, Warwick F. Vincent. 1995. Optical properties of the coastal and oceanic waters off South Island, New Zealand: regional variation. New Zealand Journal of Marine and Freshwater Research: Vol. 29. 589-602.

Wright S. W., D. P. Thomas, H. J. Marchant, H. W. Higgins, M. D. Mackey, And D. J. Mackey. 1996. Analysis of phytoplankton of the Australian sector of the Southern Ocean: Comparison of microscopy and size frequency data with interpretations of pigment HPLC data using the 'CHEMTAX' matrix factorization program. Marine Ecology Progress Series 144. 285-298.

Yılmaz A., Dilek Ediger, Özden Baştürk and Süleyman Tuğrul. 1994. Phytoplankton fluorescence and deep chlorophyll maxima in the Northeastern Mediterranean. Oceanologica Acta-Vol. 17-No:1. 69-77.

Zibordi G., G. Maracci and P. Schlittenhardt. 1990. Ocean colour analysis in coastal waters by airborne sensors. Int. J. Remote Sensing. Vol 11, No: 5. 705-725.

Zohary T., Barak Herut, Michael D. Krom, R. Fauzi C. Mantoura, Paraskevi Pitta, Stella Psarra, Ferreidoun Rassoulzadegan, Noga Stambler, Tsuneo Tanaka, T. Frede Thingstad, E. Malcolm S. Woodward. 2005. P-limited bacteria but N and P co-limited phytoplankton in the Eastern Mediterranean—a microcosm experiment. Deep-Sea Research II 52. 3011-3023.

URL1:
http://coolcosmos.ipac.caltech.edu/cosmic_classroom/ir_tutorial/irwindows.html
URL2: http://sealevel.jpl.nasa.gov/
URL3: http://www.ioccg.org/
URL4: http://daac.gsfc.nasa.gov/data/dataset/index.html

CURRICULUM VITAE

GENERAL

SURNAME NAME: ÖREK, Hasan

DATE OF BIRTH: 23/09/1973

MARITAL STATUS: Married

PRESENT ADDRESS: ODTÜ Deniz Bilimleri Enstitüsü, PK 28 Erdemli, 33731 Mersin

TEL: +90 324 5213434

FAKS: +90 324 5212327

E-MAIL: orek@ims.metu.edu.tr, hasan.orek@gmail.com

EDUCATION

BSc: 1992-1996 Aegean University Faculty of Fisheries.

MSc: An Application of Mass Blance Ecopath Model to the Trophic Structure in the Black Sea "After Anchovy Collapse".
1997-2000 Middle East Technical University Institute of Marine Sciences, Dept. Marine Biology and Fisheries.

PhD: Bio-Optical Properties of the Turkish Seas. 2001-2007. Middle East Technical University Institute of Marine Sciences, Dept. Marine Biology and Fisheries.

EXPERIENCE:

1995   Three weeks in Seal Research and Rehabilitation Centre, Netherlands
              (Train on Autopsy and Rehabilitation).

1996-1999   Working for WWF-Conservation of Mediterranean Monk Seal in
              Cilician Basin. (Field Researcher).

1999   National Training Course on Environmental Information Systems in
              Integrated Coastal Area Management 22-26 February, Izmir, Turkey.

2000   Training Course on Remote Sensing of Ocean Colour September 11-
              24, September. NATO/IOCCG OCEAN COLOUR TRAINING
              COURSE ERDEMLI, TURKEY.

2002   A NATO Advanced Study Institute. "The Ocean Carbon Cycle and
              Climate"
              5-16 August, Middle East Technical University (METU), Ankara,
              Turkey.

2005   Methods and Applications of Ocean Colour Remote Sensing in
              Coastal and Regional Seas"3-14 October 2005, Ispra, Italia.

DISSERTATIONS

Hasan Örek, Ali Cemal Gücü, Ferit Bingel. 2000. Karadeniz ekosistemindeki
değişim (Change in Black Sea Ecosystem). I. Ulusal Deniz Bilimleri Konferansı (1st
national Marine Science Conference). Z. Uysal ve İ. Salihoğlu (Eds). 86-91 pp.

Hasan Örek, Yalçın Savaş, Ali Cemal Gücü, Funda Erkan. 2001 Akdeniz Foku
(Monachus monachus Nordmann 1779) Kilikya Populasyonu IV. Ulusal Ekoloji ve
Çevre Kongresi.

Harun Güçlüsoy, **Hasan Örek** & N. Ozan Veryeri. 2001. Ege ve Akdeniz Deniz Kıyılarında Akdeniz Foku (Monachus monachus) Rehabilitasyonu ve Nekropsi Çalışmaları / Rehabilitation and Necropsies of the Monk Seal (Monachus monachus) along the Coast of the Aegean and Mediterranean Sea. II Avrasya IWRC Yaban Hayatı Rehabilitasyon Sempozyumu ve Eğitim Kursu Programı. (II. Eurasia Wild Life, Rehabilitation symposium and training programme). ANKARA.

Hasan Örek, Ali Cemal Gücü, Ferit Bingel. 2002. An application of mass balance ecopath model to the trophic structure in the black sea "after anchovy collapse" Second International Conference on "Oceanography of the Eastern Mediterranean and Black Sea: Similarities and Differences of Two Interconnected Basins"

PUBLICATIONS

Ali Cemal Gucu*,Gul Gucu, **Hasan Örek.** Habitat use and preliminary demographic evaluation of the critically endangered Mediterranean monk seal (Monachus monachus) in the Cilician Basin (Eastern Mediterranean). Biological Conservation 116 (2004) 417–431.

Hasan Örek. An Application of Mass Blance Ecopath Model To The Trophic Structure In The Black Sea "After Anchovy Collapse" MSc Thesis. 115 pages. February 2000.